1 Synthetic and analytical details

1.1 Materials and synthetic methods

All experiments were carried out using Schlenk and glove-box (argon atmosphere) techniques. All solvents were dried by passing through columns packed with activated alumina unless otherwise mentioned. Deuterated solvents (Euriso-Top GmbH) and *t*BuNH$_2$ (Sigma Aldrich), were dried over Na/K (d_6-benzene and d_8-THF) or CaH$_2$ (1,8-Diazabicyclo[5.4.0]undec-7-ene (DBU)), respectively, distilled by trap-to-trap transfer *in vacuo* and degassed by three freeze-pump-thaw cycles. DMF (Sigma Aldrich) was dried by storage over molecular sieves (4 Å). Aluminum oxide (Brockmann I, basic) was heated *in vacuo* for 3 d to 200 °C prior to use. AgCF$_3$CO$_2$ (ABCR) and bis(cyclopentadienyl)cobalt(II) (ABCR) were used as purchased. **6** and thianthrenium tetrafluoroborate were prepared according to published procedure.[1,2] *t*Bu^{15}NH$_2$ was prepared using a modified method of Bergman and coworkers (see below).[3]

1.2 Analytical methods

Elemental analyses were obtained from the Analytical laboratories at the Georg-August University on a Elementar Vario EL 3. NMR spectra were recorded on Bruker Avance III 300 or 400 MHz spectrometers and were calibrated to the residual solvent proton resonance (d_6-benzene: δ_H = 7.16 ppm, δ_C = 128.06 ppm; d_8-THF: δ_H = 3.58 ppm, δ_C = 67.2 ppm). ^{31}P chemical shifts are reported relative to external phosphoric acid. Signal multiplicities are abbreviated as: s (singlet), d (dublet), t (triplet), q (quartet), m (multiplet) and br (broad). Spectra are recorded at r.t. unless otherwise noted. Magnetic moments in solution were determined in d_8-THF or C_6D_6 at r.t. by Evans' method as modified by Sur[4] and corrected for diamagnetic contribution.

Experimental X-band EPR spectra were recorded at 23 K on a Bruker EMX spectrometer equipped with a He temperature control cryostat system (Oxford Instruments), using a frozen solution (glass) of **9** in MeTHF. The spectra were simulated by iteration of the anisotropic g-values, (super)hyperfine coupling constants, and line widths using the EPR simulation program W95EPR developed by Prof. dr. Frank Neese. W-band ELDOR NMR experiments[5] were conducted at 5.5 K on a

Bruker Elexsys E680 W-band FT-EPR spectrometer equipped with a 6 Tesla split-pair cryogenic superconducting Magnet, using a frozen solution (glass) of **9** in MeTHF. The sample was accommodated in an EN 680-1021H W-band TE011 pulse ENDOR resonator. Cryogenic temperatures were reached using a dedicated Oxford Helium flow cryostat. The spectra were simulated using the EasySpin package of Matlab scripts,[6] making use of the ENDOR ("salt") routine.

Temperature-dependent magnetic susceptibility measurements were carried out with a *Quantum-Design* MPMS-XL-5 SQUID magnetometer in the range from 295 to 2.0 K at a magnetic field of 0.5 T. The powdered sample was contained in a gelatin capsule and fixed in a non-magnetic sample holder. Each raw data file for the measured magnetic moment was corrected for the diamagnetic contribution of the gelatin capsule according to M^{dia}(capsule) = $\chi_g \cdot m \cdot H$, with an experimentally obtained gram susceptibility of the gelatin capsule. The molar susceptibility data were corrected for the diamagnetic contribution according to χ_M^{dia}(sample) = $-0.5 \cdot M \cdot 10^{-6}$ cm^3·mol^{-1}.[7] Experimental data were modelled with the *julX* program[8] using a fitting procedure to the spin Hamiltonian $\hat{H} = g\mu_B \vec{B}\,\vec{S} + D\left[\hat{S}_z^2 - \frac{1}{3}S(S+1)\right]$.

Paramagnetic impurities (*PI*) were included according to $\chi_{calc} = (1 - PI)\cdot\chi + PI\cdot\chi_{mono}$.

1.3 Syntheses

[Ir(NH*t*Bu)(N(CHCHP*t*Bu$_2$)$_2$)] (7). A mixture of LiNH*t*Bu (5.0 mg; 63 μmol; 7.3 eq) and [Ir(Cl)(N(CHCHP*t*Bu$_2$)$_2$)] (**6**) (5.0 mg; 8.6 μmol; 1 eq) is dissolved in *t*BuNH$_2$ (0.5 mL) and stirred for 2 h. All volatiles are removed *in vacuo*. Extraction of the residue with pentanes (4 x 2 mL) followed by removal of the solvent yields crude **7** as a green solid (Figure S2). Any attempts of further purification did not lead to the isolation of analytically pure material.

[Ir(NH*t*Bu)(N(CHCHP*t*Bu$_2$)$_2$)]PF$_6$ (8). A solution of crude **7** (*vide supra*) in benzene is purified by chromatography (basic alumina) using THF as eluent after exhaustive washing with benzene. Immediate oxidation with a small excess of $AgPF_6$ (3.8 mg, 15 μmol; 1.7 eq based on starting material **6**) affords a blue solution, which is filtered. The residue is extracted with THF (2 x 1 mL) and the product is precipitated from the combined THF fractions upon addition of pentanes. The residue is then washed with benzene (3 x 2 mL). Diffusion of pentanes into a solution of crude **8** in THF at -30 °C yields **8** as dark blue crystals (yield: 40%). Anal. Calc. for $C_{24}H_{50}N_2F_6P_3Ir$ (765.80): C, 37.64; H, 6.58; N, 3.66. Found: C, 38.02; H, 6.76; N, 3.32. NMR (d_8-THF [ppm]): ^{1}H (300 MHz, 24 °C): δ = 13.45 (br, 1 H, N*H*), 6.32 (AMXX'M'A', N = $|^3J_{HP} + {}^4J_{HP}|$ = 20.8 Hz, $^3J_{HH}$ =6.1 Hz, 2 H, NC*H*CHP), 5.83 (AMXX'M'A', N = $|^2J_{HP} + {}^4J_{HP}|$ = 3.0 Hz, $^3J_{HH}$ =6.1 Hz, 2 H, NCHC*H*P), 1.38 (AXX'A', N = $|^3J_{HP} + {}^5J_{HP}|$ = 7.3 Hz 36 H, PC(C*H*$_3$)$_3$), 0.95 (s, 9 H, NHC(C*H*$_3$)$_3$). ^{31}P (121 MHz, 24 °C): δ = 41.73 (s), -145.00 (hept, $^1J_{PF}$ = 710 Hz).

[Ir(N*t*Bu)(N(CHCHP*t*Bu$_2$)$_2$)]CF$_3$CO$_2$ (9). A mixture of LiNH*t*Bu (40.0 mg; 506 μmol; 2.7 eq) and [Ir(Cl)(N(CHCHP*t*Bu$_2$)$_2$)] (6) (110.6 mg; 189 μmol; 1 eq) is dissolved in *t*BuNH$_2$ (8 mL) and stirred for 2 h. All volatiles are removed *in vacuo*, $AgCF_3CO_2$ (175 mg; 792 μmol; 4.2 eq) is added. The mixture is dissolved in THF (4 mL) and shaken for 1 min. The crude product is precipitated by addition of pentanes (40 mL). The residue is dissolved in THF (4 mL) and separated by chromatography (basic aluminum oxide). After rinsing the column with benzene (20 mL), the product is eluted with DMF and dried *in vacuo* overnight. Two successive crystallizations from dichloromethane layered with pentanes affords analytically pure **9** as purple crystals which is washed with pentanes (2 x 1 mL) and dried *in vacuo* overnight (yield: 57%). Anal. Calc. for

$C_{26}H_{49}N_2F_3O_2P_2Ir$ (732.84): C, 42.61; H, 6.74; N, 3.82. Found: C, 42.39; H, 6.70; N, 3.81. NMR (d_8-THF [ppm]): 1H (300 MHz, 24 °C): δ = 32.08 (br, 2 H), 6.74 (br, 45 H), -10.78 (br, 2 H). 19F (282 MHz, 24 °C)): δ = -77.05 (s). μ_{eff}^{298K} = 1.6(2) μ_B (Evans' method in CD_2Cl_2).

[Ir(N*t*Bu)(N(CHCHP*t*Bu$_2$)$_2$)]BF$_4$ (9-BF$_4$). The synthesis is analogous to the synthesis of **9** using $AgBF_4$ instead of $AgCF_3CO_2$ as the oxidant. The spectroscopic features in the ^{1}H NMR remain unchanged.

[Ir(^{15}N*t*Bu)(N(CHCHP*t*Bu$_2$)$_2$)]CF$_3$CO$_2$ (^{15}N-9). The synthesis is carried out analogously to the unlabeled complex using Li^{15}NH*t*Bu and *t*Bu^{15}NH$_2$ as solvent.

***t*Bu^{15}NH$_2$.** A solution of $^{15}NH_4Cl$ (5.0 g; 91.5 mmol; 1 eq) in water (19 mL) is cooled to 0 °C and layered with pivaloyl chloride (15.0 mL; 120 mmol; 1.3 eq) in diethylether (50 mL). The solution is warmed to r.t. while stirring slowly avoiding mixing of the phases. Sodium hydroxide (21.4 g; 535 mmol; 5.8 eq) is dissolved in water (25 mL) and added to the aqueous phase. After slow stirring for 15 min, the phases are mixed while releasing pressure and cooling with an ice bath. The ether is removed *in vacuo* and the remaining aqueous phase extracted with dichloromethane (5 x 20 mL). All volatiles are removed *in vacuo* to yield crude pivaloyl amide. Potassium hydroxide (40 g; 1 mol; 10.9 eq) is dissolved in water (200 mL) and cooled in an ice bath. After addition of bromine (5.5 mL; 17 g; 108 mmol; 1.2 eq), the pivaloyl amide is added. The solution is stirred for 90 min at 0 °C, warmed to r.t. and stirred for another 20 min before cooling again to 0 °C. After slow addition of hydrochloric acid (36% in water; 175 mL) the solution is stirred for 15 min at 50 °C and cooled again in an ice bath while *n*-heptane (20 mL) is added. Potassium hydroxide is added until a pH value of at least 12 is reached. The aqueous phase is extracted with *n*-heptane (5 x 20 mL). The combined organic phases are extracted with hydrochloric acid (1 M; 5 x 20 mL). After removing all volatiles *in vacuo*, the flask is cooled to -50 °C and DBU (8 mL; 53.6 mmol; 0.6 eq) is added. After stirring for 16 h at r.t., all volatiles are trap-to-trap transferred to a flask with Na/K alloy. Upon thawing gas evolution can be observed. The liquid is stirred for 4 d, degassed by three freeze-pump-thaw cycles and trap-to-trap transferred to yield analytically pure *t*Bu^{15}NH$_2$ (2.0 mL; 1.4 g; 19.1 mmol; 21%).

[Ir(N*t*Bu)(N(CHCHP*t*Bu$_2$)$_2$)] (10). A mixture of **9** (70.7 mg; 96.5 µmol; 1 eq) and cobaltocene (17.8 mg; 94.1 µmol; 0.98 eq) is dissolved in THF (10 mL) and stirred for 1 h. All volatiles are removed *in vacuo*, the residue is extracted with pentanes (4 x 2 mL) and filtered. The solution is then evaporated to a total volume of about 1 mL and cooled to -50 °C. The product crystallizes upon slow evaporation of the solvent over 10 h and collected as red-brown crystals (yield: 62%). Anal. Calc. for $C_{24}H_{49}N_2P_2Ir$ (619.82): C, 46.51; H, 7.97; N, 4.52. Found: C, 46.85; H, 8.38; N, 4.33. NMR (d_6-benzene [ppm]): ^{1}H (300 MHz, 24 °C): δ = 17.52 (br, 36 H), 13.88 (br, 9 H), -46.73 (br, 2 H), -78.80 (br, 2 H). μ_{eff}^{298K} = 2.3(2) μ_B (Evans' method in d_8-THF).

[Ir(N*t*Bu)(N(CHCHP*t*Bu$_2$)$_2$)](BF$_4$)$_2$ (11). A mixture of [Ir(N*t*Bu)(N(CHCHP*t*Bu$_2$)$_2$)]BF$_4$ (9-BF$_4$) (13.4 mg; 19.0 µmol; 1.0 eq) and thianthrenium tetrafluoroborate (5.8 mg; 19.1 µmol; 1.0 eq) is dissolved in precooled MeCN (2 mL). The resulting green solution is layered with toluene (2 mL) and pentanes (2 mL) and stored at -35 °C until the crude product is completely precipitated. The solution is decanted and the residue washed with cooled (-35 °C) toluene (3 x 1 mL) and pentanes (3 x 1 mL). Drying *in vacuo* yields the analytically pure dark green product (70%). Anal. Calc. for $C_{24}H_{49}N_2B_2F_8P_2Ir$ (793.43): C, 36.33; H, 6.22; N, 3.53. Found: C, 36.36; H, 5.98; N, 3.81. NMR (d_3-acetonitrile [ppm]): ^{1}H (400 MHz, -30 °C): δ = 7.05 (AMXX'M'A', N = $|^3J_{HP} + {}^4J_{HP}|$ = 20.2 Hz, $^3J_{HH}$ =4.8 Hz, 2 H, NC*H*CHP), 6.33 (AMXX'M'A', N = $|^2J_{HP} + {}^4J_{HP}|$ = 7.6 Hz, $^3J_{HH}$ =4.8 Hz, 2 H, NCHC*H*P), 1.81 (s, 9 H, NC(C*H*$_3$)$_3$), 1.69 (AXX'A', N = $|^3J_{HP} + {}^5J_{HP}|$ = 8.9 Hz 36 H, PC(C*H*$_3$)$_3$)). ^{31}P (162 MHz, -30 °C): δ = 142.06 (s). ^{19}F (376 MHz, -30 °C): δ = -150.85 (s).

Thermal decomposition of 11. A solution of **11** (3.0 mg, 3.8 µmol) in d_3-MeCN (0.4 mL) is warmed stepwise from -30 °C to r.t. The decay is monitored by ^{31}P (Figure S14). Isobutene and nitride **1**[9] are the only products detected by ^{1}H and ^{31}P NMR spectroscopy (Figure S15).

Reaction of 10 with PMe$_3$. Precooled (-30 °C) PMe$_3$ (0.7 µL, 6.9 µmol; 1.3 eq) is added to a solution of 10 (3.3 mg; 5.3 µmol; 1 eq) in C_6D_6 (0.4 mL). The reaction is completed after 7 d at r.t. as indicated by the disappearance of the starting material in the ^{1}H-NMR spectrum. The three signals in the ^{31}P-NMR spectrum are assigned to residual PMe$_3$, [Ir(Ph$_{d5}$)(D){N(CHCHP*t*Bu$_2$)$_2$}][10] (**12**) and *t*BuNPMe$_3$[11] (Figure S16).

Reaction of 10 with CO_2. 10 (10.4 mg; 16.8 μmol; 1 eq) is dissolved in THF (1 mL), degassed by two freeze-pump-thaw cycles and cooled to -10 °C before carbon dioxide (1 bar) is added. The solution is then allowed to warm to r.t. while stirring. All volatiles are immediately removed *in vacuo*. The residue is extracted with THF (2 x 0.5 mL). Removal of volatiles at -10 °C *in vacuo* yields green [Ir(η^2-N(*t*Bu)C(O)O){N(CHCHP*t*Bu$_2$)$_2$}] (**13**) (86%). Anal. Calc. for $C_{25}H_{49}N_2O_2P_2Ir$ (663.83): C, 45.23; H, 7.44; N, 4.22. Found: C, 44.60; H, 7.65; N, 3.90. NMR (*d*$_8$-THF [ppm]): ^{1}H (300 MHz, 24 °C): δ = 7.07 (AMXX'M'A', N = $|^3J_{HP} + {}^4J_{HP}|$ = 20.6 Hz, $^3J_{HH}$ =5.8 Hz, 2 H, NC*H*CHP), 4.68 (AMXX'M'A', N = $|^2J_{HP} + {}^4J_{HP}|$ = 6.0 Hz, $^3J_{HH}$ =5.8 Hz, 2 H, NCHC*H*P), 1.63 (s, 9 H), 1.34 (AXX'A', N = $|^3J_{HP} + {}^5J_{HP}|$ = 7.2 Hz 18 H, PC(C*H*$_3$)$_3$), 1.29 (AXX'A', N = $|^3J_{HP} + {}^5J_{HP}|$ = 7.2 Hz 18 H, PC(C*H*$_3$)$_3$). ^{31}P (121 MHz, 24 °C): δ = 26.2 (s). **13** is thermally labile in solution and in the solid state. Monitoring the decay of **13** in C_6D_6 at r.t. over several hours shows the conversion into 3 products (Figure S18). Two sets of signals in the ^{31}P NMR spectrum were assigned to diastereomers of crystallographically characterized **14** that arise from frozen rotation around the O_2C–N(H)*t*Bu bond. The third signal (**A**) could not be assigned. NMR (C_6D_6 [ppm]): ^{31}P (121 MHz, 24 °C): δ = 47.0 (**14a**, d, $^2J_{PP}$ = 357.5 Hz, *Pt*Bu$_2$), 46.3 (**14b**, d, $^2J_{PP}$ = 357.5 Hz, *Pt*Bu$_2$), 45.6 (**A**), 2.64 (**14a**, d, $^2J_{PP}$ = 357.5 Hz, *Pt*Bu), 2.56 (**14b**, d, $^2J_{PP}$ = 357.5 Hz, *Pt*Bu).

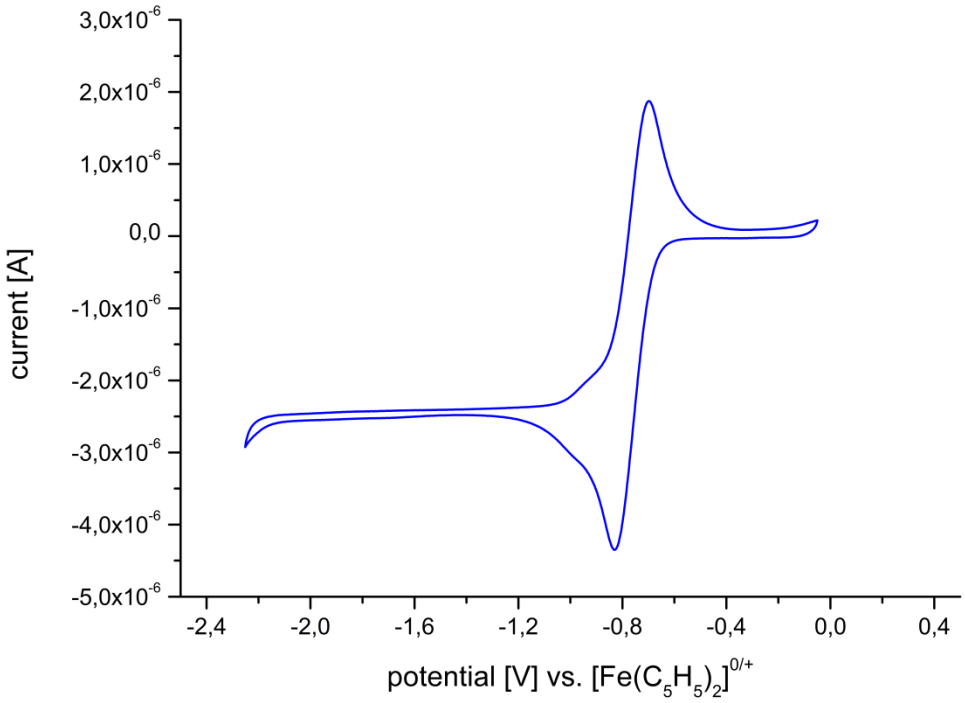

Figure S1. Cyclic voltammogramm of crude **7** in THF (scan rate 50 mV/s; 0.1 mol·L^{-1} *t*Bu$_{4p}$NPF$_6$).

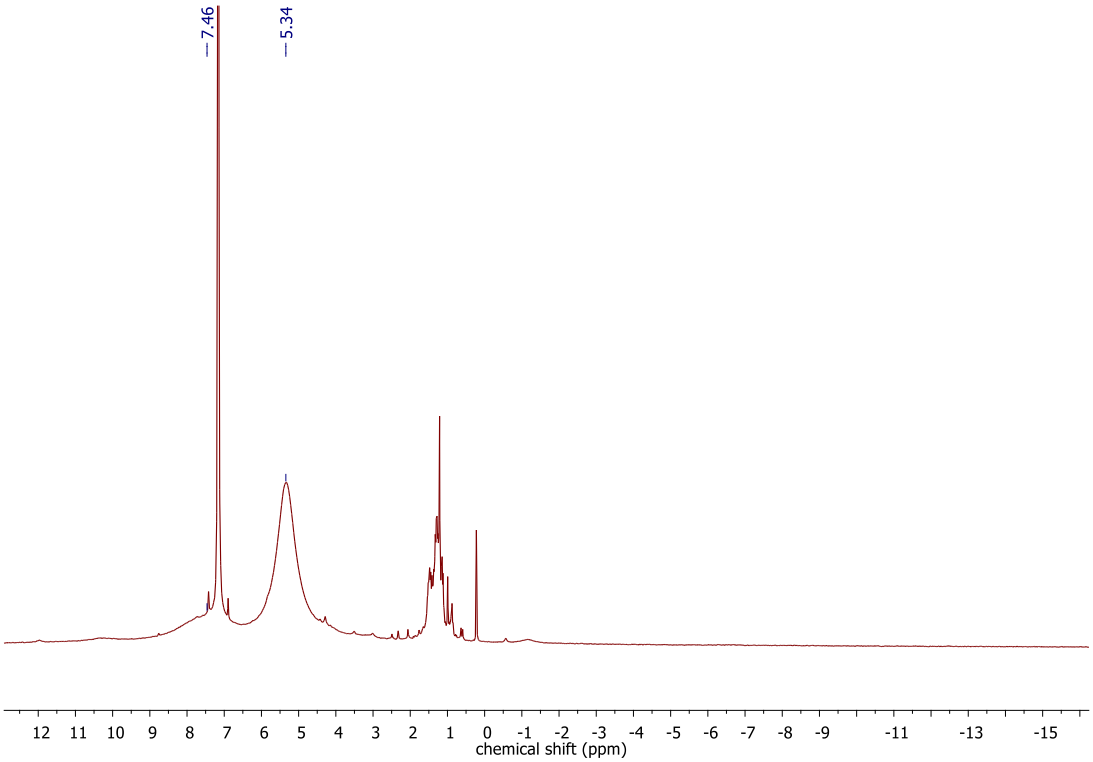

Figure S2. ^{1}H NMR spectrum of crude **7** in C$_6$D$_6$.

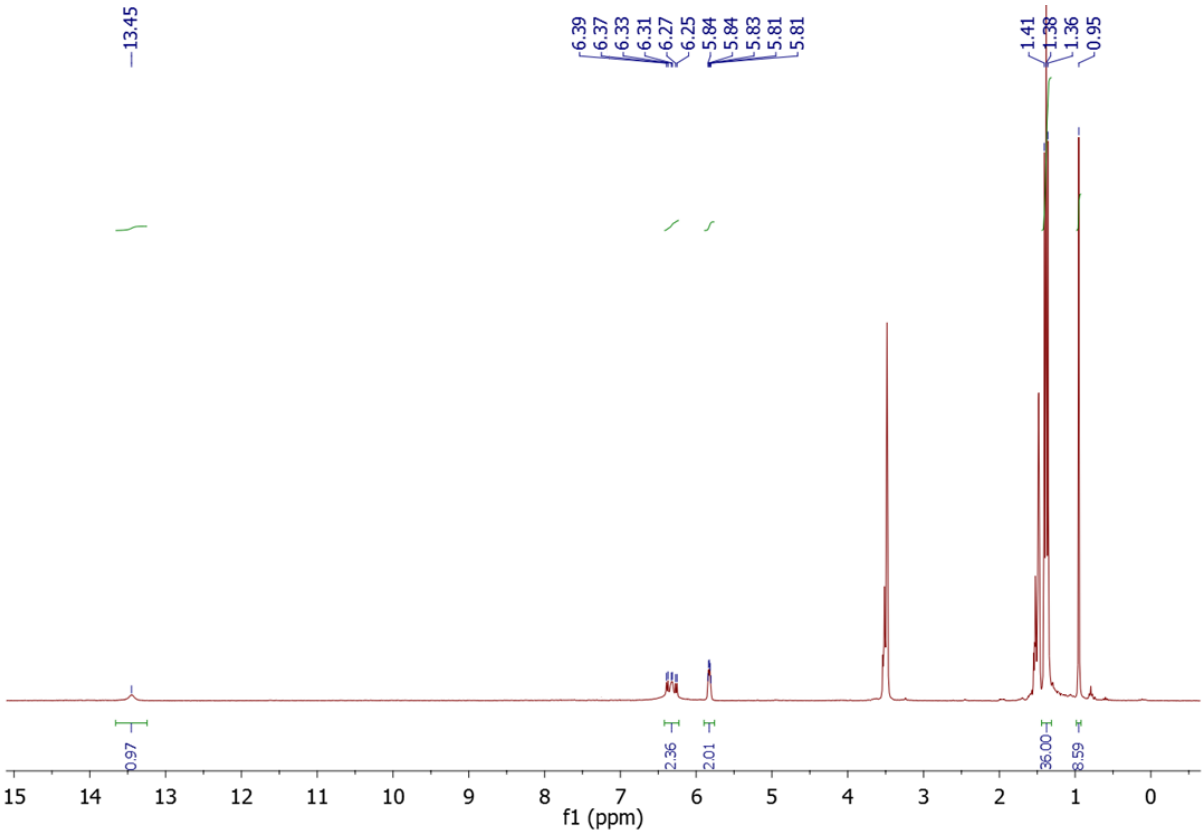

Figure S3. ^{1}H NMR spectrum of **8** in d_8-THF.

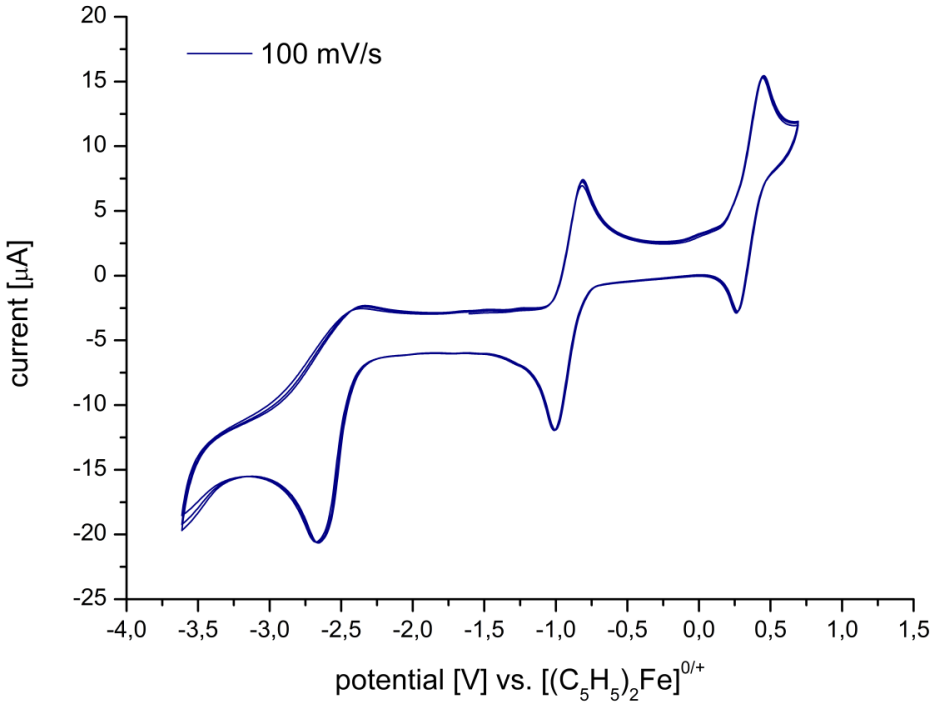

Figure S4. Cyclic voltammogramm of **9** in THF (0.1 mol·L^{-1} *t*Bu$_4$NPF$_6$).

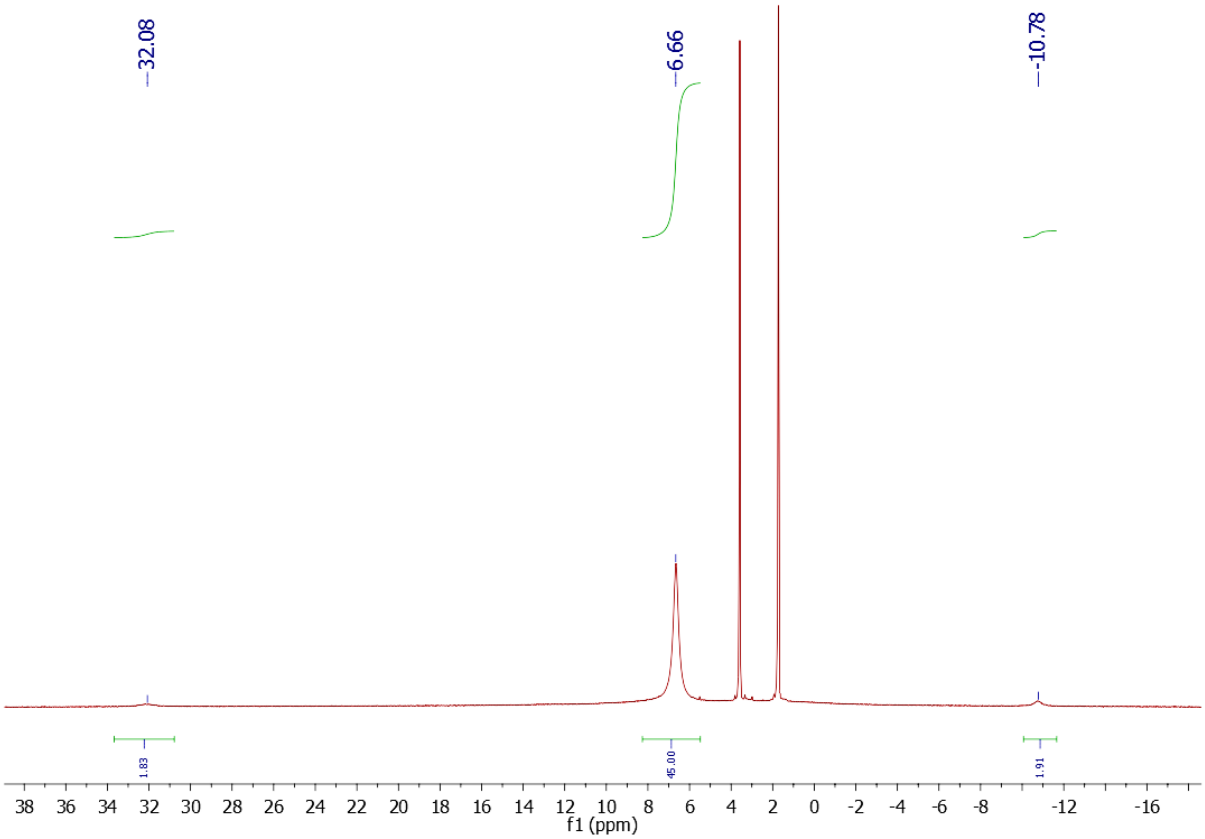

Figure S5. ^{1}H NMR spectrum of **9** in d_8-THF.

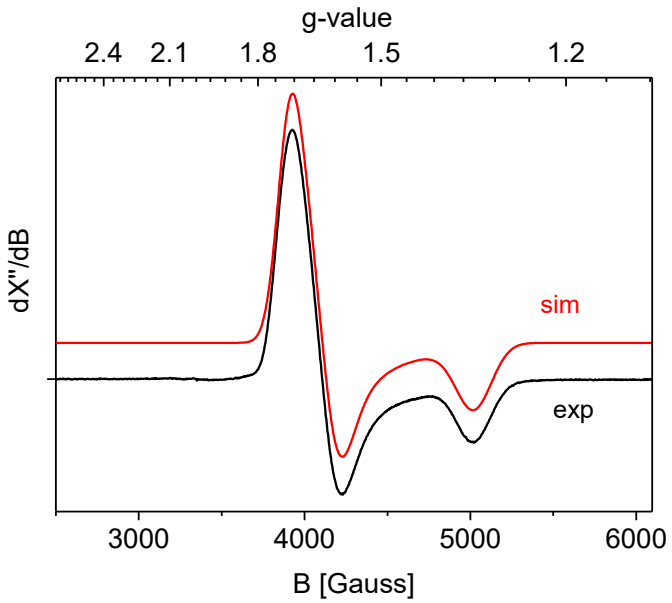

Figure S6. Experimental (black) and simulated (red) EPR spectra of **9**. Experimental conditions: Spectrum recorded in MeTHF at 23 K, frequency 9.367669 GHz, microwave power 0.632 mW, modulation amplitude 4 G. Simulation was obtained using the parameters shown in Table S1.

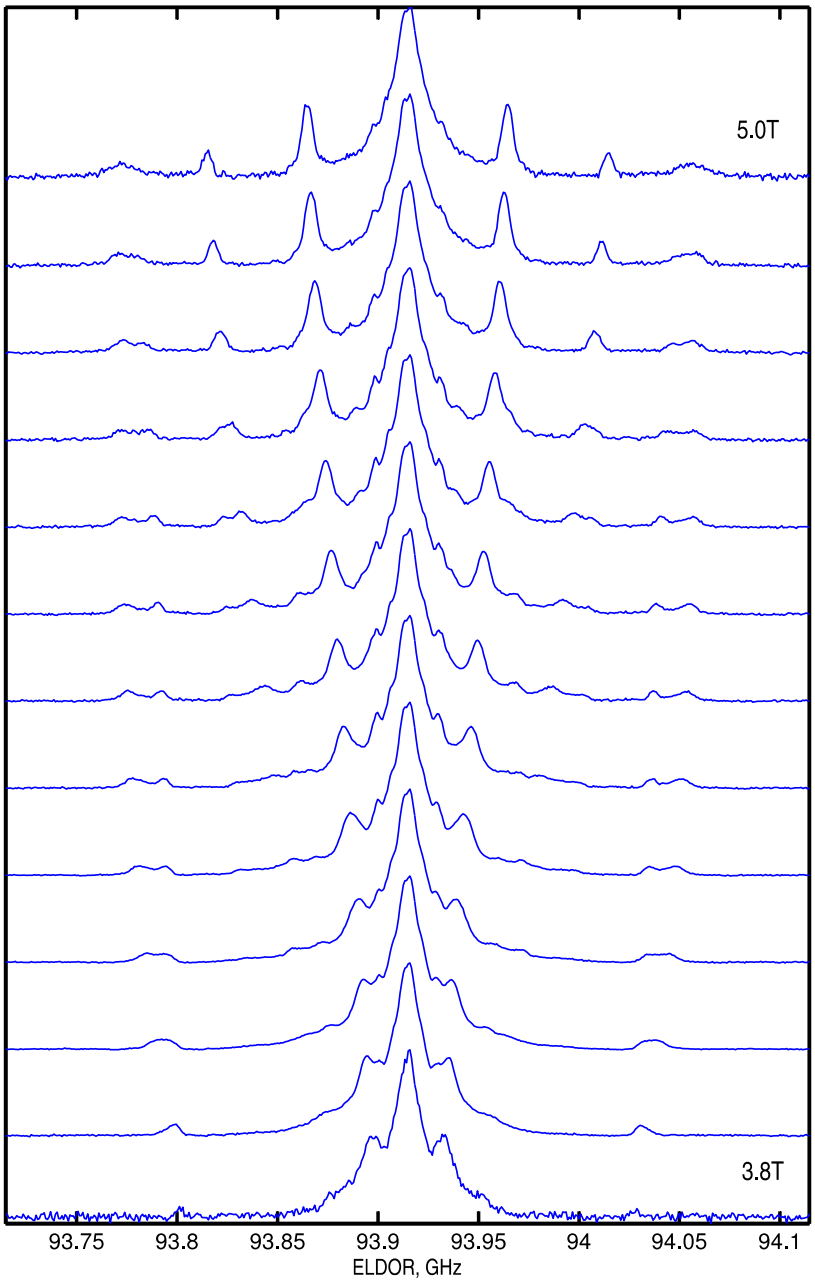

Figure S7. Raw Data of the ELDOR detected NMR spectra recorded on **^{15}N-9**. The microwave frequency of the two pulse echo observer sequence was adjusted to the resonance frequency of the Bruker TE011 W-band cavity by optimizing the symmetry of the ELDOR-NMR spectrum. The high turning angle pulse (HTA) was 5 µs. The full echo shape (tau = 600 ns) was integrated over 500 ns in order to optimize the spectral resolution. The ELDOR pattern was baseline corrected by fitting and subtracting a Lorentzian line shape corresponding to the cavity resonance. Subsequent polynomial base line corrections led to the processed spectra displayed in Figure S8.

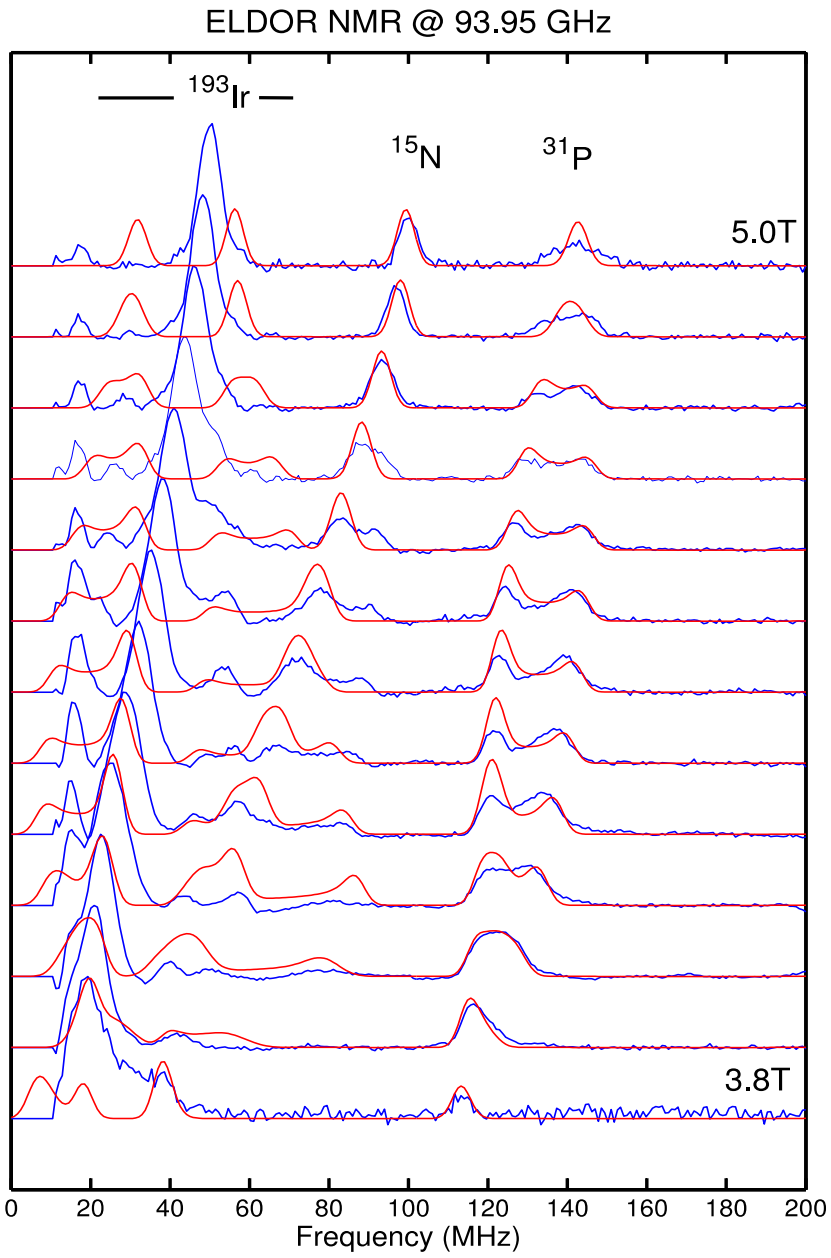

Figure S8. ELDOR detected NMR spectrum **^{15}N-9** recorded at W-band (simulations for ^{15}N and ^{31}P indicated by red line). The features below 60 MHz are dominated by contributions from ^{191}Ir and ^{193}Ir (I=3/2). The peaks up to 100 MHz (at 5.0 T) are assigned to the high frequency transition of the strongly coupled imido ^{15}N nucleus (I=1/2). Assuming alignment with the *g*-matrix principal axes the HFI tensor was simulated as A(^{15}N) = [-156 143 42] MHz, which corresponds to the ^{14}N HFI principal values A(^{14}N) = [-111 102 30] MHz. The peaks up to 140 MHz (at 5.0 T) are assigned to the ^{31}P nuclei (I=1/2) and simulated with HFI tensor A(^{31}P) = (94 94 134) MHz and Euler angles (47 99 NR) degrees which is in very good agreement with the DFT calculations for this interaction.

Table S1. Comparison of experimental and DFT calculated EPR parameters of **9**.

$[(L^{tBu})Ir(NtBu)]^+$						
g-tensor						
	g_{11}	g_{22}	g_{33}	g_{11}	g_{22}	g_{33}
Exp. (sim) X-band	**1.332**	**1.625**	**1.709**	**1.332**	**1.625**	**1.709**
	BP86, TZP			*B3LYP, TZ2P*		
DFT (restricted)	*0.619*	*0.750*	*0.847*	*0.545*	*0.689*	*0.832*
DFT	***1.330***	***1.765***	***1.867***	***1.357***	***1.708***	***1.881***
Hyperfine Interactions						
N^{t}Bu ^{14}N-atom	A^N_{11}	A^N_{22}	A^N_{33}	A^N_{11}	A^N_{22}	A^N_{33}
Exp (ELDOR simulation)	**-111**	**102**	**30**	**-111**	**102**	**30**
	BP86, TZP			*B3LYP, TZ2P*		
DFT (no SOC)	*82*	*2*	*-10*	*100*	*20*	*1*
DFT (SOC)	***-67***	***87***	***-5***	***-51***	***108***	***10***
PNP ^{14}N-atom	A^N_{11}	A^N_{22}	A^N_{33}	A^N_{11}	A^N_{22}	A^N_{33}
Exp (simulation)	NR	NR	NR	NR	NR	NR
	BP86, TZP			*B3LYP, TZ2P*		
DFT (no SOC)	*-9*	*-4*	*-4*	*-1*	*-12*	*-5*
DFT (SOC)	***-7***	***-5***	***-4***	***-9***	***-6***	***-5***
PNP ^{31}P-atoms	A^N_{11}	A^N_{22}	A^N_{33}	A^N_{11}	A^N_{22}	A^N_{33}
Exp (ELDOR simulation)[a]	**94**	**94**	**134**	**94**	**94**	**134**
	BP86, TZP			*B3LYP, TZ2P*		
DFT (no SOC) [b]	*91*	*91*	*130*	*89*	*89*	*128*
DFT (SOC) [b]	***87***	***91***	***134***	***88***	***91***	***134***
^{193}Ir	A^{Ir}_{11}	A^{Ir}_{22}	A^{Ir}_{33}	A^N_{11}	A^N_{22}	A^N_{33}
Exp (simulation)	NR	NR	NR	NR	NR	NR
	BP86, TZP			*B3LYP, TZ2P*		
DFT (no SOC)	*-35*	*-62*	*-37*	*-46*	*-75*	*-51*
DFT (SOC)	***-80***	***-29***	***-84***	***-89***	***-51***	***-96***

[a] Experimental Euler angles: [47 99 NR] degrees (gamma value meaningless).
[b] Averaged DFT Euler angles: [55 88 NR] degrees (gamma value meaningless).

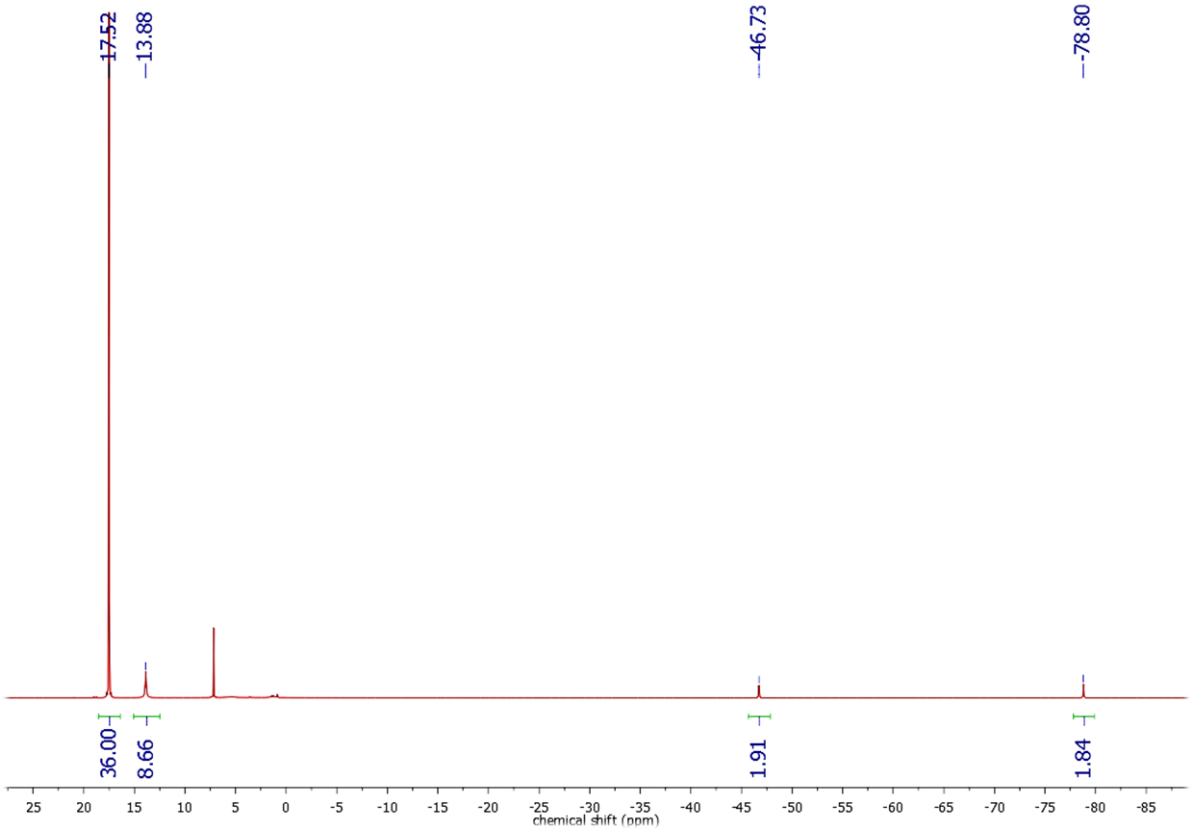

Figure S9. ^{1}H NMR spectrum of **10** in C_6D_6.

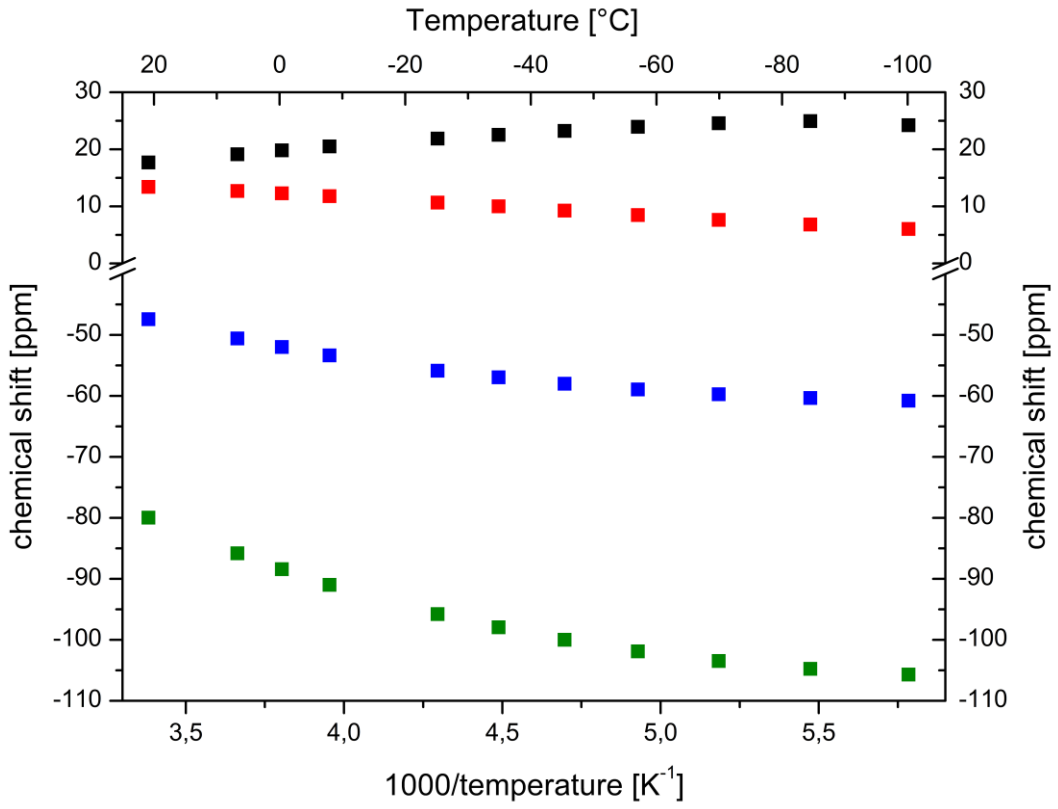

Figure S10. Temperature dependence of the ^{1}H NMR data of **10** in d_8-THF.

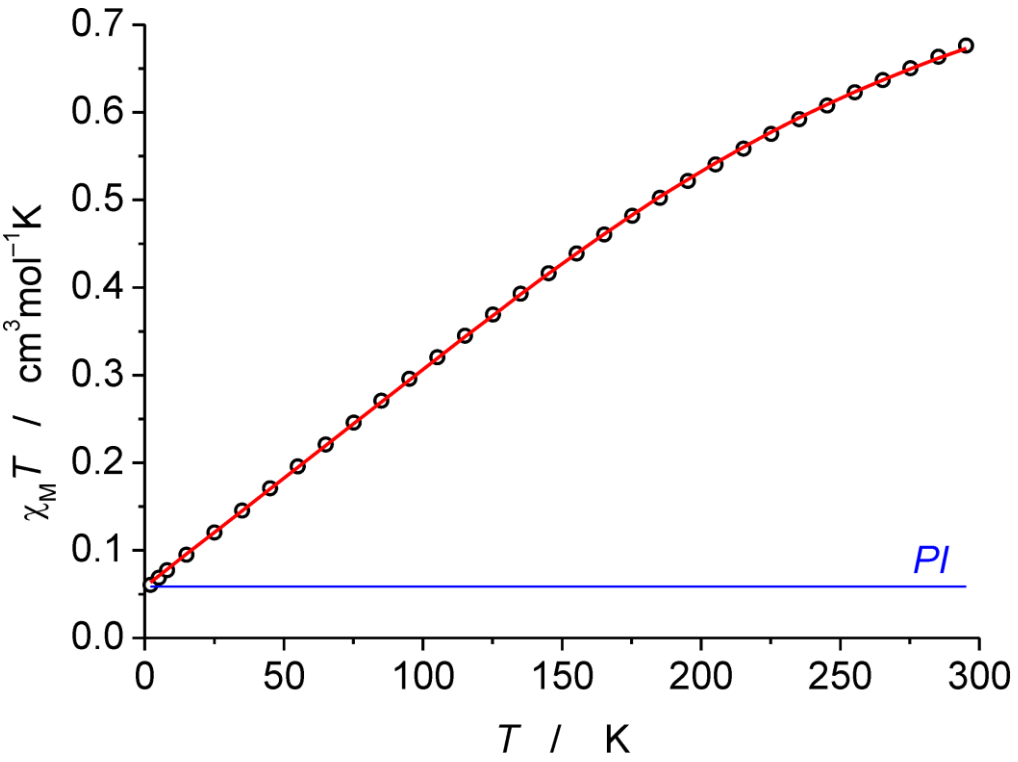

Figure S11. Temperature dependence of the experimental χT-product (circles) of microcrystalline **10** at 0.5 T. Solid lines represent the global fit using the Spin-Hamiltonian given in the experimental details (fit parameters: S = 1; g = 1.98; D = 466 cm^{-1}; PI denotes the correction from a paramagnetic impurity (15.6%) with S = 0.5).

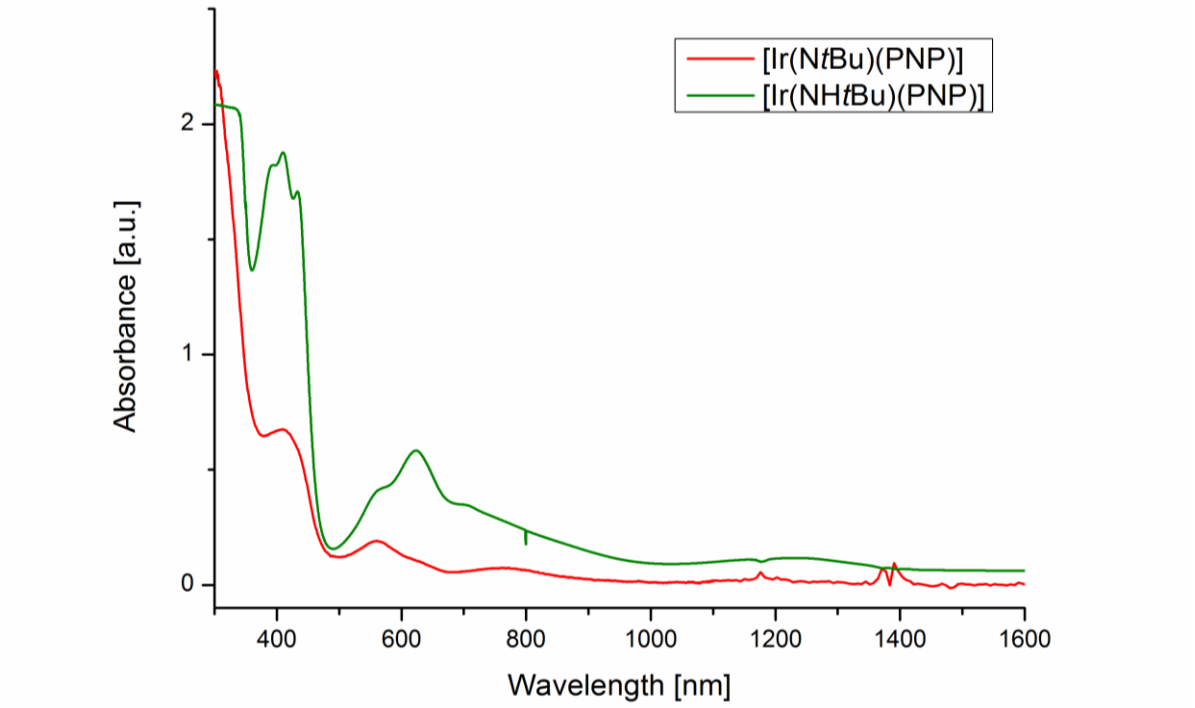

Figure S12. UV/Vis/NIR spectra of **7** (green, 0.81 mM) and **10** (red, 0.20 mM) in THF solution at r.t.

1.4 MCD measurements of MK532

MCD spectra of **10** were recorded as a frozen solution in 2-Methyltetrahydrofuran at wavelengths between 300 and 2,000 nm on a spectrometer built around an Aviv 42 CD spectrometer equipped with both photomultiplier and InGaAs detectors and an Oxford Instruments Spectromag SM4000 optical cryomagnet. A comparison with the baseline shows that signals above 1600 nm arise from the set-up.

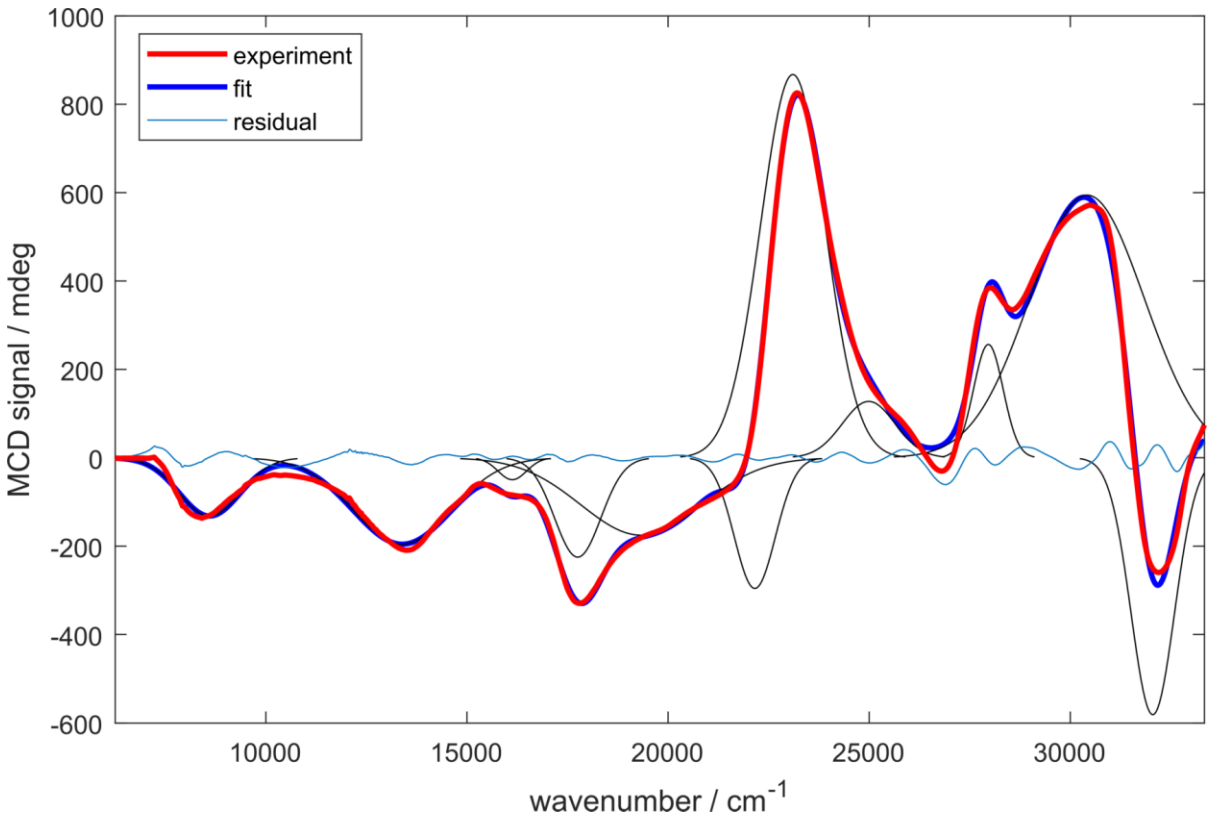

Figure S13. Deconvolution of the MCD spectrum of **10** at 1.5 K and 5 T using 11 gaussians.

Table S2. Peak positions of the gaussians used for deconvolution of **10**.

Peak / cm^{-1}	
8602	(6)
13388	(9)
16130	(20)
17752	(8)
19330	(80)
22160	(20)
23100	(50)
24990	(50)
27962	(2)
30420	(10)
32051	(2)

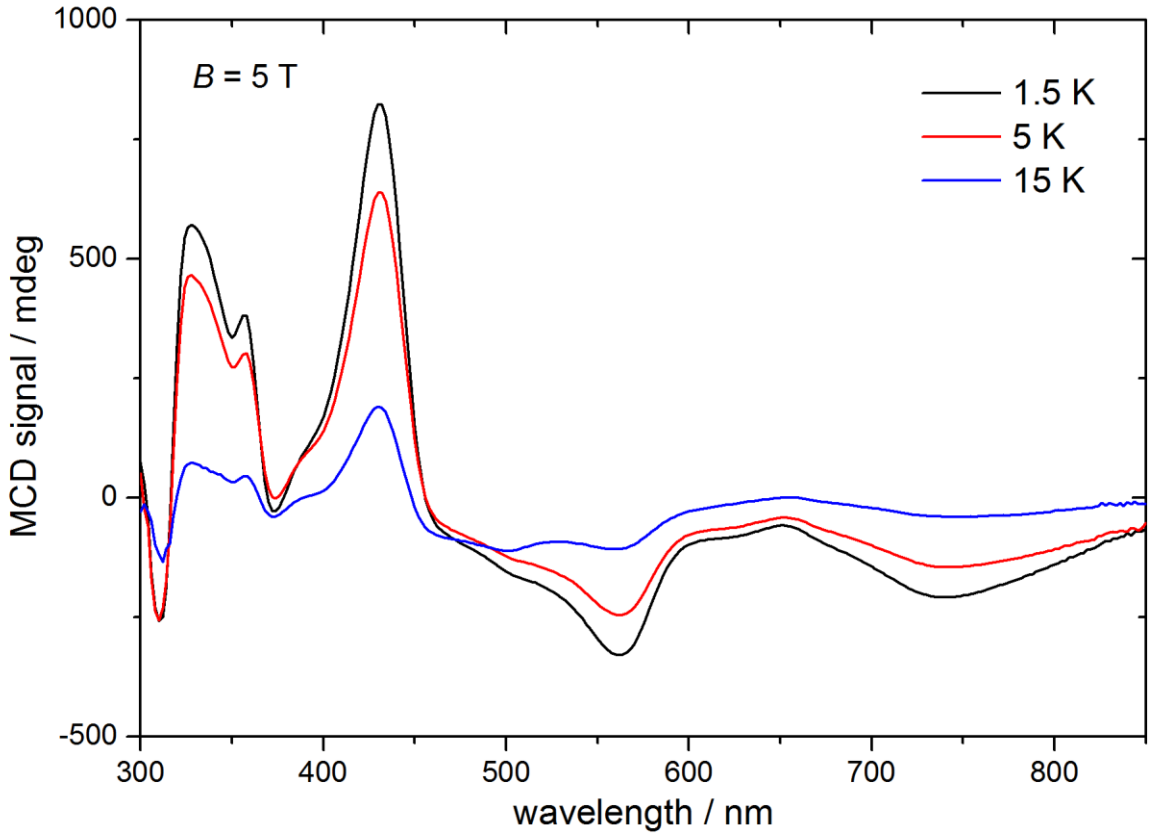

Figure S14. MCD spectra of **10** in the Vis range at 5 T and various temperatures.

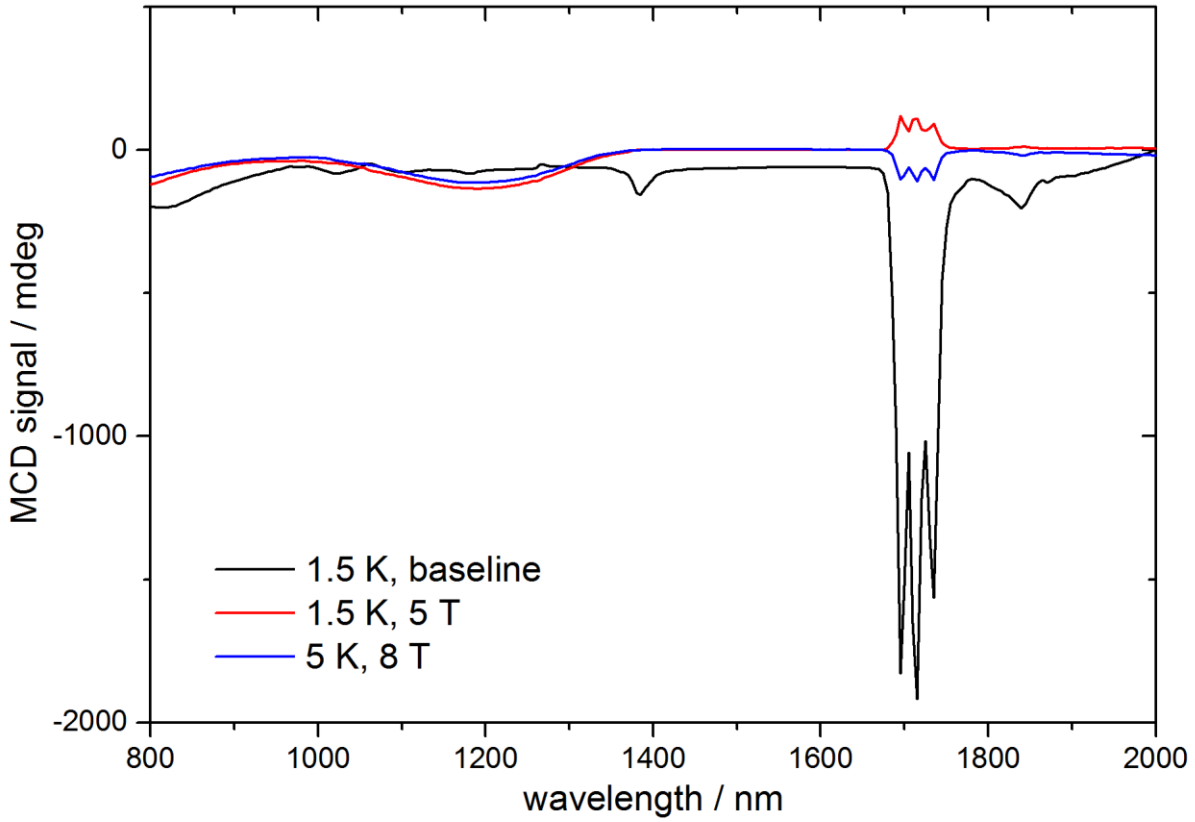

Figure S15. MCD spectra of **10** in the NIR range at different temperatures and magnetic fields.

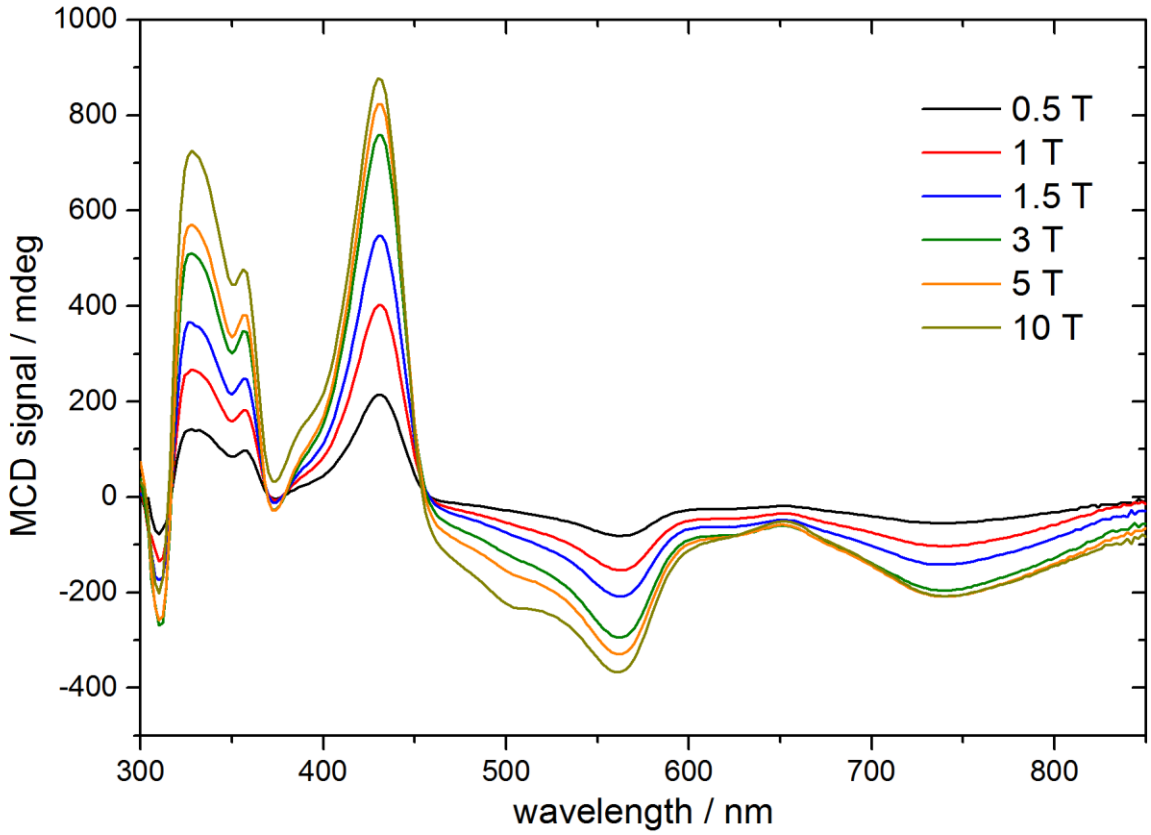

Figure S16. Variable field MCD spectra of **10** in the Vis Range at 1.5 K.

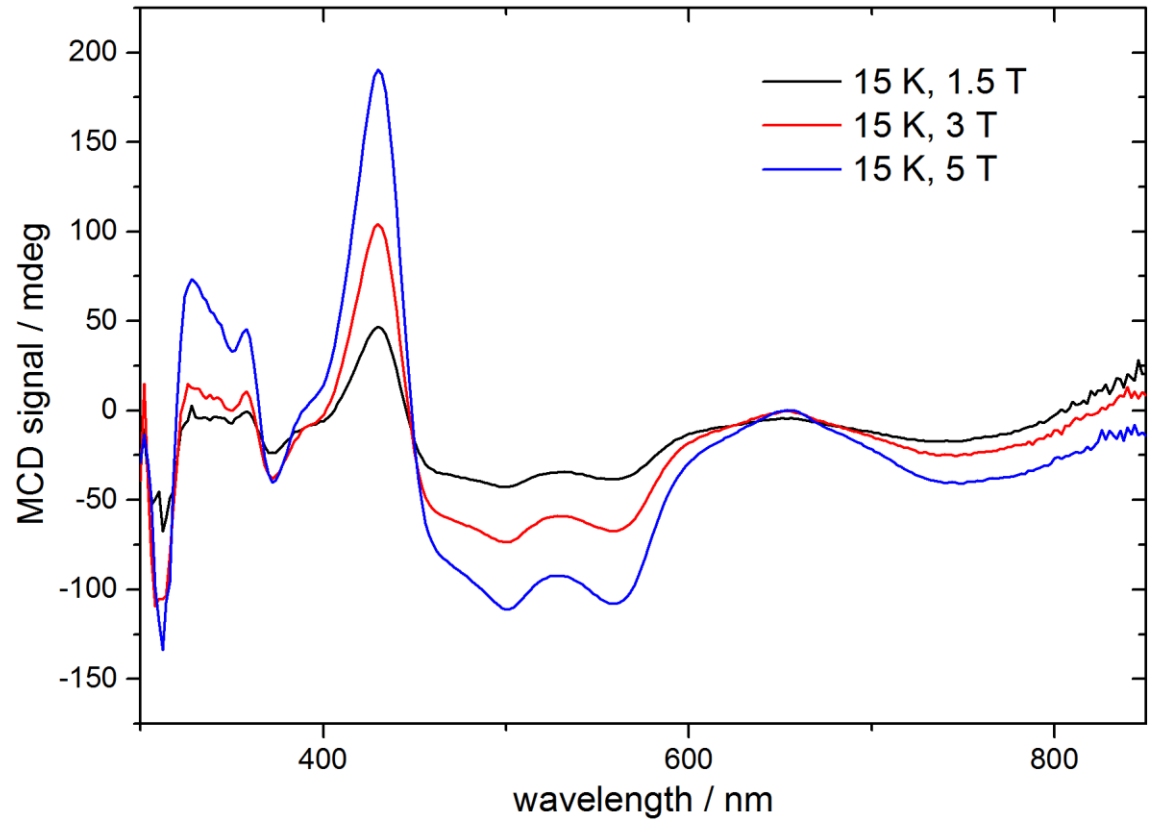

Figure S17. Variable field MCD spectra of **10** in the Vis range at 15 K.

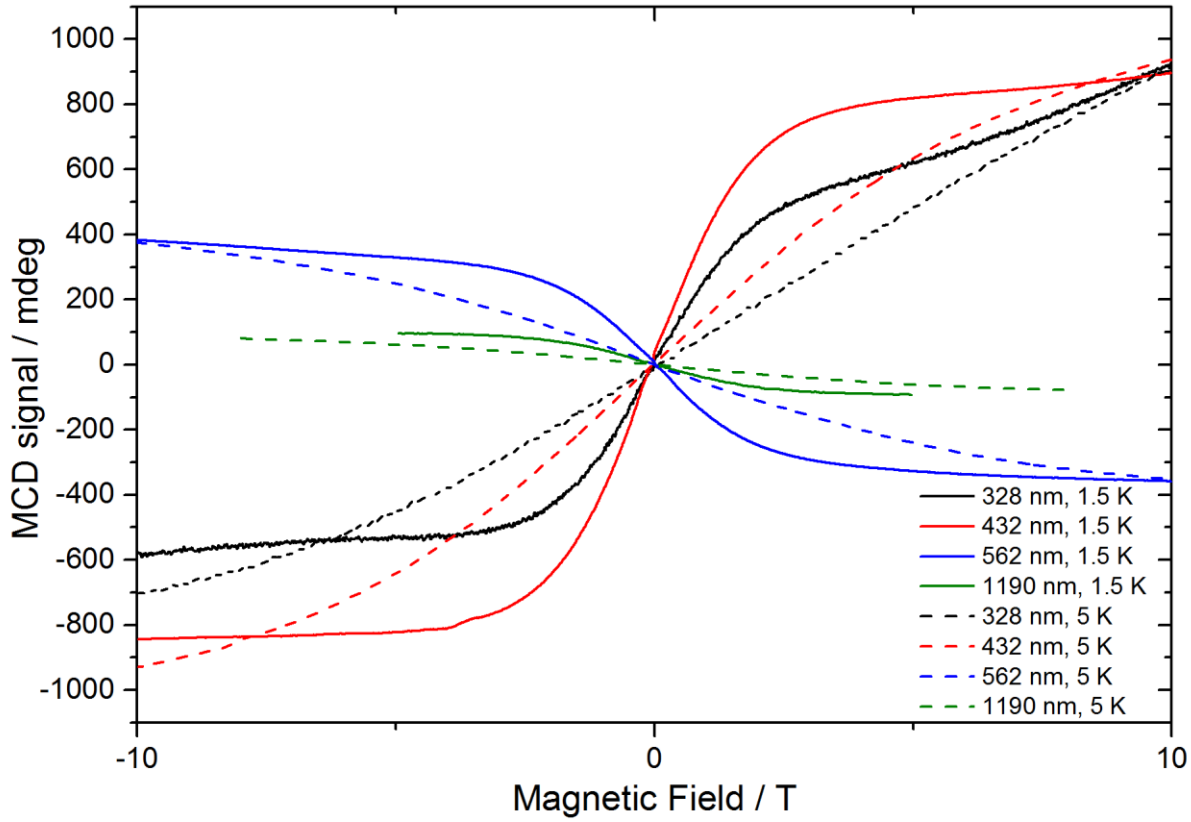

Figure S18. Field dependent MCD signals at 1.5 K and 5 K and various wavelengths.

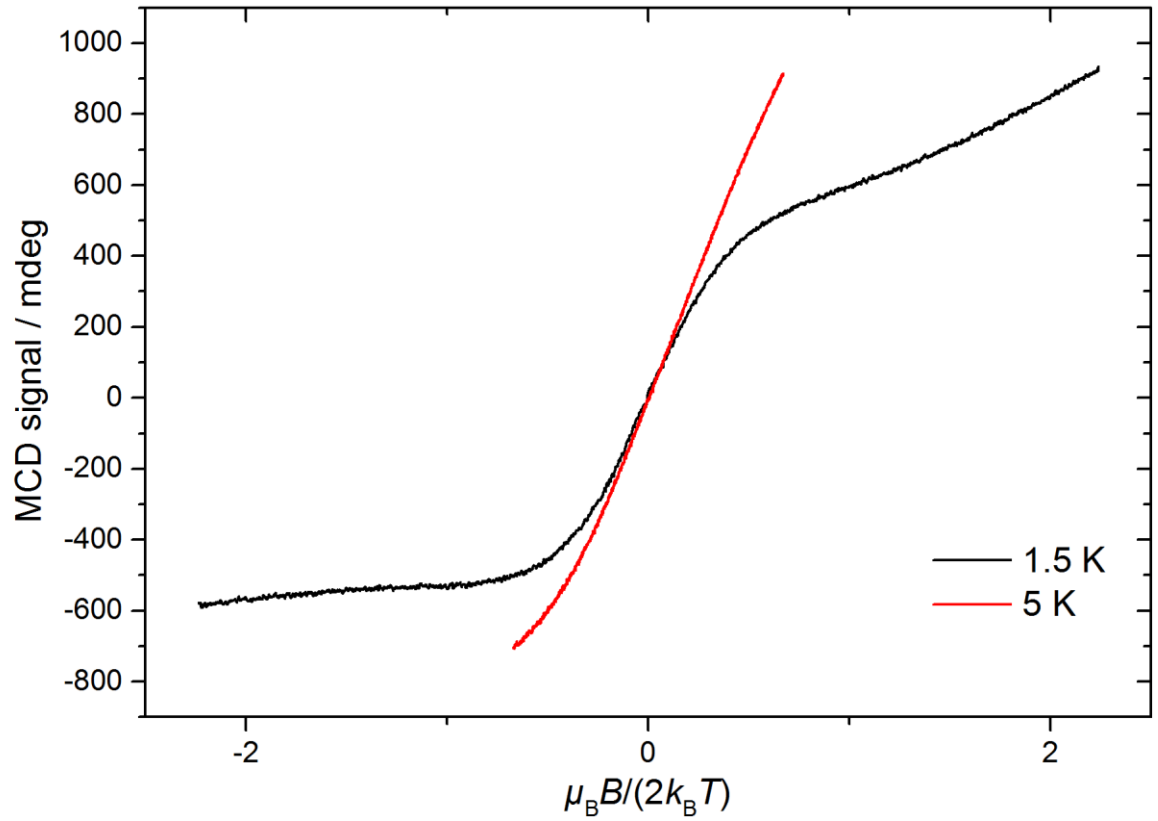

Figure S19. Plot of the MCD intensity at 328 nm over the reduced magnetic field at 1.5 K, 5 K and 15 K.

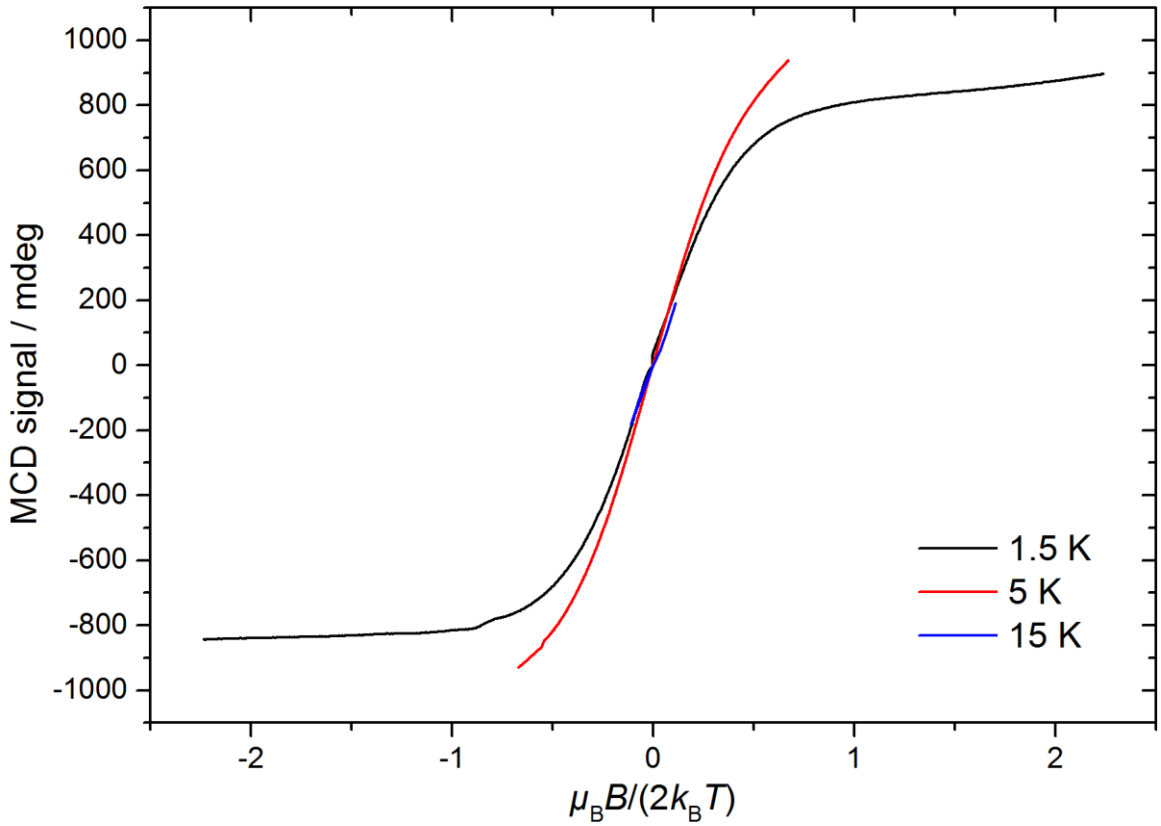

Figure S20. Plot of the MCD intensity at 432 nm over the reduced magnetic field at 1.5 K, 5 K and 15 K.

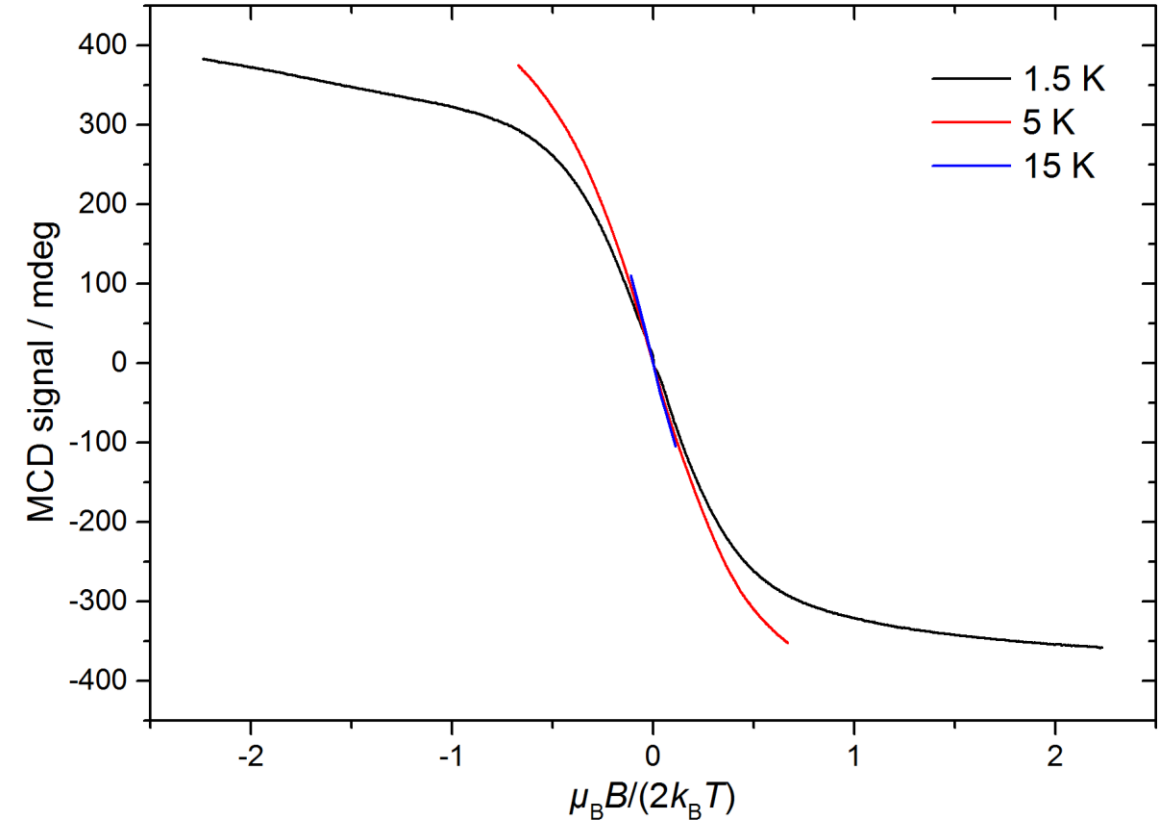

Figure S21. Plot of the MCD intensity at 562 nm over the reduced magnetic field at 1.5 K, 5 K and 15 K.

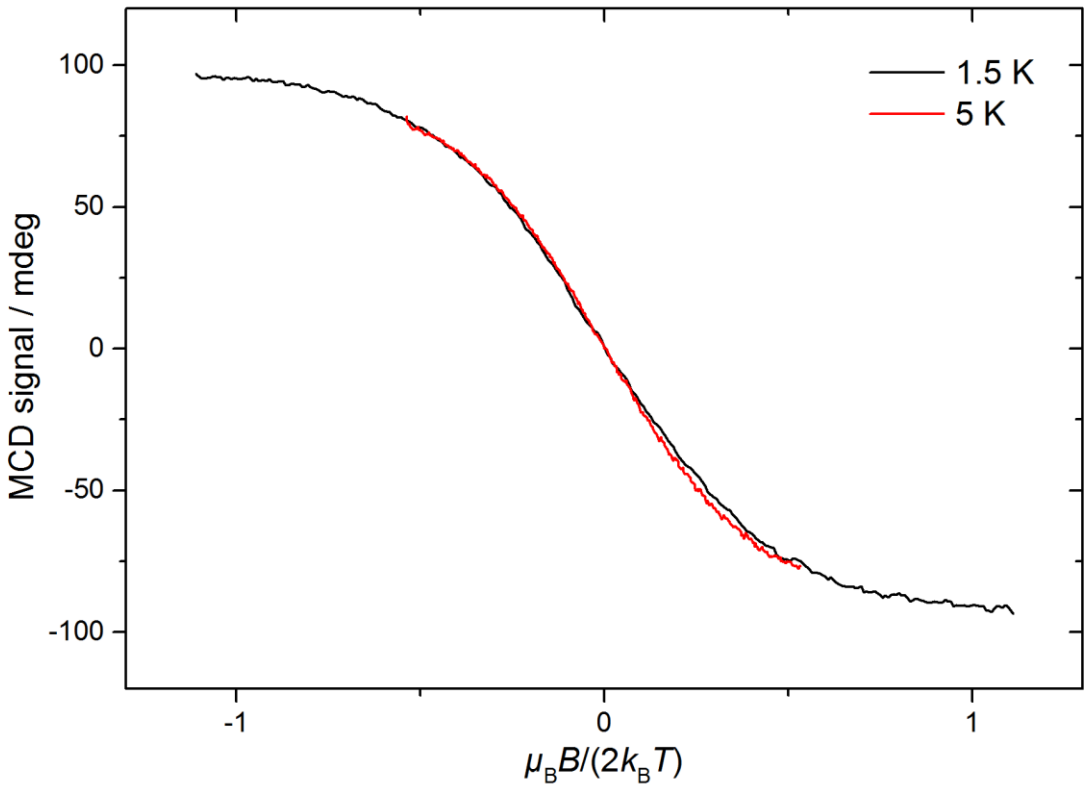

Figure S22. Plot of the MCD intensity at 1190 nm over the reduced magnetic field at 1.5 K and 5 K.

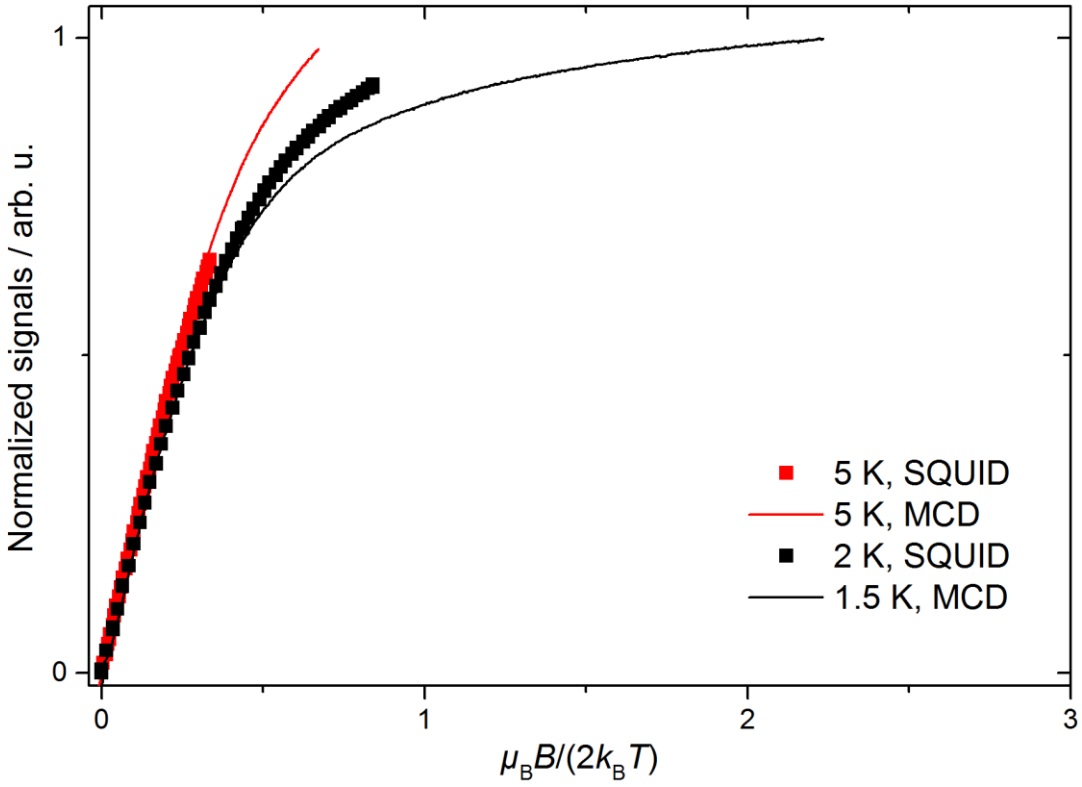

Figure S23. Comparison of normalized MCD intensities measured at 532 nm and magnetization curves acquired with SQUID magnetometry scaled to measurements at 5 K.

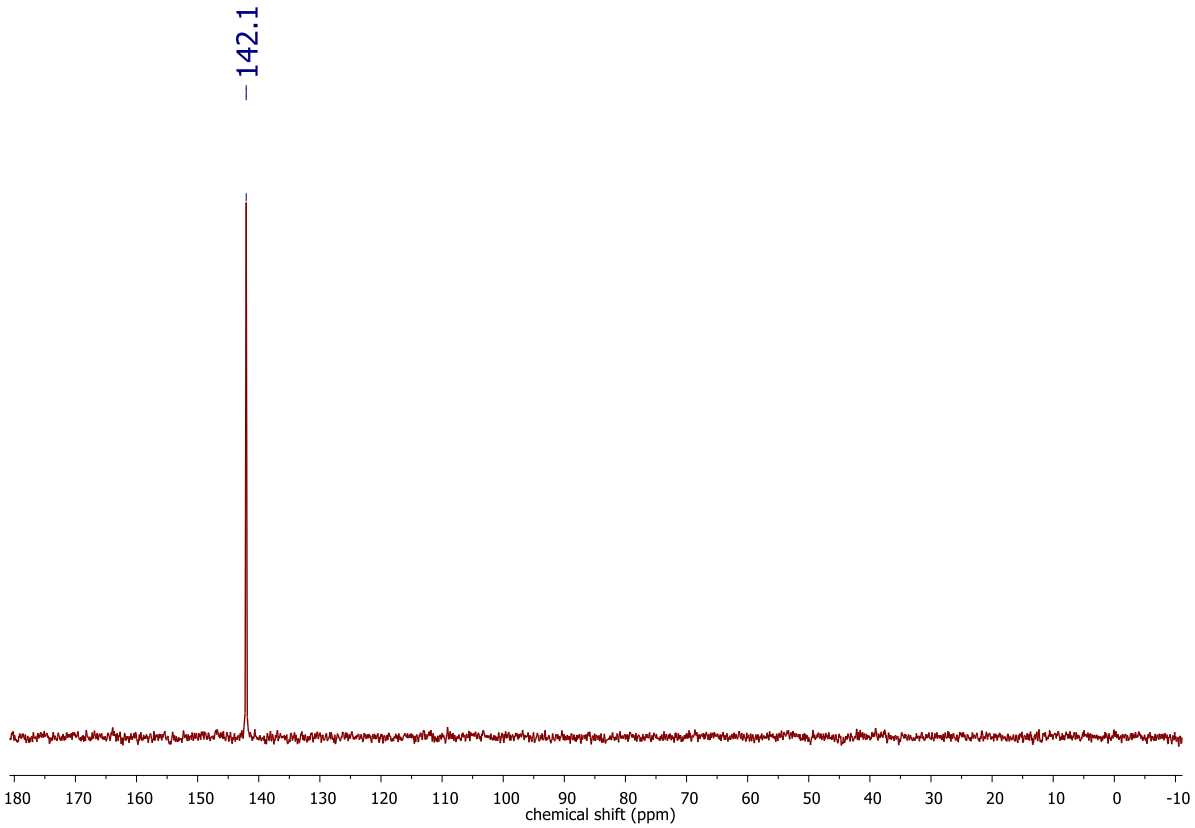

Figure S24. $^{31}P\{^{1}H\}$ NMR spectrum of **11** in d3-acetonitrile at -30 °C.

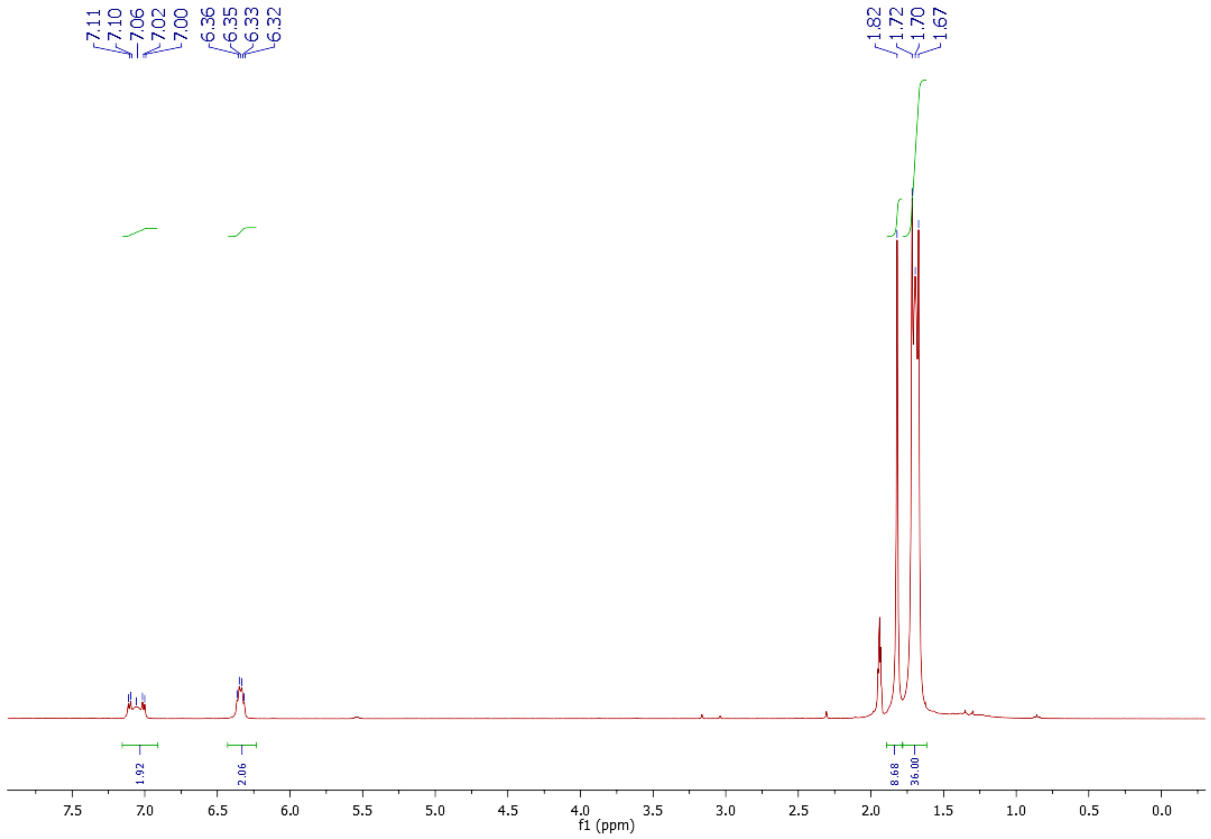

Figure S25. ^{1}H NMR spectrum of **11** in d3-acetonitrile at -30 °C.

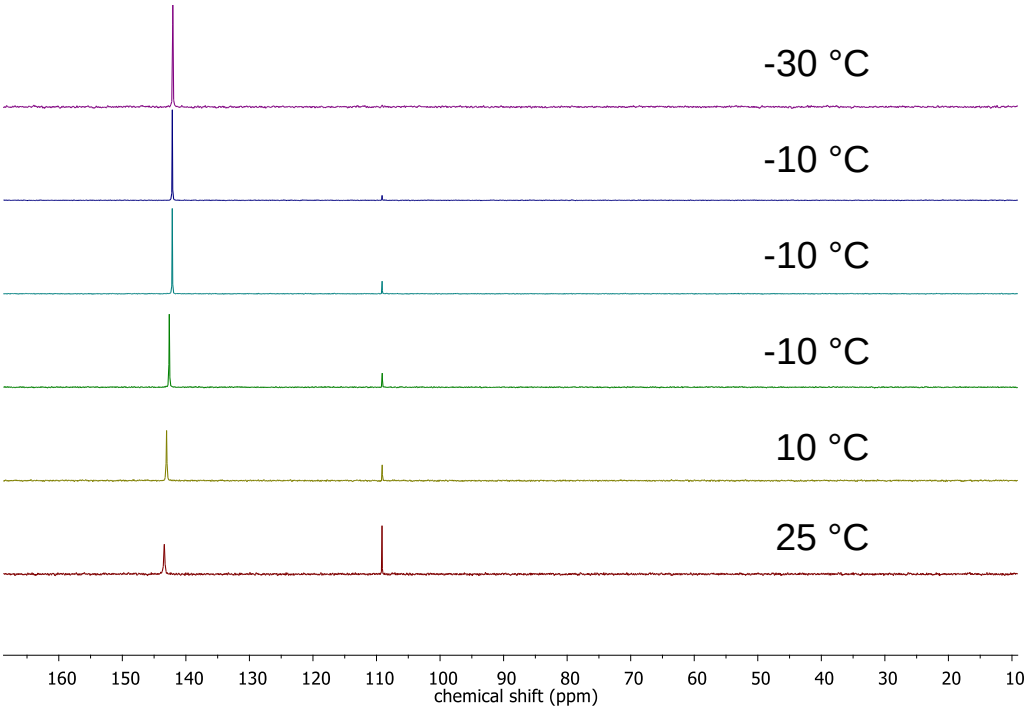

Figure S26. VT $^{31}P\{^{1}H\}$ spectra of **11** in d_3-acetonitrile from -30 °C to r.t.

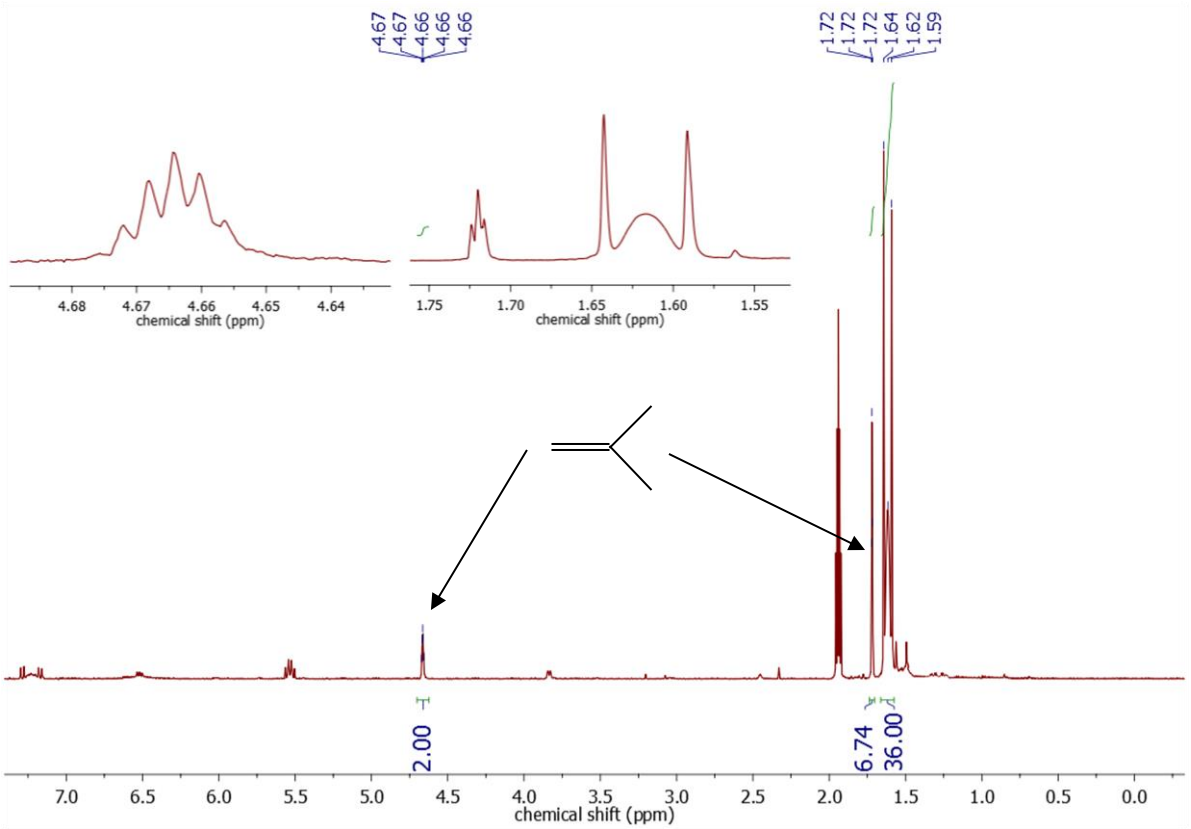

Figure S27. ^{1}H NMR spectrum at r.t. of solution of **11** in d_3-acetonitrile after 2 h showing formation of 1 eq of isobutene.

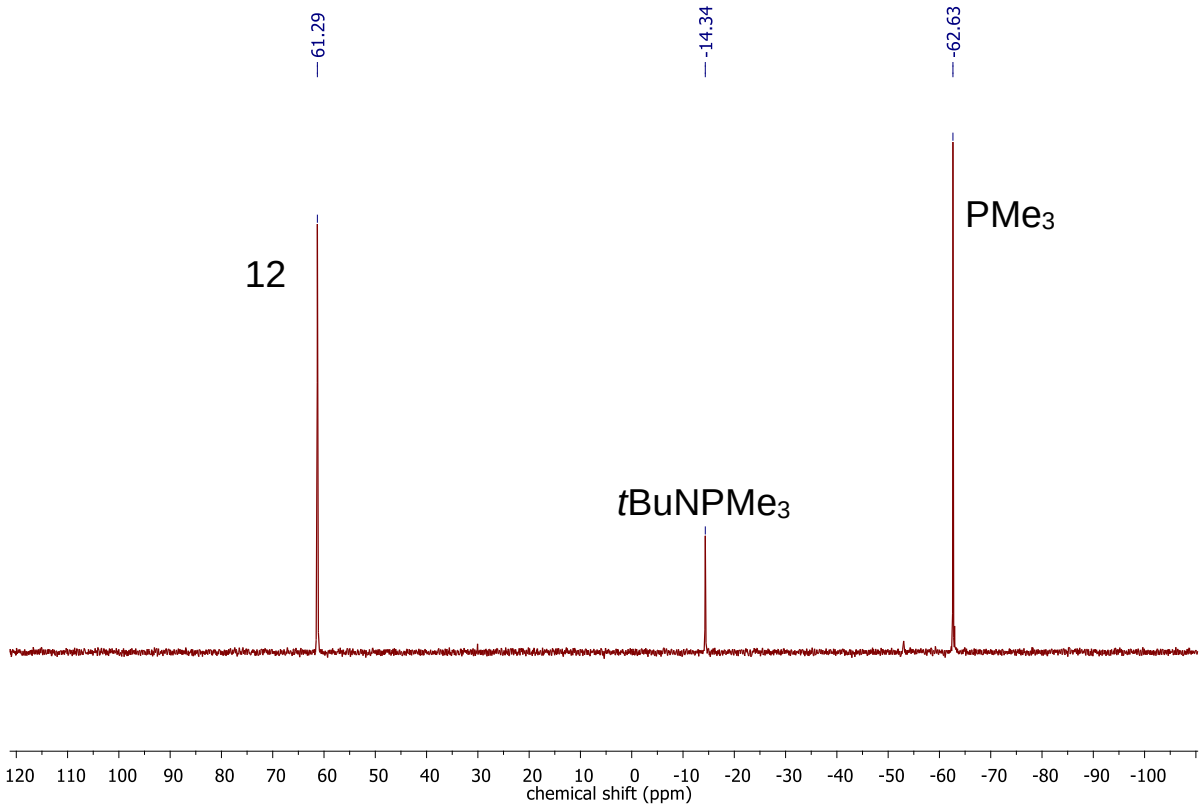

Figure S28. $^{31}P\{^{1}H\}$ NMR spectrum of reaction of **10** with PMe_3 in C_6D_6.

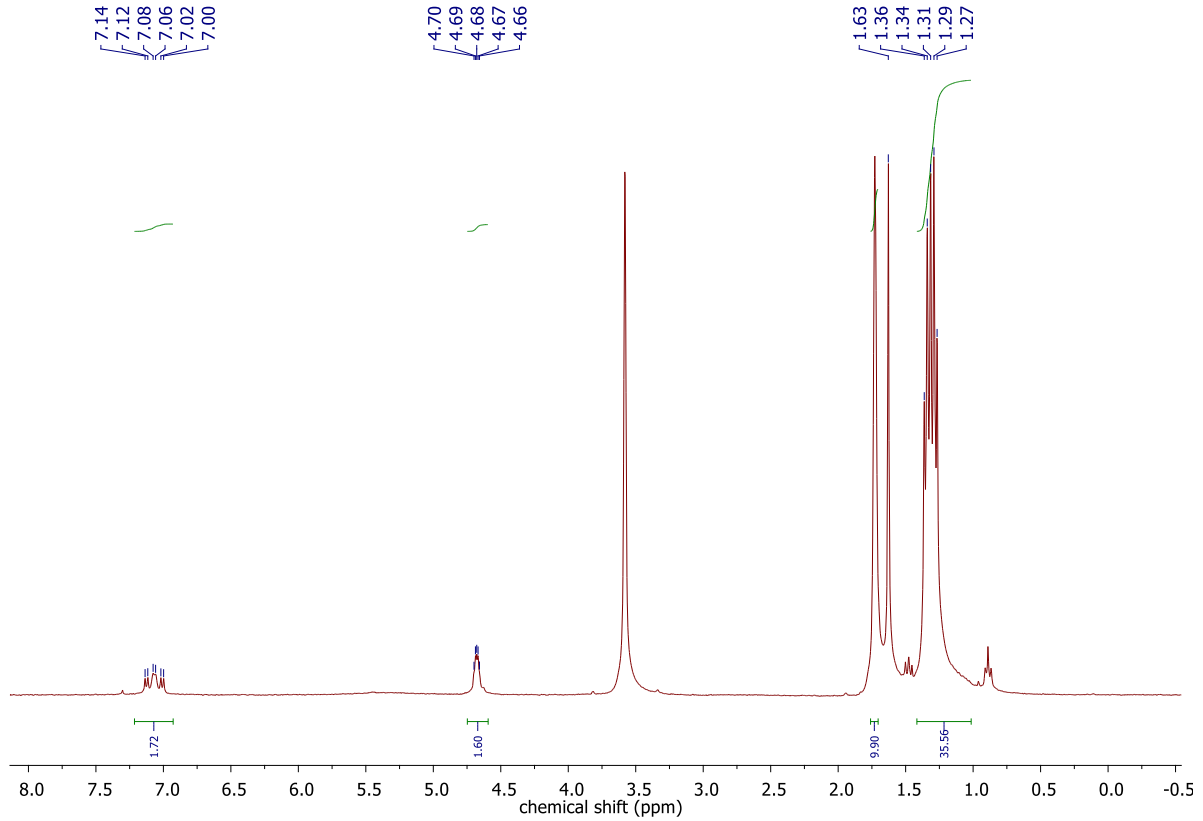

Figure S29. ^{1}H NMR spectrum of reaction product of **10** with CO_2 in d_8-THF.

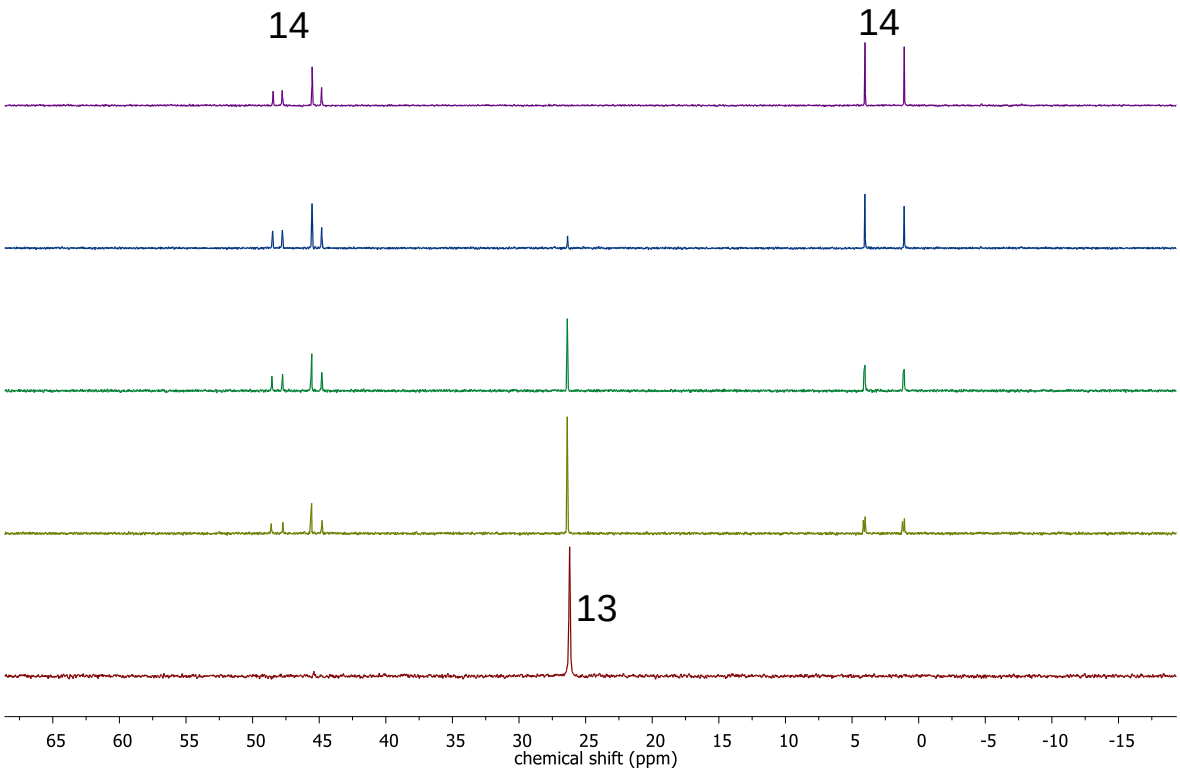

Figure S30. $^{31}P\{^{1}H\}$ NMR spectra of reaction product of **10** with CO_2 in C_6D_6 over 24h.

2 Computational details

2.1 Methods

Geometry optimizations of **9** were carried out with the Turbomole program package[12] coupled to the PQS Baker optimizer[13] via the BOpt package,[14] at the b3-lyp[15] level. We used the def2-TZVP basis set[16] (small-core pseudopotentials on Ir[17]) for the geometry optimizations together with a small grid (m4). Scalar relativistic effects were included implicitly through the use of the Ir ECPs. The optimized geometries were identified as minima through analysis of the eigenvalues of the Hessian matrix. EPR parameters[18] were calculated with the ADF[19] program system both at the BP86/TZP and at the b3-lyp/TZ2P level, using the coordinates from the structures optimized in Turbomole as input. ZORA basis sets as supplied with the ADF program were used. Three different sets of calculations were performed: Unrestricted SCALAR ZORA calculations for non-SOC corrected A-tensors; restricted SPINORBIT ZORA calculations for the g-tensors excluding spin polarization, and unrestricted SPINORBIT ZORA COLLINEAR calculations for the SOC corrected HFI-tensors and Zeeman corrected g-tensors. The molecular geometry of **10** was optimized also at the B3LYP/def2-TZVP level of theory, using the Gaussian09 program[20] (along with the D3 dispersion correction and the local correlation functional VWN5, as is also implemented in Turbomole).[21] Wiberg[22] and Mayer[23] bond orders were calculated from the Turbomole output files using the AOMix program[24] (compound **9**) and from Gaussian checkpoint files using the NBO6 program (compound **10**).[25]

Further calculations were conducted on two smaller model systems, in which the five *t*Bu groups of the pincer and the imido nitrogen were replaced by methyl groups (**10^{Me}**) or hydrogen atoms (**10^{H}**). To ensure a closest possible structural match in the ONIOM approach (see below) to the fully optimized geometry of the real system **10**, the model systems **10^{Me}** and **10^{H}** were constructed in constrained geometries where only the C-H or P-H / N-H bond lengths of the newly added hydrogen atoms (which replace the corresponding methyl or *t*Bu fragments of the five *t*Bu groups) were allowed to relax, i.e., all angles and dihedrals are kept fixed and all remaining coordinates are unaltered. Total energies for these model systems **10^{Me}** and **10^{H}** were computed using the Molpro program.[26] The coupled-cluster ansatz with single and double excitations and

perturbative triples, CCSD(T),[27] was employed in combination with the correlation-consistent polarized triple-zeta basis set cc-pVTZ(PP), which includes the relativistic pseudopotential of Figgen *et al.* (ECP60MDF) for iridium.[28] In order to reach a more reasonable estimate of the one-particle space, we also used the explicitly correlated variant, CCSD(T)-F12,[29] with the cc-pVTZ-F12 orbital and auxiliary basis sets[30] on non-metal atoms and the aug-cc-pVTZ-PP basis set on Ir;[28c] in combination with the corresponding auxiliary JKfit and MP2fit basis sets of Weigend[31] and Hill.[32] The explicitly correlated methods are, by construction, close to convergence towards the complete basis set limit already with double-zeta quality basis sets. Final energies are based on an ONIOM(F12:DFT) approach [see Lung Wa Chung, W. M. C. Sameera, Romain Ramozzi, Alister J. Page, Miho Hatanaka, Galina P. Petrova, Travis V. Harris, Xin Li, Zhuofeng Ke, Fengyi Liu, Hai-Bei Li, Lina Ding and Keiji Morokuma, *Chem. Rev.* 2015, **115**, 5678-5796 and references cited therein] according to, e.g.,

$$E_{\text{tot}}(\mathbf{10}) = E_{\text{CCSD(T)-F12}}(\mathbf{10^{Me}}) - E_{\text{B3LYP-D3}}(\mathbf{10^{Me}}) + E_{\text{B3LYP-D3}}(\mathbf{10})$$

Quasi-degenerate perturbation theory (QDPT) was used within the ORCA program[33,34] to calculate spin-orbit eigenstates for complex 10, based on the DFT-optimized geometry of the lowest-energy C_s-symmetric ^{3}A″ state. CASSCF wavefunctions were optimized employing the ZORA approximation[35] along with the ZORA-def2TZVP basis sets,[36] which include the segmented all-electron relativistically contracted SARC-ZORA-TZVPP basis set for iridium. The active space comprises the five Ir-based 5d orbitals and five occupied ligand-metal based orbitals, giving rise to a CAS(16,10) expansion. In the CASSCF calculations the orbitals were optimized by the average of 5 quintet, 45 triplet and 50 singlet roots arising from the formal d^6 configuration of the iridium(III) center. The RI and RIJCOSX[37] approximations were used along with the corresponding def2/JK auxiliary basis sets[31] and a fine grid (GridX6 in ORCA convention), respectively. The final energies are obtained from NEVPT2 calculations,[38,39,40] and the energies that enter the infinite-order QDPT treatment via a full SOMF operator[41] are thus corrected to second order (dynamic correlation).

2.2 Geometries, Energies and Electronic Structures

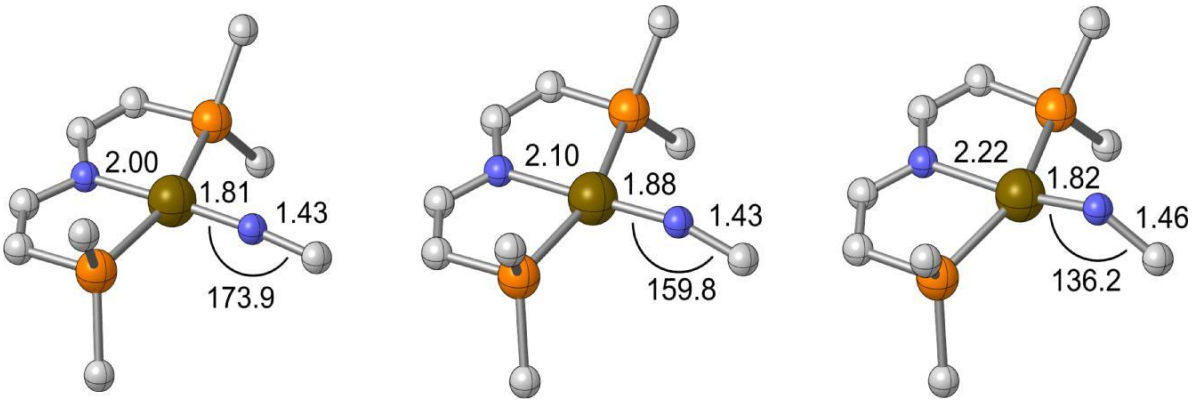

Complex **9** | **10** T: $^3A''$ (C_s) | **10** CSS: $^1A'$ (C_s)

Figure S31. DFT-optimized molecular geometries for **9** and the singlet and triplet isomers of **10**; *t*Bu groups and hydrogen atoms are omitted for clarity.

Table S3. Selected bond lengths, bond angles and computed bond orders (Wiberg/Mayer) of the DFT optimized geometries of **9** and **10**.

9					
Bond length	**(Å)**	**Wiberg**	**Mayer**	**Bond angle**	**(°)**
Ir-N(*t*Bu)	1.810	1.540	1.671	N_{PNP}-Ir-N(*t*Bu)	175.6
Ir-N_{PNP}	2.001	0.770	0.776	N_{PNP}-Ir-P_1	80.9
Ir-P_1	2.450	0.788	0.796	N_{PNP}-Ir-P_2	80.8
Ir-P_2	2.450	0.789	0.796	P_1-Ir-P_2	161.7
N-$C(Me)_3$	1.433	0.774	0.785	P_1-Ir-N(*t*Bu)	99.2
				P_2-Ir-N(*t*Bu)	99.2
				Ir-N-$C(Me)_3$	173.9

10 (triplet)					
Bond length	**(Å)**	**Wiberg**	**Mayer**	**Bond angle**	**(°)**
Ir-N(*t*Bu)	1.876	1.208	1.118	N_{PNP}-Ir-N(*t*Bu)	178.8
Ir-N_{PNP}	2.097	0.388	0.552	N_{PNP}-Ir-P_1	80.3
Ir-P_1	2.372	0.525	0.858	N_{PNP}-Ir-P_2	80.3
Ir-P_2	2.372	0.525	0.858	P_1-Ir-P_2	160.6
N-$C(Me)_3$	1.432	1.066	0.883	P_1-Ir-N(*t*Bu)	99.7
				P_2-Ir-N(*t*Bu)	99.7
				Ir-N-$C(Me)_3$	159.8

10 (CSS)					
Bond length	**(Å)**	**Wiberg**	**Mayer**	**Bond angle**	**(°)**
Ir-N(*t*Bu)	1.818	1.278	1.555	N_{PNP}-Ir-N(*t*Bu)	169.1
Ir-N_{PNP}	2.219	0.295	0.395	N_{PNP}-Ir-P_1	77.0
Ir-P_1	2.388	0.561	0.845	N_{PNP}-Ir-P_2	77.0
Ir-P_2	2.388	0.561	0.845	P_1-Ir-P_2	153.1
N-$C(Me)_3$	1.460	1.052	1.023	P_1-Ir-N(*t*Bu)	103.4
				P_2-Ir-N(*t*Bu)	103.4
				Ir-N-$C(Me)_3$	136.2

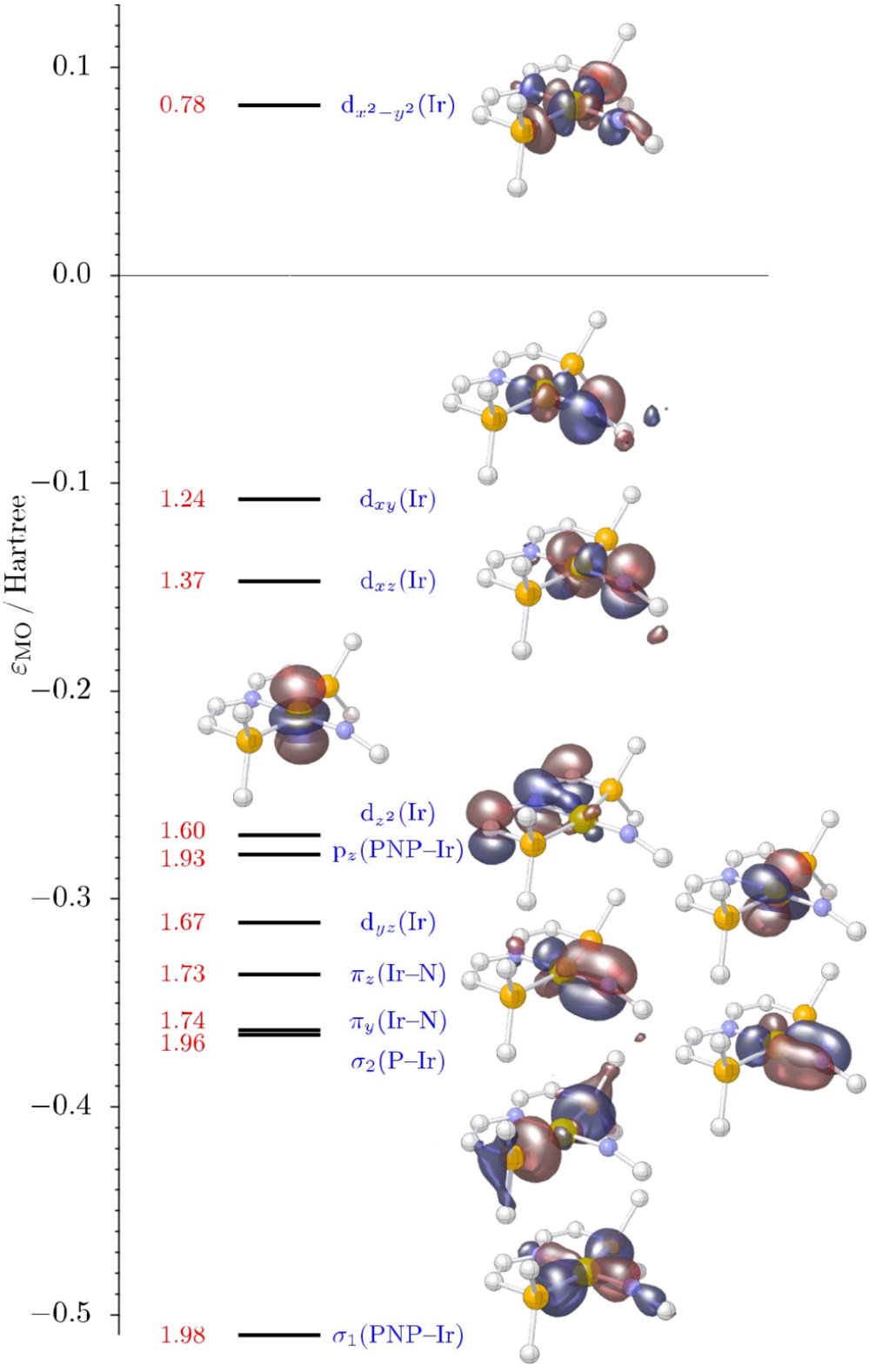

Figure S32. Active MO scheme computed at the DFT-optimized triplet geometry of **10** for a SA-CASSCF(16,10) wavefunction, state-averaged over the 5 quintet, 45 triplet, and 50 singlet CSFs, which arise from the local $5d^6$ configuration of the formal Ir^{III} center; average occupation numbers (red) and orbital labels (blue) with orbital plots at an isovalue of 0.05 $a_0^{-3/2}$ are also given.

Table S4. Total energies E_{tot} in Hartree and relative energies ΔE_{tot}(T/CSS) in kcal mol^{-1} for the triplet (T) and closed-shell singlet (CSS) states of the model systems **10**,**H**, **10**,**Me** and the full complex **10**, computed at the B3LYP-D3/def2-TZVP, CCSD(T)/cc-pVTZ, CCSD(T)-F12/VTZ-F12 and ONIOM(F12:DFT) levels.[a]

E_{tot}/Hartree			
B3LYP-D3/def2-TZVP	**10^{H}**	**10^{Me}**	**10**
T $^3A''$ (C_s)	-1054.246 880	-1250.803 043	-1840.346 035
CSS $^1A'$ (C_s)	-1054.231 023	-1250.791 004	-1840.334 556
CCSD(T)/cc-pVTZ	**10^{H}**	**10^{Me}**	
T $^3A''$ (C_s)	-1052.671 694	-1248.918 372	
CSS $^1A'$ (C_s)	-1052.664 222	-1248.914 419	
CCSD(T)-F12/VTZ-F12	**10^{H}**	**10^{Me}**	
T $^3A''$ (C_s)	-1052.866 997	-1249.190 213	
CSS $^1A'$ (C_s)	-1052.860 684	-1249.187 272	
ONIOM(F12:DFT)[a]	**10^{H}:10**	**10^{Me}:10**	
T $^3A''$ (C_s)	-1838.966 151	-1838.733 205	
CSS $^1A'$ (C_s)	-1838.964 217	-1838.730 824	

ΔE_{tot}(T/CSS)/kcal mol^{-1}			
	10^{H}	**10^{Me}**	**10**
B3LYP-D3/def2-TZVP	10.0	7.6	7.2
CCSD(T)/cc-pVTZ	4.7	2.5	
CCSD(T)-F12/VTZ-F12	4.0	1.8	
ONIOM(F12:DFT)[a]			1.2 (**10^{H}**:**10**)
			1.5 (**10^{Me}**:**10**)

[a]ONIOM(CCSD(T)-F12/VTZ-F12 : B3LYP-D3/def2-TZVP) energy on the full system employing the **10^{H}** and **10^{Me}** high-level system, respectively.

Table S5. Total energies E_{tot} in Hartree and relative energies ΔE_{tot}(T/CSS@T) in kcal mol^{-1} for the CSS states of the model system **10^{Me}** and of the full complex **10**, both computed at the corresponding DFT-optimized T geometries (α(Ir-N-tBu) = 159.8). Energies are computed at the B3LYP-D3/def2-TZVP, CCSD(T)-F12/VTZ-F12 and ONIOM(F12:DFT) levels.[a]

E_{tot}/Hartree			
CSS state at T geometry	**10^{Me}**	**10**	**10^{Me}:10**
B3LYP-D3/def2-TZVP	-1250.770 741	-1840.316 340	
CCSD(T)-F12/VTZ-F12	-1249.167 785		
ONIOM(F12:DFT)			-1838.713 384
ΔE_{tot}(T/CSS@T)/kcal mol^{-1}			
CSS state at T geometry	**10^{Me}**	**10**	**10^{Me}:10**
B3LYP-D3/def2-TZVP	20.3	18.6	
CCSD(T)-F12/VTZ-F12	14.1		
ONIOM(F12:DFT)			12.4

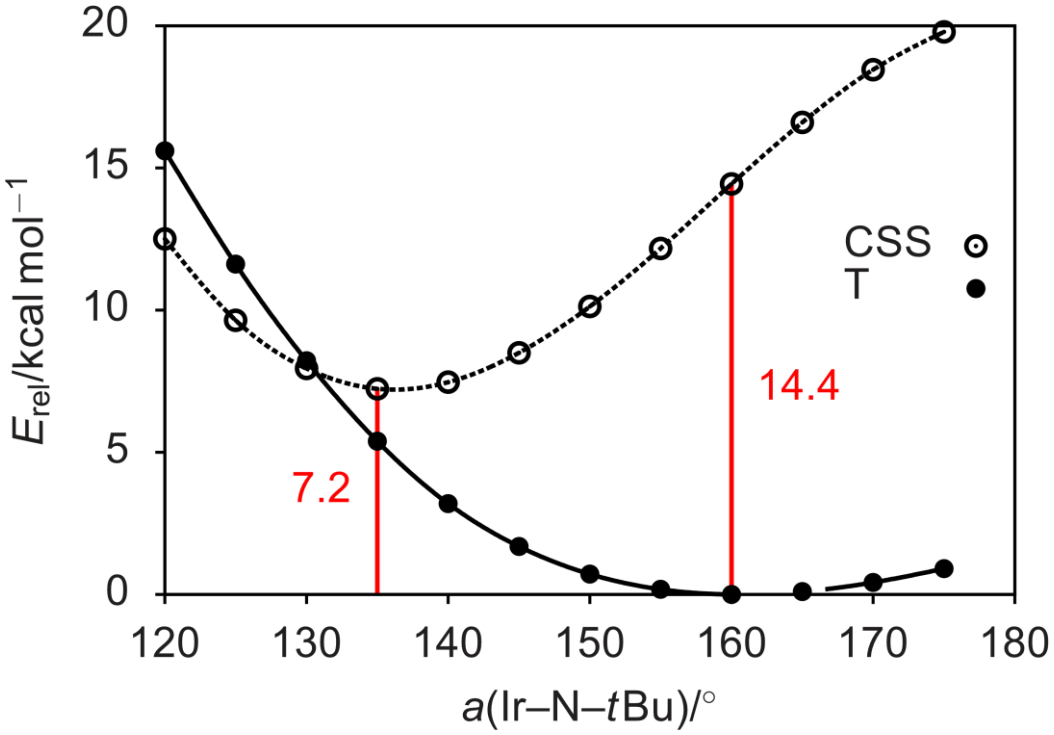

Figure S33. Relaxed potential energy scan (B3LYP-D3/def2-TZVP) along the Ir–N–*t*Bu angle for the triplet (solid) and closed-shell singlet (dashed) spin states of **10**. At the individually optimized geometries the triplet is 7.2 kcal mol^{-1} more stable than the singlet; with partially relaxed geometries fixed at an Ir–N–tBu angle of 160° the energy difference amounts to 14.4 kcal mol^{-1} (red bars in graph). If both spin states are computed at the triplet geometry, Δ*E*(T/CSS) = 18.6 kcal mol^{-1}.

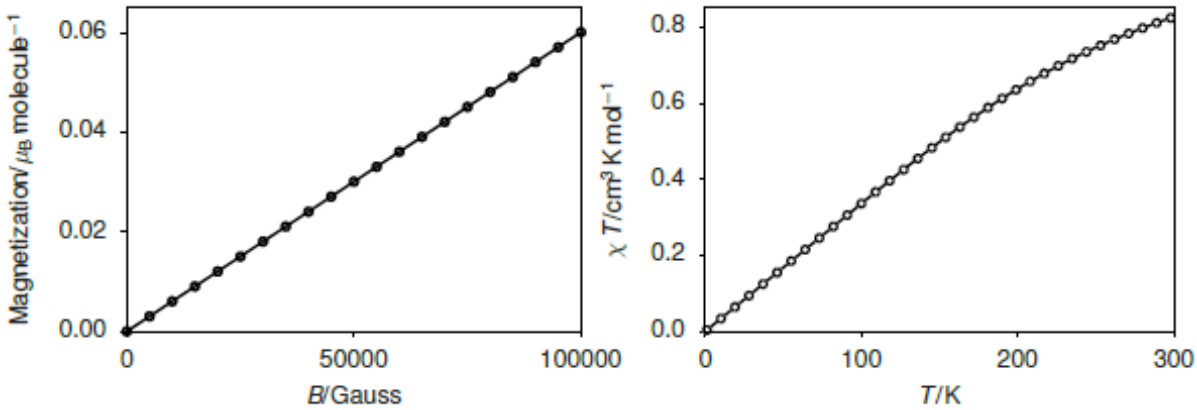

Figure S34. Magnetic properties from NEVPT2/SA-CASSCF(16,10)/def2TZVP(ZORA) calculations for 10: Magnetization in Bohr magnetons per molecule vs. magnetic field strength in Gauss (left), and magnetic susceptibility at 50 000 Gauss (right).

Table S6. State energies sorted by spin multiplicity ΔE_{state} and spin-orbit eigenvalues ΔE_{SOC} in cm^{-1} from NEVPT2/SA-CASSCF(16,10)/def2TZVP(ZORA) calculations for **10**.

		ΔE_{state}				ΔE_{state}		ΔE_{SOC}	
root	mult	CAS(16,10)	NEVPT2	root	mult	CAS(16,10)	NEVPT2	CAS(16,10)	NEVPT2
0	1	2769.1	4180.5	0	3	0.0	0.0	0.0	0.0
1	1	5086.7	5406.1	1	3	8327.9	12 678.2	497.7	450.7
2	1	7612.1	8964.2	2	3	14 107.8	18 946.2	506.4	457.9
3	1	9055.0	13 726.5	3	3	15 364.8	19 383.3	2875.7	4259.3
4	1	15 784.4	20 623.7	4	3	18 998.7	24 771.6	5554.0	5823.3
5	1	16 141.2	20 697.5	5	3	20 367.0	24 421.3	8261.9	9839.5
6	1	21 384.0	25 976.2	6	3	22 209.4	25 732.0	8948.9	12 854.6
7	1	22 450.8	26 114.1	7	3	24 087.9	25 162.1	9003.3	12 883.8
8	1	29 699.6	28 857.5	8	3	24 358.0	28 714.6	9393.1	12 907.4
9	1	30 268.2	29 097.3	9	3	26 664.6	26 414.5	9438.7	13 557.0
10	1	36 253.7	38 461.1	10	3	30 267.1	34 564.8	13 955.0	17 654.6
11	1	37 527.6	38 134.2	11	3	31 792.4	35 929.6	13 978.5	17 730.9
12	1	39 724.2	41 368.9	12	3	34 704.4	36 922.1	14 834.9	17 851.7
13	1	41 572.6	41 777.7	13	3	35 658.1	39 698.7	15 211.1	18 371.5
14	1	44 183.8	46 237.5	14	3	36 685.4	37 116.4	17 014.6	18 497.2
15	1	45 294.3	45 401.8	15	3	37 623.6	41 037.9	17 172.3	19 089.6
16	1	48 138.5	49 662.4	16	3	37 659.4	40 262.5	17 222.7	19 587.5
17	1	49 476.0	19 880.1	17	3	41 233.8	43 494.7	18 012.1	20 764.9
18	1	50 416.6	49 660.1	18	3	42 002.5	46 991.0	18 841.9	21 012.1
19	1	50 510.4	51 284.7	19	3	42 412.7	43 193.3	19 021.6	21 228.3
20	1	51 243.0	51 165.1	20	3	44 760.1	44 418.9	19 031.7	21 369.3
21	1	52 839.6	42 778.8	21	3	46 554.8	50 867.4	22 356.7	21 822.4
22	1	53 611.1	52 762.8	22	3	47 074.7	47 983.0	23 793.5	23 136.6
23	1	55 472.5	32 498.6	23	3	48 302.0	51 625.5	24 121.9	23 413.3
24	1	55 835.5	60 238.2	24	3	49 593.6	16 365.8	24 257.1	23 634.1
25	1	56 088.4	63 062.5	25	3	50 351.3	53 813.6	24 306.0	25 058.4
26	1	57 536.7	52 873.5	26	3	51 108.1	57 015.7	24 463.2	25 284.9

27	1	57 918.2	47 483.6	27	3	52 517.4	59 108.7	24 556.7	25 437.9
28	1	58 352.2	62 614.6	28	3	52 614.8	53 263.9	24 800.7	25 753.3
29	1	58 709.0	49 887.5	29	3	53 033.7	54 712.8	24 830.0	26 297.8
30	1	58 905.7	63 219.8	30	3	53 677.9	58 750.8	24 905.6	27 285.6
31	1	60 157.8	56 692.3	31	3	54 314.9	58 947.1	25 138.8	27 429.0
32	1	60 886.2	61 925.3	32	3	54 405.1	58 499.4	25 830.6	27 781.8
33	1	61 525.4	47 179.3	33	3	54 767.1	27 879.7	26 156.1	27 905.7
34	1	61 647.1	54 502.5	34	3	55 955.3	55 607.9	26 301.6	28 222.5
35	1	61 814.8	66 083.6	35	3	56 121.6	60 164.1	26 415.2	28 301.5
36	1	62 825.3	64 573.0	36	3	56 613.1	62 207.6	26 514.4	28 696.7
37	1	63 506.0	63 266.1	37	3	56 967.3	62 064.9	26 561.3	28 899.4
38	1	63 556.6	65 182.1	38	3	57 125.9	57 639.8	27 487.7	29 168.8
39	1	64 199.7	66 560.0	39	3	57 818.9	46 169.2	27 735.3	29 472.2
40	1	64 579.2	67 270.8	40	3	57 956.0	34 451.9	28 326.4	29 577.8
41	1	65 630.0	70 770.2	41	3	58 139.6	57 728.8	28 634.4	29 634.4
42	1	65 913.4	68 134.6	42	3	58 855.2	60 188.2	29 115.1	29 749.6
43	1	66 311.9	41 998.3	43	3	59 516.6	63 385.3	29 609.5	29 988.1
44	1	67 526.5	38 423.6	44	3	60 009.0	48 595.8	30 054.6	30 320.3
45	1	68 230.2	66 325.8	0	5	26 945.9	30 164.4	30 311.7	30 341.7
46	1	68 684.7	38 188.2	1	5	30 245.5	33 474.7	31 254.6	30 415.7
47	1	69 799.5	58 624.6	2	5	39 042.9	41 375.0	31 280.5	30 419.9
48	1	70 436.1	58 843.0	3	5	39 127.9	45 286.6	31 595.8	30 629.8
49	1	70 549.4	49 705.8	4	5	45 692.7	55 761.4	. . .	. . .

Table S7. Cartesian coordinates of DFT geometries (Å) for 9, 10, 10^{Me} and 10^{H}

78
Complex 9

Ir	0.8428411	4.3489227	10.0418002
P	-0.7209655	3.6275893	11.7846309
P	2.4703699	5.6797798	8.7825506
N	0.9072351	5.9678285	11.2168055
N	0.6813209	2.9447214	8.9113412
C	0.1481664	6.0785176	12.3819925
C	-0.6587786	5.1037453	12.8054898
C	-2.5734594	3.4989526	11.3295363
C	-3.4872575	3.815962	12.5280137
C	-2.935809	2.1173816	10.7730176
C	-2.8170585	4.5663302	10.2466939
C	-0.0981436	2.2475268	12.9408578
C	1.2553513	2.7282874	13.4977732
C	-1.0560517	1.9832176	14.1127527
C	0.1370432	0.94799	12.16104
C	1.6989222	7.0775867	10.9206269
C	2.4861763	7.1279413	9.8442976
C	4.2706585	5.0577226	8.8330272
C	4.6307001	4.8989524	10.3224451
C	5.2539936	6.043106	8.1824533
C	4.3921969	3.6846358	8.1605454
C	1.9299364	6.3928524	7.093006
C	2.6055199	7.7438544	6.7928785
C	2.2128776	5.4225122	5.9405613
C	0.4124543	6.6306387	7.2009137
C	0.4423783	1.9120572	7.9469995
C	0.0530888	0.5872354	8.6370549
C	1.7050192	1.6409597	7.1013998
C	-0.7111123	2.3833687	7.0298949
H	0.2550081	7.0061429	12.9363432
H	-1.2226754	5.2154875	13.7197274
H	-3.3325444	4.8254482	12.9073018
H	-4.5244278	3.7545766	12.1879469
H	-3.3753203	3.113621	13.3511819
H	-3.9778266	2.133462	10.4432716
H	-2.3277266	1.8527114	9.9096985
H	-2.8454984	1.3283636	11.51928
H	-2.561286	5.5667516	10.5993721
H	-2.2448997	4.3684212	9.3408371
H	-3.8789123	4.5686627	9.9870511
H	1.688205	1.9244133	14.0981831
H	1.9616252	2.9646448	12.7001553
H	1.151177	3.6038866	14.1374648
H	-1.2899323	2.8868376	14.6766486
H	-1.9891272	1.5209764	13.7922216
H	-0.5728762	1.2870993	14.80344
H	0.5280835	0.1927636	12.847615
H	-0.7743985	0.5462025	11.7215985
H	0.871159	1.0899209	11.3696457

H	1.6463482	7.904103	11.6229125
H	3.0974732	7.9968988	9.6506415
H	3.9371838	4.2329315	10.8386332
H	5.6289175	4.4599697	10.3930912
H	4.6478185	5.8536264	10.8470149
H	6.2715577	5.6895623	8.3690662
H	5.1288628	6.1045979	7.1019024
H	5.1804099	7.0479846	8.5999859
H	3.7607596	2.9467224	8.6525148
H	4.1404436	3.7071352	7.1016326
H	5.4277696	3.3444387	8.2419187
H	3.6883269	7.674757	6.7138739
H	2.2322065	8.1023866	5.8299935
H	2.3577574	8.5011034	7.5358271
H	1.7448941	4.4523568	6.09855
H	1.7950751	5.8382025	5.0200122
H	3.2790622	5.2723887	5.7721339
H	0.1658303	7.3087875	8.0193896
H	0.0612266	7.0903193	6.2734503
H	-0.1376866	5.7022786	7.3509328
H	-0.8383576	0.6938305	9.248782
H	-0.1475043	-0.1624803	7.870396
H	0.8664215	0.2223769	9.2626507
H	2.5200015	1.2792031	7.7267999
H	1.4754951	0.8700848	6.3643915
H	2.0378704	2.5288437	6.5711651
H	-1.6235553	2.5552702	7.5997347
H	-0.4491406	3.3023824	6.5069242
H	-0.9098865	1.6093729	6.287307

78

10 CSS: ^{1}A' (C_S): E(B3LYP-D3/def2-TZVP) = -1840.33455625

Ir	-0.100059829641	-0.137212601302	0.000000000000
P	-0.611407016584	0.081037208155	2.322508435562
P	-0.611407016584	0.081037208155	-2.322508435562
N	-2.295424203818	0.184843181801	0.000000000000
N	1.616751672236	-0.735384009975	0.000000000000
C	-2.984536577103	0.305529985217	-1.159217062320
C	-2.374661766330	0.281641785150	-2.365359968492
C	0.046435101887	1.609280345216	-3.251010766178
C	-0.065140870768	2.769113516533	-2.243959620985
C	-0.808326512020	1.969965112847	-4.479735475853
C	1.503801514224	1.442850350060	-3.690746670855
C	-0.292476298107	-1.543515252494	-3.275907037366
C	-1.154732005445	-2.607362627613	-2.569064344740
C	1.168798270499	-1.990222246651	-3.190644287967
C	-0.722143801113	-1.445995231658	-4.746303874355
C	-2.984536577103	0.305529985217	1.159217062320
C	-2.374661766330	0.281641785150	2.365359968492
C	0.046435101887	1.609280345216	3.251010766178
C	-0.808326512020	1.969965112847	4.479735475853
C	-0.065140870768	2.769113516533	2.243959620985
C	1.503801514224	1.442850350060	3.690746670855
C	-0.292476298107	-1.543515252494	3.275907037366
C	-1.154732005445	-2.607362627613	2.569064344740
C	-0.722143801113	-1.445995231658	4.746303874355
C	1.168798270499	-1.990222246651	3.190644287967
C	2.944499677249	-0.127904843001	0.000000000000
C	3.694334291245	-0.671848124027	1.235937500024
C	3.694334291245	-0.671848124027	-1.235937500024
C	2.997948482764	1.407172902043	0.000000000000
H	-4.064889547960	0.433560244686	-1.087955059884
H	-2.936915564793	0.367764702498	-3.282582141802
H	0.268927128656	3.694884074760	-2.722763809259
H	0.536890653779	2.593005601998	-1.354623997830
H	-1.097255118824	2.906712808455	-1.917753543291
H	-1.841573542083	2.179949515689	-4.205075743967
H	-0.803908392636	1.195339642934	-5.243871255187
H	-0.398324223698	2.878100167504	-4.932004113731
H	1.879422211484	2.397734612898	-4.070412895330
H	1.607904629306	0.709993688900	-4.491193425937
H	2.144470111261	1.143006410626	-2.865778257742
H	-2.218736433706	-2.383745518113	-2.642014789949
H	-0.896472656636	-2.685002209064	-1.511761851057
H	-0.972825255127	-3.577429795039	-3.041124970509
H	1.847801531850	-1.307336873684	-3.698045873257
H	1.269984101823	-2.967213567866	-3.673123483990
H	1.485132058837	-2.092415996694	-2.154087911720
H	-1.747856358934	-1.089823706658	-4.852925461203
H	-0.671727629270	-2.441253927877	-5.198377553938
H	-0.065282645330	-0.795808777020	-5.324345520719
H	-4.064889547960	0.433560244686	1.087955059884
H	-2.936915564793	0.367764702498	3.282582141802
H	-0.398324223698	2.878100167504	4.932004113731
H	-0.803908392636	1.195339642934	5.243871255187
H	-1.841573542083	2.179949515689	4.205075743967

H	-1.097255118824	2.906712808455	1.917753543291
H	0.536890653779	2.593005601998	1.354623997830
H	0.268927128656	3.694884074760	2.722763809259
H	2.144470111261	1.143006410626	2.865778257742
H	1.607904629306	0.709993688900	4.491193425937
H	1.879422211484	2.397734612898	4.070412895330
H	-2.218736433706	-2.383745518113	2.642014789949
H	-0.972825255127	-3.577429795039	3.041124970509
H	-0.896472656636	-2.685002209064	1.511761851057
H	-0.065282645330	-0.795808777020	5.324345520719
H	-0.671727629270	-2.441253927877	5.198377553938
H	-1.747856358934	-1.089823706658	4.852925461203
H	1.485132058837	-2.092415996694	2.154087911720
H	1.269984101823	-2.967213567866	3.673123483990
H	1.847801531850	-1.307336873684	3.698045873257
H	4.728890432064	-0.322038375191	1.213122194001
H	3.691800681565	-1.761653540284	1.236972833440
H	3.241346119786	-0.329384224057	2.161608751375
H	3.241346119786	-0.329384224057	-2.161608751375
H	3.691800681565	-1.761653540284	-1.236972833440
H	4.728890432064	-0.322038375191	-1.213122194001
H	2.499861494211	1.812622894010	-0.877698311606
H	4.033292406013	1.760044440750	0.000000000000
H	2.499861494211	1.812622894010	0.877698311606

33

10^{Me} CSS: ^{1}A' (C_S): E(B3LYP-D3/def2-TZVP) = -1250.79100385

Ir	-0.1000598296	-0.1372126013	0.0000000000
P	-0.6114070166	0.0810372082	2.3225084356
P	-0.6114070166	0.0810372082	-2.3225084356
N	-2.2954242038	0.1848431818	0.0000000000
N	1.6167516722	-0.7353840100	0.0000000000
C	-2.9845365771	0.3055299852	-1.1592170623
C	-2.3746617663	0.2816417851	-2.3653599685
C	0.0464351019	1.6092803452	-3.2510107662
H	-0.0324412706	2.4292008982	-2.5390963699
H	-0.5594246444	1.8649356978	-4.1219376173
H	1.0845523157	1.4907282492	-3.5642452475
C	-0.2924762981	-1.5435152525	-3.2759070374
H	-0.9017581039	-2.2952445182	-2.7764422168
H	0.7483227057	-1.8616842020	-3.2151782828
H	-0.5980710125	-1.4741555669	-4.3217052380
C	-2.9845365771	0.3055299852	1.1592170623
C	-2.3746617663	0.2816417852	2.3653599685
C	0.0464351019	1.6092803452	3.2510107662
H	-0.5594246444	1.8649356978	4.1219376173
H	-0.0324412706	2.4292008982	2.5390963699
H	1.0845523157	1.4907282492	3.5642452475
C	-0.2924762981	-1.5435152525	3.2759070374
H	-0.9017581039	-2.2952445182	2.7764422168
H	-0.5980710125	-1.4741555669	4.3217052380
H	0.7483227057	-1.8616842020	3.2151782828
C	2.9444996772	-0.1279048430	0.0000000000
H	3.4768848497	-0.5141064561	0.8775199048
H	3.4768848497	-0.5141064561	-0.8775199048
H	2.9826600047	0.9680797889	0.0000000000
H	-4.0648895480	0.4335602447	-1.0879550599
H	-2.9369155648	0.3677647025	-3.2825821418
H	-4.0648895480	0.4335602447	1.0879550599
H	-2.9369155648	0.3677647025	3.2825821418

18

10^{H} CSS: ^{1}A' (C_S): E(B3LYP-D3/def2-TZVP) = -1054.23102325

Ir	-0.1000598296	-0.1372126013	0.0000000000
P	-0.6114070166	0.0810372082	2.3225084356
P	-0.6114070166	0.0810372082	-2.3225084356
N	-2.2954242038	0.1848431818	0.0000000000
N	1.6167516722	-0.7353840100	0.0000000000
C	-2.9845365771	0.3055299852	-1.1592170623
C	-2.3746617663	0.2816417852	-2.3653599685
H	-0.1251876391	1.2105809176	-3.0087761775
H	-0.3764278291	-1.1158873747	-3.0249457230
C	-2.9845365771	0.3055299852	1.1592170623
C	-2.3746617663	0.2816417852	2.3653599685
H	-0.1251876391	1.2105809176	3.0087761775
H	-0.3764278291	-1.1158873747	3.0249457230
H	2.5536648941	-0.3067218983	0.0000000000
H	-4.0648895480	0.4335602447	-1.0879550599
H	-2.9369155648	0.3677647025	-3.2825821418
H	-4.0648895480	0.4335602447	1.0879550599
H	-2.9369155648	0.3677647025	3.2825821418

78

10 triplet: $^3A''$ (C_S): E(B3LYP-D3/def2-TZVP) = -1840.34603470

Ir	0.193210489535	-0.008666965712	0.000000000000
P	0.588388102803	-0.070722172510	2.338040753440
P	0.588388102803	-0.070722172510	-2.338040753440
N	2.243384740065	-0.449022548957	0.000000000000
N	-1.632442482625	0.421990198706	0.000000000000
C	2.928787304275	-0.583609160767	-1.173915137527
C	2.337600748559	-0.444787606992	-2.378627499739
C	-0.183488694052	-1.492037252485	-3.345726434281
C	-0.164135873721	-2.708418424201	-2.399813868861
C	0.623644276361	-1.852749035780	-4.604479652581
C	-1.631854061047	-1.192751818943	-3.741151012780
C	0.430038394728	1.609966728432	-3.214353830454
C	1.406531160240	2.550931152655	-2.482346261251
C	-0.986303954772	2.171881879914	-3.042699976193
C	0.801202131706	1.562156494380	-4.701312468823
C	2.928787304275	-0.583609160767	1.173915137527
C	2.337600748559	-0.444787606992	2.378627499739
C	-0.183488694052	-1.492037252485	3.345726434281
C	0.623644276361	-1.852749035780	4.604479652581
C	-0.164135873721	-2.708418424201	2.399813868861
C	-1.631854061047	-1.192751818943	3.741151012780
C	0.430038394728	1.609966728432	3.214353830454
C	1.406531160240	2.550931152655	2.482346261251
C	0.801202131706	1.562156494380	4.701312468823
C	-0.986303954772	2.171881879914	3.042699976193
C	-3.053787245108	0.249369615325	0.000000000000
C	-3.683515029484	0.925686868877	1.238308826969
C	-3.683515029484	0.925686868877	-1.238308826969
C	-3.402084701935	-1.253732018490	0.000000000000
H	3.992147738221	-0.807795619852	-1.098228890606
H	2.909111215518	-0.542650113666	-3.289659991781
H	-0.563265110333	-3.580347551110	-2.927711792765
H	-0.765834023200	-2.532768884000	-1.508582215151
H	0.850961051335	-2.943420848719	-2.075180461441
H	1.643241167809	-2.148510155096	-4.358600597938
H	0.664520366297	-1.042149380656	-5.329398793285
H	0.144961733963	-2.706057765492	-5.095074217569
H	-2.077532578706	-2.086115127459	-4.189033288608
H	-1.703006936346	-0.389282797206	-4.474422413010
H	-2.232391694772	-0.925142363334	-2.875128429773
H	2.443418355267	2.242254861602	-2.614020569402
H	1.196347806976	2.584011768598	-1.411906497335
H	1.293834470783	3.561336239439	-2.886730547680
H	-1.737373917082	1.582833877022	-3.566073223087
H	-1.022390609379	3.186375396494	-3.451864734152
H	-1.259999172781	2.216099399040	-1.989748123259
H	1.787897590799	1.124995548703	-4.864330581396
H	0.823673573117	2.581678410522	-5.099055438574
H	0.072838801227	1.002292063795	-5.287903756081
H	3.992147738221	-0.807795619852	1.098228890606
H	2.909111215518	-0.542650113666	3.289659991781
H	0.144961733963	-2.706057765492	5.095074217569
H	0.664520366297	-1.042149380656	5.329398793285
H	1.643241167809	-2.148510155096	4.358600597938

H	0.850961051335	-2.943420848719	2.075180461441
H	-0.765834023200	-2.532768884000	1.508582215151
H	-0.563265110333	-3.580347551110	2.927711792765
H	-2.232391694772	-0.925142363334	2.875128429773
H	-1.703006936346	-0.389282797206	4.474422413010
H	-2.077532578706	-2.086115127459	4.189033288608
H	2.443418355267	2.242254861602	2.614020569402
H	1.293834470783	3.561336239439	2.886730547680
H	1.196347806976	2.584011768598	1.411906497335
H	0.072838801227	1.002292063795	5.287903756081
H	0.823673573117	2.581678410522	5.099055438574
H	1.787897590799	1.124995548703	4.864330581396
H	-1.259999172781	2.216099399040	1.989748123259
H	-1.022390609379	3.186375396494	3.451864734152
H	-1.737373917082	1.582833877022	3.566073223087
H	-4.766761574701	0.783078660156	1.226921339473
H	-3.476622185212	1.996008621839	1.233050551600
H	-3.295765535569	0.510424625415	2.163749738194
H	-3.295765535569	0.510424625415	-2.163749738194
H	-3.476622185212	1.996008621839	-1.233050551600
H	-4.766761574701	0.783078660156	-1.226921339473
H	-2.985519559346	-1.741960718983	-0.880585997752
H	-4.485273679382	-1.401191789290	0.000000000000
H	-2.985519559346	-1.741960718983	0.880585997752

33

10^{Me} triplet: $^3A''$ (C_S): E(B3LYP-D3/def2-TZVP) = -1250.80304263

Ir	0.1932104895	-0.0086669657	0.0000000000
P	0.5883881028	-0.0707221725	2.3380407534
P	0.5883881028	-0.0707221725	-2.3380407534
N	2.2433847401	-0.4490225490	0.0000000000
N	-1.6324424826	0.4219901987	0.0000000000
C	2.9287873043	-0.5836091608	-1.1739151375
C	2.3376007486	-0.4447876070	-2.3786274997
C	-0.1834886941	-1.4920372525	-3.3457264343
H	-0.1698091188	-2.3518384315	-2.6771064672
H	0.3889618835	-1.7478682943	-4.2384839268
H	-1.2155835974	-1.2787685720	-3.6275031886
C	0.4300383947	1.6099667284	-3.2143538305
H	1.1202156667	2.2750328531	-2.6969767386
H	-0.5768315116	2.0094290873	-3.0923260593
H	0.6942326244	1.5759354191	-4.2727705152
C	2.9287873043	-0.5836091608	1.1739151375
C	2.3376007486	-0.4447876070	2.3786274997
C	-0.1834886941	-1.4920372525	3.3457264343
H	0.3889618835	-1.7478682943	4.2384839268
H	-0.1698091188	-2.3518384315	2.6771064672
H	-1.2155835974	-1.2787685720	3.6275031886
C	0.4300383947	1.6099667284	3.2143538305
H	1.1202156667	2.2750328531	2.6969767386
H	0.6942326244	1.5759354191	4.2727705152
H	-0.5768315116	2.0094290873	3.0923260593
C	-3.0537872451	0.2493696153	0.0000000000
H	-3.5018007815	0.7305287638	0.8809824348
H	-3.5018007815	0.7305287638	-0.8809824348
H	-3.3015634576	-0.8199256739	0.0000000000
H	3.9921477382	-0.8077956199	-1.0982288906
H	2.9091112155	-0.5426501137	-3.2896599918
H	3.9921477382	-0.8077956199	1.0982288906
H	2.9091112155	-0.5426501137	3.2896599918

18

10^{H} triplet: $^3A''$ (C_S): E(B3LYP-D3/def2-TZVP) = -1054.24688032

Ir	0.1932104895	-0.0086669657	0.0000000000
P	0.5883881028	-0.0707221725	2.3380407534
P	0.5883881028	-0.0707221725	-2.3380407534
N	2.2433847401	-0.4490225490	0.0000000000
N	-1.6324424826	0.4219901987	0.0000000000
C	2.9287873043	-0.5836091608	-1.1739151375
C	2.3376007486	-0.4447876070	-2.3786274997
H	0.0177109811	-1.1215530851	-3.0830601222
H	0.4711081194	1.1740617223	-2.9870724716
C	2.9287873043	-0.5836091608	1.1739151375
C	2.3376007486	-0.4447876070	2.3786274997
H	0.0177109811	-1.1215530851	3.0830601222
H	0.4711081194	1.1740617223	2.9870724716
H	-2.6360354025	0.3001050658	0.0000000000
H	3.9921477382	-0.8077956199	-1.0982288906
H	2.9091112155	-0.5426501137	-3.2896599918
H	3.9921477382	-0.8077956199	1.0982288906
H	2.9091112155	-0.5426501137	3.2896599918

3 Crystallographic details

3.1 Crystallographic Details

CCDC-1546382 (**9**), CCDC-1546383 (**10**), CCDC-1546384 (**13**), CCDC-1546385 (**14**) contain the supplementary crystallographic data for this paper. This data can be obtained free of charge via http://www.ccdc.cam.ac.uk/ products/csd/request/ (or from Cambridge Crystallographic Data Centre, 12 Union Road, Cambridge, CB2 1EZ, UK. Fax: +44-1223- 336-033; e-mail: deposit@ccdc.cam.ac.uk).

Suitable single crystals for X-ray structure determination were selected from the mother liquor under an inert gas atmosphere and transferred in protective perfluoro polyether oil on a microscope slide. The selected and mounted crystals were transferred to the cold gas stream on the diffractometer. The diffraction data were obtained at 100 K on a Bruker D8 three-circle diffractometer, equipped with a PHOTON 100 CMOS detector and an INCOATEC microfocus source with Quazar mirror optics (Mo-Kα radiation, λ= 0.71073 Å).The data obtained were integrated with SAINT and a semi-empirical absorption correction from equivalents with SADABS was applied. The structure was solved and refined using the Bruker SHELX 2014 software package.[42] All non-hydrogen atoms were refined with anisotropic displacement parameters. All C-H hydrogen atoms were refined isotropically on calculated positions by using a riding model with their U_{iso} values constrained to 1.5 U_{eq} of their pivot atoms for terminal sp3 carbon atoms and 1.2 times for all other carbon atoms.

3.2 X-ray Single-Crystal Structure Analysis of 9

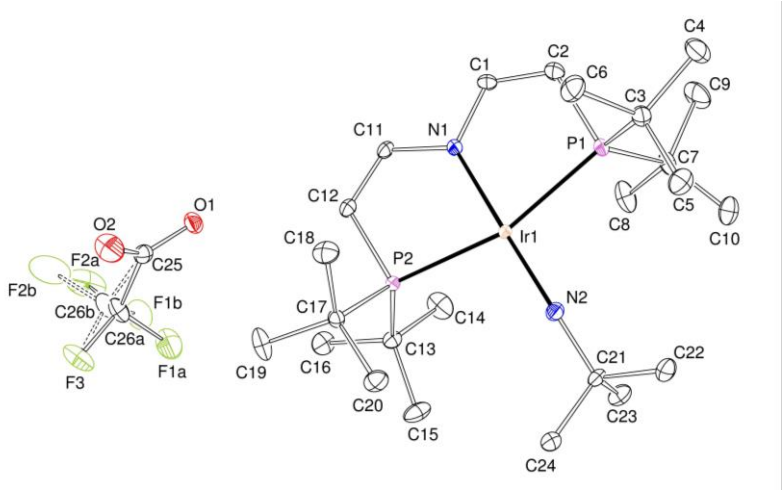

Figure S35. Thermal ellipsoid plot of **9** with the anisotropic displacement parameters drawn at the 50% probability level. The asymmetric unit contains one cationic complex molecule and one disordered CF_3COO anion with a population of 0.878(2) on the main domain. The disordered anion was refined using some restraints (SADI) and constraints (EADP).

Table S8. Crystal data and structure refinement for **9**.

Identification code	mo_CV_MK_29012016_a (MK402)
CCDC-No	1546382
Empirical formula	$C_{26}H_{49}F_3IrN_2O_2P_2$
Formula weight	732.81
Temperature	103(2) K
Wavelength	0.71073 Å
Crystal system	Orthorhombic
Space group	Pbca
Unit cell dimensions	a = 14.6519(6) Å α= 90°

	b = 15.5746(6) Å β= 90°
	c = 27.2406(10) Å γ = 90°
Volume	6216.2(4) $Å^3$
Z	8
Density (calculated)	1.566 Mg/m^3
Absorption coefficient	4.441 mm^{-1}
F(000)	2952
Crystal size	0.268 x 0.198 x 0.144 mm^3
Crystal shape and color	Block, clear dark blue-violet
Theta range for data collection	2.425 to 33.249°
Index ranges	-22<=h<=22, -23<=k<=23, -41<=l<=41
Reflections collected	270012
Independent reflections	11918 [R(int) = 0.0484]
Completeness to theta	= 25.242° 99.9 %
Max. and min. transmission	0.7465 and 0.5967
Refinement method	Full-matrix least-squares on F^2
Data / restraints / parameters	11918 / 12 / 350
Goodness-of-fit on F^2	1.031
Final R indices [I>2sigma(I)]	R1 = 0.0193, wR2 = 0.0362
R indices (all data)	R1 = 0.0278, wR2 = 0.0386
Largest diff. peak and hole	0.900 and -0.725 $eÅ^{-3}$

Table S9. Bond lengths [Å] and angles [°] for **9**.

C(1)-C(2)	1.332(2)	C(17)-P(2)	1.8718(14)
C(1)-N(1)	1.4020(19)	C(21)-N(2)	1.4437(18)
C(2)-P(1)	1.7879(16)	C(21)-C(24)	1.537(2)
C(3)-C(5)	1.528(2)	C(21)-C(23)	1.539(2)
C(3)-C(4)	1.538(2)	C(21)-C(22)	1.541(2)
C(3)-C(6)	1.540(2)	F(3)-C(26B)	1.296(17)
C(3)-P(1)	1.8748(16)	F(3)-C(26A)	1.325(3)
C(7)-C(10)	1.530(2)	C(25)-O(2)	1.229(2)
C(7)-C(8)	1.535(2)	C(25)-O(1)	1.2412(19)
C(7)-C(9)	1.536(2)	C(25)-C(26A)	1.552(4)
C(7)-P(1)	1.8832(16)	C(25)-C(26B)	1.63(4)
C(11)-C(12)	1.335(2)	N(1)-Ir(1)	1.9792(12)
C(11)-N(1)	1.4048(18)	N(2)-Ir(1)	1.8053(12)
C(12)-P(2)	1.7907(15)	P(1)-Ir(1)	2.3890(4)
C(13)-C(15)	1.524(2)	P(2)-Ir(1)	2.3879(4)
C(13)-C(16)	1.532(2)	C(26A)-F(1A)	1.349(3)
C(13)-C(14)	1.537(2)	C(26A)-F(2A)	1.350(3)
C(13)-P(2)	1.8770(15)	C(26B)-F(1B)	1.218(16)
C(17)-C(20)	1.527(2)	C(26B)-F(2B)	1.361(16)
C(17)-C(19)	1.529(2)	C(2)-C(1)-N(1)	121.23(14)
C(17)-C(18)	1.535(2)	C(1)-C(2)-P(1)	115.48(12)

C(5)-C(3)-C(4)	109.65(13)	C(19)-C(17)-C(18)	108.77(13)
C(5)-C(3)-C(6)	108.63(13)	C(20)-C(17)-P(2)	110.56(10)
C(4)-C(3)-C(6)	109.33(14)	C(19)-C(17)-P(2)	113.74(10)
C(5)-C(3)-P(1)	111.36(11)	C(18)-C(17)-P(2)	105.10(10)
C(4)-C(3)-P(1)	112.47(11)	N(2)-C(21)-C(24)	111.10(12)
C(6)-C(3)-P(1)	105.23(11)	N(2)-C(21)-C(23)	107.96(12)
C(10)-C(7)-C(8)	110.27(15)	C(24)-C(21)-C(23)	109.88(13)
C(10)-C(7)-C(9)	109.06(14)	N(2)-C(21)-C(22)	111.36(12)
C(8)-C(7)-C(9)	108.20(14)	C(24)-C(21)-C(22)	106.71(12)
C(10)-C(7)-P(1)	112.26(11)	C(23)-C(21)-C(22)	109.84(13)
C(8)-C(7)-P(1)	105.00(11)	O(2)-C(25)-O(1)	131.68(16)
C(9)-C(7)-P(1)	111.93(12)	O(2)-C(25)-C(26A)	115.49(16)
C(12)-C(11)-N(1)	121.78(13)	O(1)-C(25)-C(26A)	112.82(15)
C(11)-C(12)-P(2)	114.45(11)	O(2)-C(25)-C(26B)	110.9(4)
C(15)-C(13)-C(16)	108.66(13)	O(1)-C(25)-C(26B)	116.9(4)
C(15)-C(13)-C(14)	109.10(14)	C(1)-N(1)-C(11)	114.34(12)
C(16)-C(13)-C(14)	108.63(13)	C(1)-N(1)-Ir(1)	122.76(10)
C(15)-C(13)-P(2)	112.28(10)	C(11)-N(1)-Ir(1)	122.85(10)
C(16)-C(13)-P(2)	112.58(10)	C(21)-N(2)-Ir(1)	171.31(11)
C(14)-C(13)-P(2)	105.46(11)	C(2)-P(1)-C(3)	103.77(8)
C(20)-C(17)-C(19)	110.13(13)	C(2)-P(1)-C(7)	103.10(8)
C(20)-C(17)-C(18)	108.27(12)	C(3)-P(1)-C(7)	115.06(7)

C(2)-P(1)-Ir(1)	99.32(5)	F(1B)-C(26B)-F(2B)	110.5(18)
C(3)-P(1)-Ir(1)	117.85(5)	F(3)-C(26B)-F(2B)	100.5(14)
C(7)-P(1)-Ir(1)	114.35(5)	F(1B)-C(26B)-C(25)	112.6(18)
C(12)-P(2)-C(17)	104.76(7)	F(3)-C(26B)-C(25)	112.1(16)
C(12)-P(2)-C(13)	102.38(7)	F(2B)-C(26B)-C(25)	101.0(15)
C(17)-P(2)-C(13)	113.97(7)		
C(12)-P(2)-Ir(1)	100.04(5)		
C(17)-P(2)-Ir(1)	116.54(5)		
C(13)-P(2)-Ir(1)	116.08(5)		
N(2)-Ir(1)-N(1)	175.55(5)		
N(2)-Ir(1)-P(2)	99.54(4)		
N(1)-Ir(1)-P(2)	80.86(4)		
N(2)-Ir(1)-P(1)	98.19(4)		
N(1)-Ir(1)-P(1)	81.18(4)		
P(2)-Ir(1)-P(1)	161.909(13)		
F(3)-C(26A)-F(1A)	105.0(2)		
F(3)-C(26A)-F(2A)	106.9(2)		
F(1A)-C(26A)-F(2A)	103.9(2)		
F(3)-C(26A)-C(25)	115.1(2)		
F(1A)-C(26A)-C(25)	114.3(2)		
F(2A)-C(26A)-C(25)	110.8(2)		
F(1B)-C(26B)-F(3)	118(2)		

Table S10. Torsion angles [°] for **9**.

N(1)-C(1)-C(2)-P(1)	1.9(2)	C(10)-C(7)-P(1)-C(3)	50.29(14)
N(1)-C(11)-C(12)-P(2)	-1.81(19)	C(8)-C(7)-P(1)-C(3)	170.11(11)
C(2)-C(1)-N(1)-C(11)	-179.17(15)	C(9)-C(7)-P(1)-C(3)	-72.73(14)
C(2)-C(1)-N(1)-Ir(1)	-1.5(2)	C(10)-C(7)-P(1)-Ir(1)	-90.74(12)
C(12)-C(11)-N(1)-C(1)	178.76(14)	C(8)-C(7)-P(1)-Ir(1)	29.08(13)
C(12)-C(11)-N(1)-Ir(1)	1.1(2)	C(9)-C(7)-P(1)-Ir(1)	146.23(11)
C(1)-C(2)-P(1)-C(3)	-123.23(14)	C(11)-C(12)-P(2)-C(17)	122.60(12)
C(1)-C(2)-P(1)-C(7)	116.46(14)	C(11)-C(12)-P(2)-C(13)	-118.20(12)
C(1)-C(2)-P(1)-Ir(1)	-1.39(15)	C(11)-C(12)-P(2)-Ir(1)	1.54(12)
C(5)-C(3)-P(1)-C(2)	173.71(11)	C(20)-C(17)-P(2)-C(12)	-170.66(11)
C(4)-C(3)-P(1)-C(2)	-62.75(13)	C(19)-C(17)-P(2)-C(12)	64.83(13)
C(6)-C(3)-P(1)-C(2)	56.19(12)	C(18)-C(17)-P(2)-C(12)	-54.03(11)
C(5)-C(3)-P(1)-C(7)	-74.44(13)	C(20)-C(17)-P(2)-C(13)	78.25(12)
C(4)-C(3)-P(1)-C(7)	49.09(14)	C(19)-C(17)-P(2)-C(13)	-46.26(14)
C(6)-C(3)-P(1)-C(7)	168.04(11)	C(18)-C(17)-P(2)-C(13)	-165.13(10)
C(5)-C(3)-P(1)-Ir(1)	65.17(12)	C(20)-C(17)-P(2)-Ir(1)	-61.20(11)
C(4)-C(3)-P(1)-Ir(1)	-171.30(10)	C(19)-C(17)-P(2)-Ir(1)	174.29(10)
C(6)-C(3)-P(1)-Ir(1)	-52.35(12)	C(18)-C(17)-P(2)-Ir(1)	55.42(11)
C(10)-C(7)-P(1)-C(2)	162.54(12)	C(15)-C(13)-P(2)-C(12)	-170.42(12)
C(8)-C(7)-P(1)-C(2)	-77.65(13)	C(16)-C(13)-P(2)-C(12)	-47.41(12)
C(9)-C(7)-P(1)-C(2)	39.51(14)	C(14)-C(13)-P(2)-C(12)	70.88(12)

C(15)-C(13)-P(2)-C(17)	-57.89(13)	O(1)-C(25)-C(26A)-F(1A)	40.3(2)
C(16)-C(13)-P(2)-C(17)	65.12(12)	O(2)-C(25)-C(26A)-F(2A)	104.0(2)
C(14)-C(13)-P(2)-C(17)	-176.59(11)	O(1)-C(25)-C(26A)-F(2A)	-76.7(2)
C(15)-C(13)-P(2)-Ir(1)	81.75(12)	O(2)-C(25)-C(26B)-F(1B)	-174.6(9)
C(16)-C(13)-P(2)-Ir(1)	-155.23(9)	O(1)-C(25)-C(26B)-F(1B)	12.6(12)
C(14)-C(13)-P(2)-Ir(1)	-36.94(12)	O(2)-C(25)-C(26B)-F(3)	-38.7(9)
O(2)-C(25)-C(26A)-F(3)	-17.5(3)	O(1)-C(25)-C(26B)-F(3)	148.6(6)
O(1)-C(25)-C(26A)-F(3)	161.88(16)	O(2)-C(25)-C(26B)-F(2B)	67.5(9)
O(2)-C(25)-C(26A)-F(1A)	-139.05(19)	O(1)-C(25)-C(26B)-F(2B)	-105.2(7)

Symmetry transformations used to generate equivalent atoms: -

3.3 X-ray Single-Crystal Structure Analysis of 10.

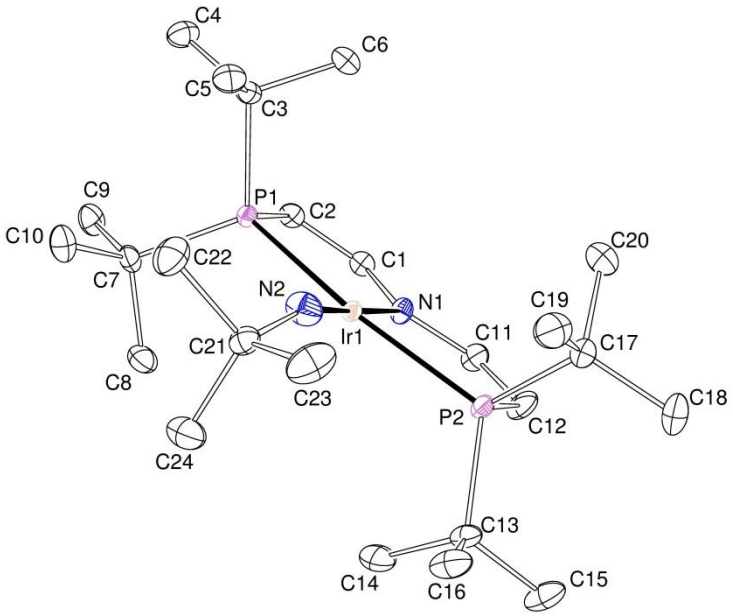

Figure S36. Thermal ellipsoid plot of **10** with the anisotropic displacement parameters drawn at the 50% probability level.

Table S11. Crystal data and structure refinement for **10**.

Identification code	mo_CV_MM_140915_0m_a (MK352)	
CCDC-No	1546383	
Empirical formula	$C_{24}H_{49}IrN_2P_2$	
Formula weight	619.79	
Temperature	100(2) K	
Wavelength	0.71073 Å	
Crystal system	Monoclinic	
Space group	$P2_1/c$	
Unit cell dimensions	a = 11.0958(6) Å	α= 90°
	b = 15.4511(8) Å	β= 100.560(2)°
	c = 16.0856(9) Å	γ = 90°

Volume	2711.0(3) $Å^3$
Z	4
Density (calculated)	1.519 Mg/m^3
Absorption coefficient	5.056 mm^{-1}
F(000)	1256
Crystal size	0.194 x 0.167 x 0.090 mm^3
Crystal shape and color	Plate, clear light orange-brown
Theta range for data collection	1.867 to 27.182°
Index ranges	-14<=h<=14, -19<=k<=19, -20<=l<=20
Reflections collected	77516
Independent reflections	6022 [R(int) = 0.0378]
Completeness to theta	= 25.242° 100.0 %
Max. and min. transmission	0.7455 and 0.5898
Refinement method	Full-matrix least-squares on F^2
Data / restraints / parameters	6022 / 0 / 277
Goodness-of-fit on F^2	1.192
Final R indices [I>2sigma(I)]	R1 = 0.0175, wR2 = 0.0340
R indices (all data)	R1 = 0.0253, wR2 = 0.0374
Largest diff. peak and hole	1.407 and -0.968 $eÅ^{-3}$

Table S12. Bond lengths [Å] and angles [°] for **10**.

C(1)-C(2)	1.342(3)
C(1)-N(1)	1.373(3)
C(2)-P(1)	1.782(2)
C(3)-C(5)	1.527(3)
C(3)-C(4)	1.534(3)
C(3)-C(6)	1.540(3)
C(3)-P(1)	1.883(2)
C(7)-C(10)	1.527(4)
C(7)-C(9)	1.539(3)
C(7)-C(8)	1.540(4)
C(7)-P(1)	1.889(2)
C(11)-C(12)	1.333(4)
C(11)-N(1)	1.373(3)
C(12)-P(2)	1.783(3)
C(13)-C(16)	1.526(4)
C(13)-C(15)	1.531(4)
C(13)-C(14)	1.538(4)
C(13)-P(2)	1.883(3)
C(17)-C(19)	1.530(4)
C(17)-C(18)	1.533(4)
C(17)-C(20)	1.538(4)
C(17)-P(2)	1.882(3)
C(21)-N(2)	1.438(3)
C(21)-C(24)	1.528(4)
C(21)-C(23)	1.537(4)
C(21)-C(22)	1.542(4)
N(1)-Ir(1)	2.059(2)
N(2)-Ir(1)	1.868(2)
P(1)-Ir(1)	2.3411(6)
P(2)-Ir(1)	2.3471(6)
C(2)-C(1)-N(1)	122.0(2)
C(1)-C(2)-P(1)	114.97(18)
C(5)-C(3)-C(4)	109.4(2)
C(5)-C(3)-C(6)	108.3(2)
C(4)-C(3)-C(6)	108.8(2)
C(5)-C(3)-P(1)	110.75(17)
C(4)-C(3)-P(1)	114.20(17)
C(6)-C(3)-P(1)	105.21(17)
C(10)-C(7)-C(9)	109.5(2)
C(10)-C(7)-C(8)	109.1(2)
C(9)-C(7)-C(8)	107.8(2)
C(10)-C(7)-P(1)	112.55(17)
C(9)-C(7)-P(1)	113.10(18)
C(8)-C(7)-P(1)	104.40(16)
C(12)-C(11)-N(1)	121.7(2)
C(11)-C(12)-P(2)	115.7(2)
C(16)-C(13)-C(15)	108.9(2)
C(16)-C(13)-C(14)	109.0(2)

C(15)-C(13)-C(14)	107.9(2)
C(16)-C(13)-P(2)	112.86(18)
C(15)-C(13)-P(2)	113.81(19)
C(14)-C(13)-P(2)	104.03(18)
C(19)-C(17)-C(18)	109.8(2)
C(19)-C(17)-C(20)	108.0(2)
C(18)-C(17)-C(20)	109.3(2)
C(19)-C(17)-P(2)	110.35(19)
C(18)-C(17)-P(2)	114.0(2)
C(20)-C(17)-P(2)	105.12(19)
N(2)-C(21)-C(24)	110.6(2)
N(2)-C(21)-C(23)	110.5(2)
C(24)-C(21)-C(23)	110.0(2)
N(2)-C(21)-C(22)	110.8(2)
C(24)-C(21)-C(22)	109.8(2)
C(23)-C(21)-C(22)	105.1(2)
C(11)-N(1)-C(1)	117.8(2)
C(11)-N(1)-Ir(1)	121.22(16)
C(1)-N(1)-Ir(1)	120.96(16)
C(21)-N(2)-Ir(1)	157.20(19)
C(2)-P(1)-C(3)	104.63(11)
C(2)-P(1)-C(7)	102.60(11)
C(3)-P(1)-C(7)	112.36(11)
C(2)-P(1)-Ir(1)	101.23(8)
C(3)-P(1)-Ir(1)	114.69(8)
C(7)-P(1)-Ir(1)	118.67(8)
C(12)-P(2)-C(17)	104.45(13)
C(12)-P(2)-C(13)	103.00(12)
C(17)-P(2)-C(13)	112.59(12)
C(12)-P(2)-Ir(1)	100.76(9)
C(17)-P(2)-Ir(1)	114.16(9)
C(13)-P(2)-Ir(1)	119.15(9)
N(2)-Ir(1)-N(1)	178.61(9)
N(2)-Ir(1)-P(1)	99.20(8)
N(1)-Ir(1)-P(1)	80.78(6)
N(2)-Ir(1)-P(2)	99.32(8)
N(1)-Ir(1)-P(2)	80.67(6)
P(1)-Ir(1)-P(2)	161.39(2)

Table S13. Torsion angles [°] for **10**.

C(1)-C(1)-C(2)-P(1)	-1.0(3)
N(1)-C(11)-C(12)-P(2)	0.7(4)
C(12)-C(11)-N(1)-C(1)	177.5(2)
C(12)-C(11)-N(1)-Ir(1)	-1.5(3)
C(2)-C(1)-N(1)-C(11)	-179.1(2)
C(2)-C(1)-N(1)-Ir(1)	-0.1(3)
C(24)-C(21)-N(2)-Ir(1)	1.2(6)
C(23)-C(21)-N(2)-Ir(1)	123.2(5)
C(22)-C(21)-N(2)-Ir(1)	-120.8(5)
C(1)-C(2)-P(1)-C(3)	120.9(2)
C(1)-C(2)-P(1)-C(7)	-121.7(2)
C(1)-C(2)-P(1)-Ir(1)	1.4(2)
C(5)-C(3)-P(1)-C(2)	-167.34(17)
C(4)-C(3)-P(1)-C(2)	68.7(2)
C(6)-C(3)-P(1)-C(2)	-50.49(19)
C(5)-C(3)-P(1)-C(7)	82.10(19)
C(4)-C(3)-P(1)-C(7)	-41.9(2)
C(6)-C(3)-P(1)-C(7)	-161.05(16)
C(5)-C(3)-P(1)-Ir(1)	-57.37(18)
C(4)-C(3)-P(1)-Ir(1)	178.67(16)
C(6)-C(3)-P(1)-Ir(1)	59.48(17)
C(10)-C(7)-P(1)-C(2)	-165.16(19)
C(9)-C(7)-P(1)-C(2)	-40.4(2)
C(8)-C(7)-P(1)-C(2)	76.61(19)
C(10)-C(7)-P(1)-C(3)	-53.3(2)
C(9)-C(7)-P(1)-C(3)	71.5(2)
C(8)-C(7)-P(1)-C(3)	-171.56(17)
C(10)-C(7)-P(1)-Ir(1)	84.37(19)
C(9)-C(7)-P(1)-Ir(1)	-150.83(15)
C(8)-C(7)-P(1)-Ir(1)	-33.9(2)
C(11)-C(12)-P(2)-C(17)	-118.5(2)
C(11)-C(12)-P(2)-C(13)	123.7(2)
C(11)-C(12)-P(2)-Ir(1)	0.2(2)
C(19)-C(17)-P(2)-C(12)	170.02(19)
C(18)-C(17)-P(2)-C(12)	-65.8(2)
C(20)-C(17)-P(2)-C(12)	53.8(2)
C(19)-C(17)-P(2)-C(13)	-78.9(2)
C(18)-C(17)-P(2)-C(13)	45.2(3)
C(20)-C(17)-P(2)-C(13)	164.87(18)
C(19)-C(17)-P(2)-Ir(1)	60.9(2)
C(18)-C(17)-P(2)-Ir(1)	-174.90(19)
C(20)-C(17)-P(2)-Ir(1)	-55.2(2)
C(16)-C(13)-P(2)-C(12)	166.6(2)
C(15)-C(13)-P(2)-C(12)	41.8(2)
C(14)-C(13)-P(2)-C(12)	-75.4(2)
C(16)-C(13)-P(2)-C(17)	54.7(2)

C(15)-C(13)-P(2)-C(17)	-70.2(2)	C(14)-C(13)-P(2)-Ir(1)	35.0(2)
C(14)-C(13)-P(2)-C(17)	172.67(18)	C(21)-N(2)-Ir(1)-P(1)	91.9(5)
C(16)-C(13)-P(2)-Ir(1)	-83.0(2)	C(21)-N(2)-Ir(1)-P(2)	-89.9(5)
C(15)-C(13)-P(2)-Ir(1)	152.13(17)		

Symmetry transformations used to generate equivalent atoms: -

3.4 X-ray Single-Crystal Structure Analysis of 12

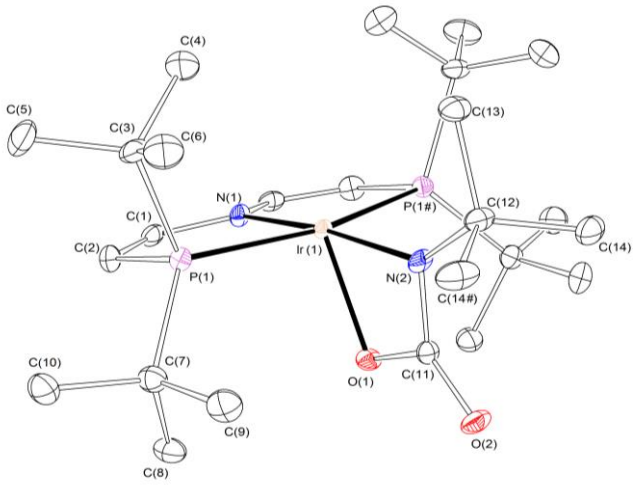

Figure S37. Thermal ellipsoid plot of **12** with the anisotropic displacement parameters drawn at the 50% probability level. The asymmetric unit contains only a half complex molecule.

Table S14. Crystal data and structure refinement for **12**.

Identification code	mo_CV_MK_200616_0m_a (MK460)	
CCDC-No	1546384	
Empirical formula	$C_{25}H_{49}IrN_2O_2P_2$	
Formula weight	663.80	
Temperature	100(2) K	
Wavelength	0.71073 Å	
Crystal system	Monoclinic	
Space group	$P2_1/m$	
Unit cell dimensions	a = 7.9728(3) Å	α= 90°
	b = 21.7175(9) Å	β= 113.5590(10)°
	c = 8.7383(3) Å	γ = 90°
Volume	1386.92(9) $Å^3$	
Z	2	

Density (calculated)	1.590 Mg/m^3
Absorption coefficient	4.952 mm^{-1}
F(000)	672
Crystal size	0.083 x 0.055 x 0.038 mm^3
Crystal shape and color	Block, clear light yellow
Theta range for data collection	2.543 to 28.359°
Index ranges	-9<=h<=10, -29<=k<=29, -11<=l<=11
Reflections collected	38483
Independent reflections	3557 [R(int) = 0.0637]
Completeness to theta	= 25.242° 100.0 %
Max. and min. transmission	0.7457 and 0.6561
Refinement method	Full-matrix least-squares on F^2
Data / restraints / parameters	3557 / 0 / 165
Goodness-of-fit on F^2	1.120
Final R indices [I>2sigma(I)]	R1 = 0.0212, wR2 = 0.0369
R indices (all data)	R1 = 0.0272, wR2 = 0.0380
Largest diff. peak and hole	0.621 and -1.775 $eÅ^{-3}$

Table S15. Bond lengths [Å] and angles [°] for **12**.

C(1)-C(2)	1.335(3)	C(2)-C(1)-N(1)	121.8(2)
C(1)-N(1)	1.384(3)	C(1)-C(2)-P(1)	116.06(18)
C(2)-P(1)	1.784(2)	C(5)-C(3)-C(6)	109.8(2)
C(3)-C(5)	1.530(3)	C(5)-C(3)-C(4)	109.3(2)
C(3)-C(6)	1.534(3)	C(6)-C(3)-C(4)	107.7(2)
C(3)-C(4)	1.540(3)	C(5)-C(3)-P(1)	112.13(17)
C(3)-P(1)	1.893(2)	C(6)-C(3)-P(1)	104.91(17)
C(7)-C(8)	1.530(3)	C(4)-C(3)-P(1)	112.83(17)
C(7)-C(10)	1.533(3)	C(8)-C(7)-C(10)	110.0(2)
C(7)-C(9)	1.537(3)	C(8)-C(7)-C(9)	108.1(2)
C(7)-P(1)	1.877(2)	C(10)-C(7)-C(9)	108.7(2)
C(11)-O(2)	1.237(4)	C(8)-C(7)-P(1)	111.62(17)
C(11)-N(2)	1.327(4)	C(10)-C(7)-P(1)	112.54(17)
C(11)-O(1)	1.366(4)	C(9)-C(7)-P(1)	105.60(16)
C(11)-Ir(1)	2.565(3)	O(2)-C(11)-N(2)	132.8(3)
C(12)-N(2)	1.476(4)	O(2)-C(11)-O(1)	120.7(3)
C(12)-C(13)	1.527(4)	N(2)-C(11)-O(1)	106.5(3)
C(12)-C(14)#1	1.538(3)	O(2)-C(11)-Ir(1)	171.9(2)
C(12)-C(14)	1.538(3)	N(2)-C(11)-Ir(1)	55.27(16)
N(1)-C(1)#1	1.384(3)	O(1)-C(11)-Ir(1)	51.20(14)
N(1)-Ir(1)	2.021(3)	N(2)-C(12)-C(13)	109.8(3)
N(2)-Ir(1)	2.112(3)	N(2)-C(12)-C(14)#1	110.44(18)
O(1)-Ir(1)	2.013(2)	C(13)-C(12)-C(14)#1	108.69(18)
P(1)-Ir(1)	2.3698(6)	N(2)-C(12)-C(14)	110.44(18)
Ir(1)-P(1)#1	2.3698(6)	C(13)-C(12)-C(14)	108.69(18)

C(14)#1-C(12)-C(14)	108.7(3)	O(1)-Ir(1)-N(2)	63.01(10)
C(1)#1-N(1)-C(1)	117.4(3)	N(1)-Ir(1)-N(2)	173.52(11)
C(1)#1-N(1)-Ir(1)	120.86(14)	O(1)-Ir(1)-P(1)	94.781(17)
C(1)-N(1)-Ir(1)	120.86(14)	N(1)-Ir(1)-P(1)	81.524(15)
C(11)-N(2)-C(12)	122.7(3)	N(2)-Ir(1)-P(1)	98.643(14)
C(11)-N(2)-Ir(1)	93.65(19)	O(1)-Ir(1)-P(1)#1	94.780(17)
C(12)-N(2)-Ir(1)	143.7(2)	N(1)-Ir(1)-P(1)#1	81.524(15)
C(11)-O(1)-Ir(1)	96.88(18)	N(2)-Ir(1)-P(1)#1	98.643(14)
C(2)-P(1)-C(7)	104.37(11)	P(1)-Ir(1)-P(1)#1	162.60(3)
C(2)-P(1)-C(3)	103.36(11)	O(1)-Ir(1)-C(11)	31.92(9)
C(7)-P(1)-C(3)	112.48(11)	N(1)-Ir(1)-C(11)	142.43(11)
C(2)-P(1)-Ir(1)	99.12(8)	N(2)-Ir(1)-C(11)	31.09(10)
C(7)-P(1)-Ir(1)	122.21(8)	P(1)-Ir(1)-C(11)	97.901(15)
C(3)-P(1)-Ir(1)	112.08(8)	P(1)#1-Ir(1)-C(11)	97.900(15)
O(1)-Ir(1)-N(1)	110.51(10)		

Symmetry transformations used to generate equivalent atoms: #1 x,-y+3/2,z

Table S16. Torsion angles [°] for **12**.

N(1)-C(1)-C(2)-P(1)	-1.2(3)	C(8)-C(7)-P(1)-C(2)	-171.35(17)
C(2)-C(1)-N(1)-C(1)#1	-175.33(17)	C(10)-C(7)-P(1)-C(2)	64.4(2)
C(2)-C(1)-N(1)-Ir(1)	-5.8(4)	C(9)-C(7)-P(1)-C(2)	-54.08(18)
O(2)-C(11)-N(2)-C(12)	0.000(2)	C(8)-C(7)-P(1)-C(3)	77.29(19)
O(1)-C(11)-N(2)-C(12)	180.000(1)	C(10)-C(7)-P(1)-C(3)	-47.0(2)
Ir(1)-C(11)-N(2)-C(12)	180.000(1)	C(9)-C(7)-P(1)-C(3)	-165.44(16)
O(2)-C(11)-N(2)-Ir(1)	180.000(1)	C(8)-C(7)-P(1)-Ir(1)	-60.57(19)
O(1)-C(11)-N(2)-Ir(1)	0.000(1)	C(10)-C(7)-P(1)-Ir(1)	175.16(14)
C(13)-C(12)-N(2)-C(11)	180.000(1)	C(9)-C(7)-P(1)-Ir(1)	56.70(18)
C(14)#1-C(12)-N(2)-C(11)	60.14(19)	C(5)-C(3)-P(1)-C(2)	-160.87(18)
C(14)-C(12)-N(2)-C(11)	-60.14(19)	C(6)-C(3)-P(1)-C(2)	80.01(18)
C(13)-C(12)-N(2)-Ir(1)	0.000(1)	C(4)-C(3)-P(1)-C(2)	-36.9(2)
C(14)#1-C(12)-N(2)-Ir(1)	-119.86(19)	C(5)-C(3)-P(1)-C(7)	-48.9(2)
C(14)-C(12)-N(2)-Ir(1)	119.86(19)	C(6)-C(3)-P(1)-C(7)	-168.00(16)
O(2)-C(11)-O(1)-Ir(1)	180.000(1)	C(4)-C(3)-P(1)-C(7)	75.0(2)
N(2)-C(11)-O(1)-Ir(1)	0.000(1)	C(5)-C(3)-P(1)-Ir(1)	93.33(18)
C(1)-C(2)-P(1)-C(7)	132.6(2)	C(6)-C(3)-P(1)-Ir(1)	-25.78(18)
C(1)-C(2)-P(1)-C(3)	-109.6(2)	C(4)-C(3)-P(1)-Ir(1)	-142.73(17)
C(1)-C(2)-P(1)-Ir(1)	5.8(2)		

Symmetry transformations used to generate equivalent atoms: #1 x,-y+3/2,z

3.5 X-ray Single-Crystal Structure Analysis of 13

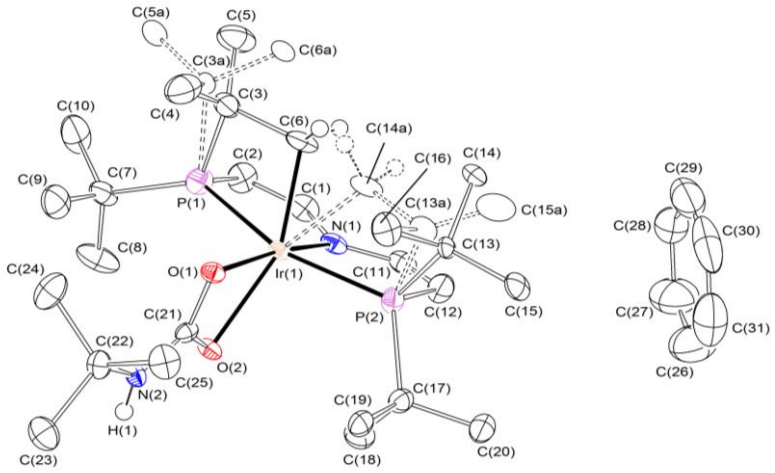

Figure S38. Thermal ellipsoid plot of **13** with the anisotropic displacement parameters drawn at the 50% probability level. The asymmetric unit contains one disordered complex molecule and one benzene solvent molecule. The benzene molecule was refined as regular hexagon using AFIX 66 command and some restraints (RIGU). The disordered tertiary butyl groups were refined with population of 0.815(5) on the main domain using some restraints (SADI) and constraints (EADP).

Table S17. Crystal data and structure refinement for **13**.

Identification code	mo_CV_MK_290616_0m_a (MK461)
CCDC-No	1546385
Empirical formula	$C_{31}H_{55}IrN_2O_2P_2$
Formula weight	741.91
Temperature	100(2) K
Wavelength	0.71073 Å
Crystal system	Monoclinic
Space group	$P2_1/c$
Unit cell dimensions	a = 11.2846(10) Å α= 90°

	b = 14.9634(13) Å β= 92.013(3)°
	c = 19.8058(17) Å γ = 90°
Volume	3342.3(5) Å^3
Z	4
Density (calculated)	1.474 Mg/m^3
Absorption coefficient	4.119 mm^{-1}
F(000)	1512
Crystal size	0.101 x 0.099 x 0.032 mm^3
Crystal shape and color	Block, clear light yellow
Theta range for data collection	2.058 to 28.391°
Index ranges	-15<=h<=14, -19<=k<=19, -26<=l<=26
Reflections collected	88414
Independent reflections	8344 [R(int) = 0.1228]
Completeness to theta	= 25.242° 100.0 %
Max. and min. transmission	0.7457 and 0.6559
Refinement method	Full-matrix least-squares on F^2
Data / restraints / parameters	8344 / 54 / 371
Goodness-of-fit on F^2	1.073
Final R indices [I>2sigma(I)]	R1 = 0.0399, wR2 = 0.0642
R indices (all data)	R1 = 0.0696, wR2 = 0.0712
Largest diff. peak and hole	1.247 and -1.731 eÅ^{-3}

Table S18. Bond lengths [Å] and angles [°] for **13**.

C(1)-C(2)	1.347(7)	C(11)-N(1)	1.360(6)
C(1)-N(1)	1.372(6)	C(12)-P(2)	1.776(5)
C(2)-P(1)	1.771(5)	C(17)-C(20)	1.527(7)
C(3)-C(4)	1.492(9)	C(17)-C(18)	1.533(7)
C(3)-C(5)	1.517(9)	C(17)-C(19)	1.536(7)
C(3)-C(6)	1.565(9)	C(17)-P(2)	1.893(5)
C(3)-P(1)	1.821(7)	C(21)-O(2)	1.275(5)
C(6)-Ir(1)	2.098(6)	C(21)-O(1)	1.290(5)
C(13)-C(15)	1.509(7)	C(21)-N(2)	1.334(6)
C(13)-C(16)	1.526(7)	C(21)-Ir(1)	2.565(5)
C(13)-C(14)	1.559(7)	C(22)-N(2)	1.468(6)
C(13)-P(2)	1.938(6)	C(22)-C(23)	1.516(7)
C(6A)-C(3A)	1.566(15)	C(22)-C(25)	1.518(6)
C(5A)-C(3A)	1.548(15)	C(22)-C(24)	1.521(7)
C(3A)-C(4)	1.577(14)	N(1)-Ir(1)	2.022(4)
C(3A)-P(1)	2.010(17)	N(2)-H(1)	0.81(6)
C(15A)-C(13A)	1.35(5)	O(1)-Ir(1)	2.129(3)
C(14A)-C(13A)	1.60(2)	O(2)-Ir(1)	2.262(3)
C(14A)-Ir(1)	2.12(3)	P(1)-Ir(1)	2.2902(13)
C(13A)-C(16)	1.56(3)	P(2)-Ir(1)	2.3416(13)
C(13A)-P(2)	1.759(18)	C(2)-C(1)-N(1)	122.9(5)
C(7)-C(9)	1.523(8)	C(1)-C(2)-P(1)	114.7(4)
C(7)-C(8)	1.530(8)	C(4)-C(3)-C(5)	109.3(6)
C(7)-C(10)	1.534(7)	C(4)-C(3)-C(6)	109.8(5)
C(7)-P(1)	1.849(5)	C(5)-C(3)-C(6)	113.3(6)
C(11)-C(12)	1.333(7)	C(4)-C(3)-P(1)	116.2(4)

C(5)-C(3)-P(1)	116.4(5)	C(10)-C(7)-P(1)	110.9(4)
C(6)-C(3)-P(1)	90.7(4)	C(12)-C(11)-N(1)	122.6(5)
C(3)-C(6)-Ir(1)	104.8(4)	C(11)-C(12)-P(2)	116.0(4)
C(15)-C(13)-C(16)	110.1(5)	C(20)-C(17)-C(18)	107.6(4)
C(15)-C(13)-C(14)	107.4(5)	C(20)-C(17)-C(19)	111.0(4)
C(16)-C(13)-C(14)	109.0(5)	C(18)-C(17)-C(19)	108.7(4)
C(15)-C(13)-P(2)	116.4(4)	C(20)-C(17)-P(2)	113.4(4)
C(16)-C(13)-P(2)	106.7(3)	C(18)-C(17)-P(2)	106.2(3)
C(14)-C(13)-P(2)	107.0(4)	C(19)-C(17)-P(2)	109.8(3)
C(5A)-C(3A)-C(6A)	103.0(17)	O(2)-C(21)-O(1)	117.7(4)
C(5A)-C(3A)-C(4)	110.2(15)	O(2)-C(21)-N(2)	120.1(4)
C(6A)-C(3A)-C(4)	115.7(15)	O(1)-C(21)-N(2)	122.1(4)
C(5A)-C(3A)-P(1)	113.3(14)	O(2)-C(21)-Ir(1)	61.8(2)
C(6A)-C(3A)-P(1)	112.1(14)	O(1)-C(21)-Ir(1)	55.9(2)
C(4)-C(3A)-P(1)	102.9(8)	N(2)-C(21)-Ir(1)	178.0(3)
C(13A)-C(14A)-Ir(1)	113.1(15)	N(2)-C(22)-C(23)	106.8(4)
C(15A)-C(13A)-C(16)	122(2)	N(2)-C(22)-C(25)	109.6(4)
C(15A)-C(13A)-C(14A)	110(3)	C(23)-C(22)-C(25)	109.6(4)
C(16)-C(13A)-C(14A)	107(2)	N(2)-C(22)-C(24)	110.2(4)
C(15A)-C(13A)-P(2)	115(3)	C(23)-C(22)-C(24)	110.0(4)
C(16)-C(13A)-P(2)	114.1(17)	C(25)-C(22)-C(24)	110.6(4)
C(14A)-C(13A)-P(2)	80.6(13)	C(11)-N(1)-C(1)	120.1(4)
C(9)-C(7)-C(8)	108.0(5)	C(11)-N(1)-Ir(1)	120.0(3)
C(9)-C(7)-C(10)	109.6(5)	C(1)-N(1)-Ir(1)	118.6(3)
C(8)-C(7)-C(10)	109.3(5)	C(21)-N(2)-C(22)	127.2(4)
C(9)-C(7)-P(1)	111.3(4)	C(21)-N(2)-H(1)	114(4)
C(8)-C(7)-P(1)	107.6(4)	C(22)-N(2)-H(1)	119(4)

C(21)-O(1)-Ir(1)	94.0(3)	C(14A)-Ir(1)-O(1)	101.1(8)
C(21)-O(2)-Ir(1)	88.4(3)	N(1)-Ir(1)-O(2)	112.08(13)
C(2)-P(1)-C(3)	108.7(3)	C(6)-Ir(1)-O(2)	155.18(19)
C(2)-P(1)-C(7)	106.4(3)	C(14A)-Ir(1)-O(2)	149.2(6)
C(3)-P(1)-C(7)	118.6(3)	O(1)-Ir(1)-O(2)	59.93(11)
C(2)-P(1)-C(3A)	104.5(5)	N(1)-Ir(1)-P(1)	83.22(12)
C(7)-P(1)-C(3A)	104.8(6)	C(6)-Ir(1)-P(1)	66.65(16)
C(2)-P(1)-Ir(1)	100.43(18)	C(14A)-Ir(1)-P(1)	109.5(7)
C(3)-P(1)-Ir(1)	89.7(2)	O(1)-Ir(1)-P(1)	98.11(9)
C(7)-P(1)-Ir(1)	130.39(17)	O(2)-Ir(1)-P(1)	97.75(9)
C(3A)-P(1)-Ir(1)	107.8(5)	N(1)-Ir(1)-P(2)	82.22(12)
C(13A)-P(2)-C(12)	105.9(11)	C(6)-Ir(1)-P(2)	100.93(17)
C(13A)-P(2)-C(17)	126.4(9)	C(14A)-Ir(1)-P(2)	58.1(7)
C(12)-P(2)-C(17)	103.5(2)	O(1)-Ir(1)-P(2)	97.89(9)
C(12)-P(2)-C(13)	108.8(2)	O(2)-Ir(1)-P(2)	98.29(9)
C(17)-P(2)-C(13)	108.4(2)	P(1)-Ir(1)-P(2)	161.49(5)
C(13A)-P(2)-Ir(1)	97.7(9)	N(1)-Ir(1)-C(21)	141.89(15)
C(12)-P(2)-Ir(1)	99.02(18)	C(6)-Ir(1)-C(21)	130.0(2)
C(17)-P(2)-Ir(1)	120.58(16)	C(14A)-Ir(1)-C(21)	127.5(7)
C(13)-P(2)-Ir(1)	114.82(17)	O(1)-Ir(1)-C(21)	30.12(12)
N(1)-Ir(1)-C(6)	86.1(2)	O(2)-Ir(1)-C(21)	29.81(12)
N(1)-Ir(1)-C(14A)	85.8(8)	P(1)-Ir(1)-C(21)	99.15(10)
N(1)-Ir(1)-O(1)	171.99(13)	P(2)-Ir(1)-C(21)	99.36(10)
C(6)-Ir(1)-O(1)	101.72(19)		

Symmetry transformations used to generate equivalent atoms: -

Table S19. Torsion angles [°] for **13**.

N(1)-C(1)-C(2)-P(1)	3.6(7)
C(4)-C(3)-C(6)-Ir(1)	93.2(5)
C(5)-C(3)-C(6)-Ir(1)	-144.3(5)
P(1)-C(3)-C(6)-Ir(1)	-25.1(4)
Ir(1)-C(14A)-C(13A)-C(15A)	142(2)
Ir(1)-C(14A)-C(13A)-C(16)	-83.2(18)
Ir(1)-C(14A)-C(13A)-P(2)	29.2(19)
N(1)-C(11)-C(12)-P(2)	2.2(7)
C(31)-C(26)-C(27)-C(28)	0.0
C(26)-C(27)-C(28)-C(29)	0.0
C(27)-C(28)-C(29)-C(30)	0.0
C(28)-C(29)-C(30)-C(31)	0.0
C(29)-C(30)-C(31)-C(26)	0.0
C(27)-C(26)-C(31)-C(30)	0.0
C(12)-C(11)-N(1)-C(1)	168.1(5)
C(12)-C(11)-N(1)-Ir(1)	1.5(7)
C(2)-C(1)-N(1)-C(11)	-167.7(5)
C(2)-C(1)-N(1)-Ir(1)	-1.0(7)
O(2)-C(21)-N(2)-C(22)	-179.7(4)
O(1)-C(21)-N(2)-C(22)	0.4(7)
C(23)-C(22)-N(2)-C(21)	-178.1(4)
C(25)-C(22)-N(2)-C(21)	-59.4(6)
C(24)-C(22)-N(2)-C(21)	62.5(6)
O(2)-C(21)-O(1)-Ir(1)	0.0(4)
N(2)-C(21)-O(1)-Ir(1)	180.0(4)
O(1)-C(21)-O(2)-Ir(1)	0.0(4)
N(2)-C(21)-O(2)-Ir(1)	-179.9(4)
C(1)-C(2)-P(1)-C(3)	89.3(5)
C(1)-C(2)-P(1)-C(7)	-141.8(4)
C(1)-C(2)-P(1)-C(3A)	107.7(7)
C(1)-C(2)-P(1)-Ir(1)	-4.0(5)
C(4)-C(3)-P(1)-C(2)	168.6(5)
C(5)-C(3)-P(1)-C(2)	37.7(6)
C(6)-C(3)-P(1)-C(2)	-78.9(4)
C(4)-C(3)-P(1)-C(7)	46.9(6)
C(5)-C(3)-P(1)-C(7)	-84.0(6)
C(6)-C(3)-P(1)-C(7)	159.4(3)
C(4)-C(3)-P(1)-Ir(1)	-90.5(5)
C(5)-C(3)-P(1)-Ir(1)	138.6(5)
C(6)-C(3)-P(1)-Ir(1)	22.0(3)
C(9)-C(7)-P(1)-C(2)	176.9(4)
C(8)-C(7)-P(1)-C(2)	58.7(4)
C(10)-C(7)-P(1)-C(2)	-60.7(5)
C(9)-C(7)-P(1)-C(3)	-60.2(5)
C(8)-C(7)-P(1)-C(3)	-178.4(4)
C(10)-C(7)-P(1)-C(3)	62.1(6)
C(9)-C(7)-P(1)-C(3A)	-72.7(6)
C(8)-C(7)-P(1)-C(3A)	169.1(5)
C(10)-C(7)-P(1)-C(3A)	49.6(6)
C(9)-C(7)-P(1)-Ir(1)	57.0(5)

C(8)-C(7)-P(1)-Ir(1)	-61.2(5)	C(11)-C(12)-P(2)-Ir(1)	-3.9(4)
C(10)-C(7)-P(1)-Ir(1)	179.3(4)	C(20)-C(17)-P(2)-C(13A)	-68.4(14)
C(15A)-C(13A)-P(2)-C(12)	-31(3)	C(18)-C(17)-P(2)-C(13A)	173.7(14)
C(16)-C(13A)-P(2)-C(12)	-178.3(12)	C(19)-C(17)-P(2)-C(13A)	56.4(14)
C(14A)-C(13A)-P(2)-C(12)	77.5(16)	C(20)-C(17)-P(2)-C(12)	53.4(4)
C(15A)-C(13A)-P(2)-C(17)	90(3)	C(18)-C(17)-P(2)-C(12)	-64.5(4)
C(16)-C(13A)-P(2)-C(17)	-57(2)	C(19)-C(17)-P(2)-C(12)	178.2(3)
C(14A)-C(13A)-P(2)-C(17)	-161.7(12)	C(20)-C(17)-P(2)-C(13)	-62.1(4)
C(15A)-C(13A)-P(2)-Ir(1)	-132(2)	C(18)-C(17)-P(2)-C(13)	-180.0(3)
C(16)-C(13A)-P(2)-Ir(1)	80.0(14)	C(19)-C(17)-P(2)-C(13)	62.7(4)
C(14A)-C(13A)-P(2)-Ir(1)	-24.2(16)	C(20)-C(17)-P(2)-Ir(1)	162.6(3)
C(11)-C(12)-P(2)-C(13A)	-104.7(10)	C(18)-C(17)-P(2)-Ir(1)	44.7(4)
C(11)-C(12)-P(2)-C(17)	120.7(4)	C(19)-C(17)-P(2)-Ir(1)	-72.6(4)
C(11)-C(12)-P(2)-C(13)	-124.1(4)		

Symmetry transformations used to generate equivalent atoms: -

4 References

[1] J. Meiners, M. G. Scheibel, M.-H. Lemée-Cailleau, S. A. Mason, M. B. Boeddinghaus,T. F. Fässler, E. Herdtweck, M. M. Khusniyarov, S. Schneider, *Angew. Chemie Int. Ed.* 2011, **50**, 8184.

[2] B. Boduszek, H. J. Shine, *J. Org. Chem.* 1988, **53** (21), 5142.

[3] D. S. Glueck, J. Wu, F. J. Hollander, R. G. Bergman, *J. Am. Chem. Soc.* 1991, **113**, 2041.

[4] S. K. Sur, *J. Magn. Res.* 1989, **82**, 169.

[5] A. Schweiger, G. Jeschke, Principles of Pulse Electron Paramagnetic Resonance. A. Schweiger, G. Jeschke, Eds., (Oxford University Press, Oxford, 2001).

[6] (a) S. Stoll, A. Schweiger, *J. Magn. Reson.* 2006, **178**, 42. (b) S. Stoll, R.D. Britt, *PhysChemChemPhys* 2009, **11**, 6614.

[7] O. Kahn, *Molecular Magnetism*, VCH Publishers Inc., New York, 1993.

[8] Full-matrix diagonalization of the spin Hamiltonian for zero-field splitting and Zeeman splitting was performed with the *julX* program (E. Bill, Max-Planck Institute for Chemical Energy Conversion, Mülheim/Ruhr, Germany, 2008**)**. Matrix diagonalization is done with the routine *ZHEEV* from the *LAPACK* numerical package. Parameter optimization is performed with the simplex routine *AMOEBA* from *NUMERICAL RECIPES*.

[9] M. G. Scheibel, B. Askevold, F. W. Heinemann, E. J. Reijerse, B. de Bruin, S. Schneider, *Nat. Chem.* 2012, **4**, 552.

[10] M. Kinauer, M. G. Scheibel, J. Abbenseth, F. W. Heinemann, P. Stollberg, C. Würtele, S. Schneider, *Dalton Trans.* 2014, **43**, 4506.

[11] O. Starzewski, T. Dieck, *Inorg. Chem.* 1979, **18** (12), 3307.

[12] R. Ahlrichs, Turbomole Version 6.5, Theoretical Chemistry Group, University of Karlsruhe.

[13] PQS version 2.4, 2001, Parallel Quantum Solutions, Fayettevile, Arkansas (USA); the Baker optimizer is available separately from PQS upon request: I. Baker, *J. Comput. Chem.* 1986, **7**, 385–395.

[14] P. H. M. Budzelaar, *J. Comput. Chem.* 2007, **28**, 2226–2236.

[15] a) C. Lee, W. Yang, R. G. Parr, *Phys. Rev. B* 1988, **37**, 785–789; b) A. D. Becke, *J. Chem. Phys.* 1993, **98**, 1372–1377; c) A. D. Becke, *J. Chem. Phys.* 1993, **98**, 5648–5652; d) Calculations were performed using the Turbomole functional "b3-lyp", which is not completely identical to the Gaussian "B3LYP" functional.

[16] a) F. Weigend, R. Ahlrichs, *Phys. Chem. Chem. Phys.* 2005, **7**, 3297–3305; b) F. Weigend, M. Häser, H. Patzelt, R. Ahlrichs, *Chem. Phys. Lett.* 1998, **294**, 143.

[17] a) Turbomole basisset library, Turbomole Version 6.5; b) D. Andrae, U. Haeussermann, M. Dolg, H. Stoll, H. Preuss, *Theor. Chim. Acta* 1990, **77**, 123.

[18] Lead reference for calculation of g-tensor (Zeeman interactions) parameters: E. van Lenthe, A. van der Avoird, P. E. S Wormer, *J. Chem. Phys.* 1997, **107**, 2488. Lead reference for calculation of A-tensor (Nuclear magnetic dipole hyperfine interactions) parameters: E. van Lenthe, A. van der Avoird, P. E. S. Wormer, *J. Chem. Phys.* 1998, **108**, 4783.

[19] ADF2013: a) E.J. Baerends, D. E. Ellis, P. Ros, *Chem. Phys.* 1973, **2**, 41. b) L. Versluis, T. Ziegler, J. Chem. Phys., 1988, **88**, 322. c) G. te Velde, E. J. Baerends, *J. Comput. Phys.*, 1992, **99**, 84. d) C. Fonseca Guerra, J. G. Snijders, G. te Velde, E. J. Baerends, *Theor. Chem. Acc.*, 1998, **99**, 391.

[20] *Gaussian 09, Revision D.01*, M. J. Frisch, G. W. Trucks, H. B. Schlegel, G. E. Scuseria, M. A. Robb, J. R. Cheeseman, G. Scalmani, V. Barone, B. Mennucci, G. A. Petersson, H. Nakatsuji, M. Caricato, X. Li, H. P. Hratchian, A. F. Izmaylov, J. Bloino, G. Zheng, J. L. Sonnenberg, M. Hada, M. Ehara, K. Toyota, R. Fukuda, J. Hasegawa, M. Ishida, T. Nakajima, Y. Honda, O. Kitao, H. Nakai, T. Vreven, J. A. Montgomery, Jr., J. E. Peralta, F. Ogliaro, M. Bearpark, J. J. Heyd, E. Brothers, K. N. Kudin, V. N. Staroverov, T. Keith, R. Kobayashi, J. Normand, K. Raghavachari, A. Rendell, J. C. Burant, S. S. Iyengar, J. Tomasi, M. Cossi, N. Rega, J. M. Millam, M. Klene, J. E. Knox, J. B. Cross, V. Bakken, C. Adamo, J. Jaramillo, R. Gomperts, R. E. Stratmann, O. Yazyev, A. J. Austin, R. Cammi, C. Pomelli, J. W. Ochterski, R. L. Martin, K. Morokuma, Ö. Farkas, V. G. Zakrzewski, G. A. Voth, P. Salvador, J. J. Dannenberg, S. Dapprich, A. D. Daniels, O. J. B. Foresman, J. V. Ortiz, J. Cioslowski, D. J. Fox (Gaussian, Inc., Wallingford, CT), 2013, see http://www.gaussian.com.

[21] S. Grimme, J. Antony, S. Ehrlich, H. Krieg, *J. Chem. Phys.* 2010, **132**, 154104.

[22] K. B. Wiberg, *Tetrahedron*, 1968, **24**, 1083.

[23] a) I. Mayer, *Chem. Phys. Lett.* **1983**, *97*, 270. b) I. Mayer, *Chem. Phys. Lett.* 1984, **110**, 440. c) I. Mayer, *Int. J. Quantum Chem.* 1986, **29**, 73. d) I. Mayer, *Int. J. Quantum Chem.* 1986, **29**, 477. e) A. J. Bridgeman, G. Cavigliasso, L. R. Ireland, J. Rothery, *J. Chem. Soc., Dalton Trans.* 2001, **14**, 2095.

[24] a) S. I. Gorelsky, AOMix: Program for Molecular Orbital Analysis, http://www.sg-chem.net/, University of Ottawa, version 6.53, 2011. b) S. I. Gorelsky, A. B. P. Lever, *J. Organomet. Chem.* 2001, **635**, 187.

[25] *NBO 6.0.,* E. D. Glendening, J. K. Badenhoop, A. E. Reed, J. E. Carpenter, J. A. Bohmann, C. M. Morales, C. R. Landis, F. Weinhold, Theoretical Chemistry Institute, University of Wisconsin, Madison 2013.

[26] *MOLPRO, version 2015.1*, a package of *ab initio* programs, H.-J. Werner, P. J. Knowles, G. Knizia, F. R. Manby, M. Schütz, P. Celani, W. Györffy, D. Kats, T. Korona, R. Lindh, A. Mitrushenkov, G. Rauhut, K. R. Shamasundar, T. B. Adler, R. D. Amos, A. Bernhardsson, A. Berning, D. L. Cooper, M. J. O. Deegan, A. J. Dobbyn, F. Eckert, E. Goll, C. Hampel, A. Hesselmann, G. Hetzer, T. Hrenar,

G. Jansen, C. Köppl, Y. Liu, A. W. Lloyd, R. A. Mata, A. J. May, S. J. McNicholas, W. Meyer, M. E. Mura, A. Nicklass, D. P. O'Neill, P. Palmieri, D. Peng, K. Pflüger, R. Pitzer, M. Reiher, T. Shiozaki, H. Stoll, A. J. Stone, R. Tarroni, T. Thorsteinsson, M. Wang (University College Cardiff Consultants Ltd., Cardiff, UK), 2015, see http://www.molpro.net.

[27] K. Raghavachari, G. W. Trucks, J. A. Pople, M. Head-Gordon, *Chem. Phys. Lett.*, 1989, **157**, 479.

[28] a) T. H. Dunning, Jr., *J. Chem. Phys*., 1989, **90**, 1007. b) D. E. Woon, T. H. Dunning, Jr., *J. Chem. Phys.*, 1993, **98**, 1358. c) D. Figgen, K. A. Peterson, M. Dolg, H. Stoll, *J. Chem. Phys.*, 2009, **130**, 164108.

[29] a) S. Ten-no, *Chem. Phys. Lett.*, 2004, **398**, 56. b) T. B. Adler, G. Knizia, H.-J. Werner, *J. Chem. Phys.*, 2007, **127**, 221106.

[30] a) K. A. Peterson, T. B. Adler, H.-J. Werner, *J. Chem. Phys.*, 2008, **128**, 084102. b) K. E. Yousaf, K. A. Peterson, *J. Chem. Phys.*, 2008, **129**, 184108. c) S. Kritikou, J. G. Hill, *J. Chem. Theory Comput.*, 2015, **11**, 5269.

[31] F. Weigend, *J. Comput. Chem*. 2008, **29**, 167-175.

[32] J. G. Hill, *J. Chem. Phys*. 2011, **135**, 044105/1-044105/4.

[33] *ORCA version 4.0.1, an* ab initio, *DFT and semiempirical SCF-MO package*, F. Neese, F. Wennmohs, with contributions from D. Aravena, M. Atanasov, U. Becker, D. Bykov, V. G. Chilkuri, D. Datta, A. K. Dutta, D. Ganyushin, Y. Guo, A. Hansen, L. Huntington, R. Izsák, C. Kollmar, S. Kossmann, M. Krupička, D. Lenk, D. G. Liakos, D. Manganas, D. A. Pantazis, T. Petrenko, P. Pinski, C. Reimann, M. Retegan, C. Riplinger, T. Risthaus, M. Roemelt, M. Saitow, B. Sandhöfer, I. Schapiro, K. Sivalingam, G. Stoychev, B. Wezisla, *and with contributions from collaborators* M. Kállay, S. Grimme, E. Valeev, G. Chan, J. Pittner, M. Brehm (Max-Planck-Institut für Chemische Energiekonversion, Mülheim a. d. Ruhr, Germany), 2017, see https://orcaforum.cec.mpg.de/.

[34] F. Neese, *WIREs Comput. Mol. Sci*. 2012, **2**, 73-78.

[35] C. van Wüllen, *J. Chem. Phys*. 1998, **109**, 392-399.

[36] D. A. Pantazis, X.-Y. Chen, C. R. Landis, F. Neese, *J. Chem. Theory Comput*. 2008, **4**, 908-919.

[37] F. Neese, F. Wennmohs, A. Hansen, U. Becker, *Chem. Phys*. 2009, **356**, 98-109.

[38] C. Angeli, R. Cimiraglia, S. Evangelisti, T. Leininger, J.-P. Malrieu, *J. Chem. Phys*. 2001, **114**, 10252-10264.

[39] C. Angeli, R. Cimiraglia, J.-P. Malrieu, *Chem. Phys. Lett*. 2001, **350**, 297-305.

[40] C. Angeli, R. Cimiraglia, J.-P. Malrieu, *J. Chem. Phys*. 2002, **117**, 9138-9153.

[41] B. A. Heß, C. M. Marian, U. Wahlgren, O. Gropen, *Chem. Phys. Lett*. 1996, **251**, 365-371.

[42] a) APEX2 v2014.9-0 (SAINT/SADABS/SHELXT/SHELXL), Bruker AXS Inc., Madison, WI, USA, 2014. b) George M. Sheldrick, *Acta Cryst.,* 2015, A71, 3-8. c) George M. Sheldrick, *Acta Cryst*., 2015, C71, 3. d) George M. Sheldrick, *Acta Cryst*., 2008, A64, 112.